“Evaluating the potential of metabolic reprogramming of macrophages for glioblastoma therapy”

Dissertation

Zur Erlangung des Grades

„Doktor

der Naturwissenschaften“

Am Fachbereich Biologie

der Johannes Gutenberg-Universität

in Mainz

Carsten Geiß

geb. am 01.05.1991 in Weinheim

Mainz, den 22.04.2021

Abstract

Even if cancer therapy is making continuous progress, the prognosis for several tumor types remains poor. Especially for glioblastoma, the most common malignant primary brain tumor, current treatments only marginally improve patient's overall survival. Hence, there is a great demand for novel therapeutic approaches. A promising strategy is the use of the body's own immune cells (like T cells or macrophages) to specifically attack and eliminate tumor cells. T cell-based tumor therapy has gained much interest in the recent years. Similarly, macrophages show many promising qualities, speaking in favor of their use for therapeutic purposes. But before developing macrophage-based therapeutic strategies more knowledge of their characteristics is needed, especially of their inflammatory phenotypes which are strongly regulated through metabolic alterations.

The experiments described in the publications presented in this thesis were performed in order to shed some light on the immunometabolism of macrophages and its possible manipulation for therapeutic use. Prior to these experiments a major problem affecting the work with tumor samples or primary cells, namely the scarcity of this material, has been addressed. In *"Assessing the reliability of gene expression measurements in very-low-numbers of human monocyte-derived macrophages"* the possibility to scale down the number of primary human macrophages required for experimental analyses has been evaluated and confirmed. This result built the basis for the following protein-protein interaction analyses, leading to the identification of a so far unknown possible regulator of the immune status of macrophages. Furthermore, the established low cell number approach was a requirement to perform the experiments described in *"Metabolic and inflammatory reprogramming of macrophages by ONC201 translates in a pro-inflammatory environment even in presence of glioblastoma cells"*, demonstrating the feasibility to introduce a pro-inflammatory phenotype in macrophages by manipulating their metabolism even if they are co-cultured with glioblastoma cell lines. Since a pro-inflammatory phenotype is typically suppressed by glioblastoma cells, the published results underline the major impact of metabolism on immune cell functions. Finally, if and how these findings can be used for glioblastoma therapy will be critically discussed.

Zusammenfassung

Auch wenn die Therapie von Krebserkrankungen kontinuierlich Fortschritte erzielt, ist die Prognose für einige Tumorarten weiterhin schlecht. Insbesondere beim Glioblastom, dem häufigsten bösartigen primären Hirntumor, führen auch modernste Behandlungsmethoden nur zu einer geringfügigen Verlängerung der Lebenszeit, weshalb dringend neuartige Therapieansätze benötigt werden. Eine vielversprechende Strategie ist der Einsatz von körpereigenen Immunzellen (wie beispielsweise T-Zellen oder Makrophagen) zur spezifischen Bekämpfung der Tumorzellen. Die T-Zell-basierte Tumortherapie hat in den letzten Jahren viel Aufmerksamkeit bekommen, aber auch Makrophagen weisen diverse vielversprechende Eigenschaften auf, die für ihren therapeutischen Einsatz sprechen. Bevor jedoch Strategien zur Tumortherapie unter Verwendung von Makrophagen entwickelt werden können, ist eine genauere Charakterisierung dieser Zellen notwendig. Insbesondere ihre inflammatorischen Phänotypen, die maßgeblich durch den zellulären Metabolismus reguliert werden, bedürfen intensiverer Untersuchungen.

Die in dieser Dissertation vorgestellten Publikationen befassen sich mit dem Immunstoffwechsel von Makrophagen und dessen mögliche Manipulation zu therapeutischen Zwecken. Zuvor wurde das Problem der Materialknappheit, das insbesondere bei der Arbeit mit Tumorproben oder primären Zellen auftritt, adressiert. In der Publikation *„Assessing the reliability of gene expression measurements in very-low-numbers of human monocyte-derived macrophages“* wird gezeigt, dass es möglich ist die Anzahl primärer humaner Makrophagen für experimentelle Analysen um ein Vielfaches zu reduzieren. Dieses Ergebnis bildete die Grundlage für Protein-Protein-Interaktionsanalysen, welche zur Identifizierung eines bisher unbekannten möglichen Regulators des inflammatorischen Profils von Makrophagen führten. Darüber hinaus bildete die Möglichkeit der Verwendung geringerer Zellzahlen die Voraussetzung für die Durchführung der in *„Metabolic and inflammatory reprogramming of macrophages by ONC201 translates in a pro-inflammatory environment even in presence of glioblastoma cells“* beschriebenen Experimente. Diese Publikation beschreibt die Induktion eines pro-inflammatorischen Phänotyps in Makrophagen durch Manipu-

lation ihres Stoffwechsels, auch in Anwesenheit von Glioblastom-Zelllinien. Da ein pro-inflammatorischer Phänotyp typischerweise von Glioblastomzellen unterdrückt wird, veranschaulichen diese Ergebnisse den starken Einfluss des Metabolismus auf die Funktionen der Immunzellen. Ob und wie diese Erkenntnisse für die Glioblastom-Therapie genutzt werden können, wird im Anschluss kritisch diskutiert.

Table of contents

1 Introduction

Using our own immune system to treat cancer is a very promising approach which gained a lot of interest in the recent years. This cumulative thesis is based on two publications, focusing on the metabolic reprogramming of human macrophages as possible tools for the treatment of glioblastoma, a primary brain tumor.

1.1 Brain tumors: a brief introduction

In general, the term “brain tumor” describes the growth of abnormal cells in brain tissues. These tumors can be benign (neither invade nearby tissue nor spread to other parts of the body) or malignant (can invade nearby tissue and/or spread to other parts of the body). They are further classified into primary brain tumors, originating in the brain, and secondary (or metastatic) brain tumors, derived from cancer cells spread to the brain from other organs. To characterize brain tumors the World Health Organization (WHO) released a classification system, which was lastly restructured in 2016. Since this restructuring the classification is also based on molecular alterations and not only on histopathologic features as it was in 2007[1,2]. Based on the WHO criteria, brain tumors are graded from I to IV. Grade I is representing benign, slow growing tumors whereas grade IV is corresponding to infiltrative, fast growing tumors. Primary brain tumors can arise from different brain tissues and are therefore grouped by their cellular origin.

The latest comprehensive summary of the current descriptive epidemiology of brain tumors is the *“CBTRUS Statistical Report: Primary Brain and Other Central Nervous System Tumors Diagnosed in the United States in 2013-2017”*, including 415,411 records of brain and other central nervous system (CNS) tumors (123,484 malignant and 291,927 non-malignant)[3]. According to this study, 80.8% of all malignant primary brain and other CNS tumors are gliomas (see Figure 1A). These tumors arise from glial cells (oligodendrocytes, astrocytes, microglia, and ependymal cells), which normally have mainly supportive and protective functions. Gliomas developing from astrocytes, are called astrocytomas and make up around 78% of all gliomas (see Figure 1B). The most frequent representative of astrocytoma is glioblastoma (GB), a grade IV

brain tumor characterized by uncontrolled cellular proliferation, local infiltration, extensive genomic instability, tendency for necrosis, angiogenesis, and resistance to current therapies (see chapter 1.2). To underline its high heterogeneity in appearance the term “glioblastoma multiforme” has been introduced in 1926[4]. But after the revision of the WHO-nomenclature in 2007, it is simply called “glioblastoma”[1]. Interestingly, even though GBs are very invasive they rarely intravasate and metastasize from the brain[5]. Only in rare cases GBs can spread to other parts of the body like liver and bone [6]. A possible explanation for this phenomenon can be found in the early patient mortality.

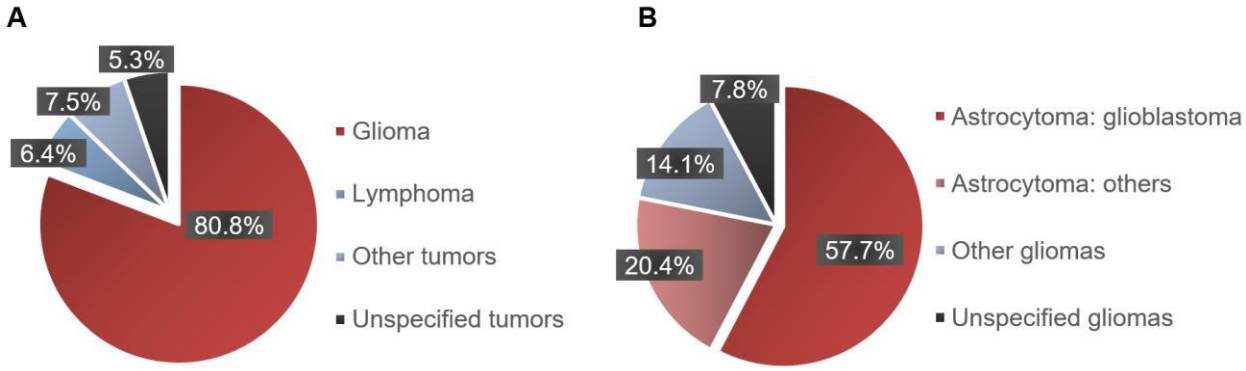

Figure 1: Incidence of brain tumors and gliomas in the United States from 2013 to 2017. A: Distribution of malignant primary brain and other CNS tumors. B: Distribution of primary brain and other CNS gliomas. The glioma sub-group astrocytoma has been further subdivided into glioblastoma and other astrocytomas to illustrate the high percentage of glioblastoma. Diagrams based on *“CBTRUS Statistical Report: Primary Brain and Other Central Nervous System Tumors Diagnosed in the United States in 2013-2017”* [3].

1.2 Glioblastoma: incidence, symptoms, and diagnosis

As shown above, GB represents 57.7% of all primary brain and other CNS gliomas (this accounts for 48.6% of all malignant primary brain and other CNS tumors) with an incidence rate of 3.23 per 100,000 population. For the years 2020 and 2021 the number of projected cases of glioblastoma in the United States is 12,800 and 12,970, respectively. The relative survival rate shows that 36.0% of patients with malignant brain and other CNS tumors were still alive after five years, whereas only 7.2% of glioblastoma patients survived. The median survival for glioblastoma, regardless of treatment, was 8 months. The incidence of glioblastoma increased with age (95% of patients were older than 40 years, median age 65) and was 1.59 times higher in males compared

to females. 90% of all diagnosed GBs were primary tumors (arise de novo), whereas only 10% were secondary tumors (arise from lower-grade tumors)[7]. Secondary tumors, correlating with a longer survival, were more often diagnosed in younger patients (mean age 45 years)[8].

The causes for brain and other CNS tumors are various and many risk factors have been investigated. So far, only ionizing radiation could be identified as a positive risk factor[9]. But in general these tumors are characterized by dysregulation of key signaling pathways involving cell survival, growth, proliferation, and apoptosis due to genomic mutations[7]. Interestingly, even if no genetic predispositions are known, the diagnosis of a first-degree family member increases the risk approximately two-fold[10]. On the other hand, having an allergy or other atopic disease decreased the risk for these tumors[11].

The most common locations for GBs are the frontal and temporal lobes of the brain, but in rare cases also other brain areas are affected[3]. Patients typically show symptoms of increased intracranial pressure, like headaches, neurological defects, and seizures[12]. The diagnosis is based on histological features including anaplasia, mitotic activity, microvascular proliferation, and necrosis[13]. Mutation of the isocitrate dehydrogenase correlates with secondary GB and better prognosis, possibly caused by increased genome-wide methylation[14].

1.2.1 Glioblastoma therapy

The standard of care for glioblastoma patients consists of maximal safe resection followed by chemo- and radiotherapy[15]. This treatment extends the median overall survival to about 16 months[16]. A gross surgical resection prolongs the overall survival time[17] and maximizes quality of life[18]. Moreover, the use of fluorescent dyes to improve the identification of the tumor edge, prolongs progression-free survival[19]. Nevertheless, a complete surgical resection of the tumor still remains almost impossible since the tumors lack a clear margin and tumor cells infiltrate the surrounding healthy tissue[18].

Chemo- and radiotherapies also show limited success. Radiotherapy faces the problem that only a small area around the tumor margin can be targeted, possibly not covering the whole spreading

area of migrating tumor cells[20]. Due to the accumulation of GB driver mutations in astrocyte-like neural stem cells in the subventricular zone[21], targeting radiotherapy towards this area maybe improves patient outcome, but these results are strongly discussed[22]. A major restriction for chemotherapy is the blood-brain barrier (BBB), which stays impassable for most chemotherapeutics even after losing integrity during tumor progression[23]. Since 2005 temozolomide (TMZ) is commonly used as first line chemotherapeutic agent for newly diagnosed glioblastoma[15]. The efficiency of chemotherapeutic therapies relies on several factors, which can vary from patient to patient or change during treatment. Unfortunately, even if an initial efficacy can be observed, tumors often acquire therapy resistance and recur[12]. One mechanism of therapeutic resistance is the expression of O6-methylguanine methyltransferase, an enzyme normally repairing DNA damages, including the damages induced by TMZ. The expression of this enzyme is controlled through the methylation of its promoter, linking the promoter methylation status directly to the efficiency of TMZ therapy. In case TMZ therapy resistance has developed, nitrosureas or a combination of procarbazine, lomustine and vincristine can be used as second line treatments yet showing higher toxicity and poorer efficacy compared to TMZ[24]. However, even using state-of-the-art technologies, GB recurrence is detected within approximately 7 months in almost all cases[15].

Unfortunately, also novel approaches, like anti-angiogenic therapies using antibodies (e.g., Bevacizumab), were ultimately ineffective at treating GB in clinical trials[25–27]. Other strategies aim at stimulating the immune system of the patient to detect and eliminate the tumor cells. This process, called cancer immunosurveillance, is a physiological process that happens on a regular basis and prevents the accumulation of transformed cells and the establishment of tumors. Nevertheless, in few cases the transformed cells are able to evade the immune system[28,29]. To overcome this mechanism cancer immunotherapies are currently tested or already in clinical use. The field of immunotherapies made great progress since the discovery and clinical implementation of immune checkpoint inhibitors, mostly targeting cytotoxic T-lymphocyte protein 4 (CTLA-4), programmed cell death protein 1 (PD-1) or programmed cell death 1 ligand 1 (PD-L1)[30]. However, even if this approach shows high potential in several kinds of cancer and clinical trials including

GB are ongoing[31], until this day, there was no breakthrough using immune checkpoint inhibitors for GB therapy. An explanation for these failures may be found in the systemic and intra-tumoral immunosuppression induced by GB cells[32]. Besides, there is evidence that a high number of patients receiving immunotherapy have to struggle with adverse events[33].

Since the success of immune checkpoint inhibition in GB treatment is limited, recent immunotherapy strategies aim at combinatorial strategies to overcome the immune resistance. Anyway, to find suitable drug combinations a deeper understanding of GB induced immunosuppression is mandatory. Of particular note would be the characterization of GB heterogeneity, which is thought to contribute to immunotherapy resistance[34].

1.2.2 Tumor heterogeneity

Like other types of tumors glioblastoma consist of a heterogenous cell population in and around the tumor mass, making each tumor unique. This inter- and intra-tumoral heterogeneity is partly based on the tumor cells which can be differentiated or undifferentiated and vary in morphology, proliferation rate or self-renewal capacity[35,36]. Furthermore, surrounding, or invading cells contribute to tumor heterogeneity. Especially GBs are very heterogenous tumors, defined by tumor cells, tumor-initiating cells (or stem-like cells), endothelial cells, pericytes, fibroblasts and immune cells[37]. These tumor-associated cells are interacting with the tumor cells and thereby typically promote tumor growth and progression[38]. Moreover, local conditions and the genetic background influence the tumor composition, as exemplified at the tumor core which is more hypoxic and contains more anti-inflammatory $CD163^+$ tumor-associated macrophages than the peritumoral area[39]. This complex tumor diversity of phenotypes is a major reason for (chemo)therapy resistance and tumor recurrence since it allows the adaptation to various conditions or treatments[40].

Nevertheless, based on the efforts of *The Cancer Genome Atlas* network GBs and low-grade gliomas could be grouped in different subtypes based on their genetic profile[41,42]. Subsequent studies further redefined the classification of glioblastoma to the three most relevant subtypes:

proneural, mesenchymal, and classical[42]. According to literature the proneural subtype is commonly related to a more favorable outcome and mesenchymal to a poor survival[42–44].

However, since patients with tumors exhibiting isocitrate dehydrogenase mutations usually show an increased survival and these tumors are consistently classified as proneural, the meaningfulness of molecular subtyping is probably affected. Besides, a common problem for tumor subtyping arises with the acquisition of biopsies from only one single random location of the tumor. As a result of the high intra-tumoral heterogeneity varied molecular subtypes can coexist in the tumor mass, leading to a mixed cellular population of different subtypes[34]. This heterogeneity is not only a problem for the identification of therapeutic targets, but a high heterogeneity is also limiting the effects of treatment and decreases overall survival[45].

1.2.3 Glioblastoma microenvironment

As described above, tumor cells are not only in contact with each other, they are also strongly interacting with surrounding and infiltrating cells of other cell types. These interactions lead to the promotion of GB cell proliferation (as exemplified by neurons secreting neuroligin-3[46]) or the suppression of anti-tumor immune responses (e.g., of infiltrating macrophages, or the CNS-resident macrophages called microglia[47]). The crosstalk between different cell types is largely defined by the conditions in the milieu around the tumor, which is further known as tumor microenvironment (TME). The abundance of specific cell types or cytokines can shift the TME from an inflammatory towards an anti-inflammatory/immunosuppressive phenotype, influencing tumor therapy and patient survival (see Figure 2). To state a few examples: Regulatory T cells (Tregs), probably attracted by C-C motif chemokine (CCL) 2 and CCL22 secreted by GB cells[48,49], shift the tumor cytokine milieu towards immunosuppression[50], preventing the production of Interleukin (IL)-12 and thereby restrict the function of infiltrating T cells[51]. Another example are myeloid-derived suppressor cells (MDSCs), whose infiltration negatively correlates with T cell infiltration[52]. Interestingly, the level of CCL2 expression correlates with poor prognosis accompanied by a high infiltration of Tregs, MDSCs, and tumor-associated microglia/macrophages (TAMs)[48]. Likewise, colony

stimulating factor-1 (CSF-1) and stromal cell-derived factor 1 (SDF-1) contribute to TAM recruitment[53,54]. Due to the immunosuppressive conditions, these TAMs undergo an inflammatory reprogramming towards a tumor-supportive phenotype and thus promote tumor invasion[55]. Transforming growth factor ß (TGF-ß) also works immunosuppressive, for example by inducing Tregs or blocking proliferation and activation of other T cells, macrophages and natural killer (NK) cells (see [56] for a review). The involvement of microglia and macrophages in tumor growth and proliferation has been addressed in several studies and will be explained in more detail in chapter 1.3.

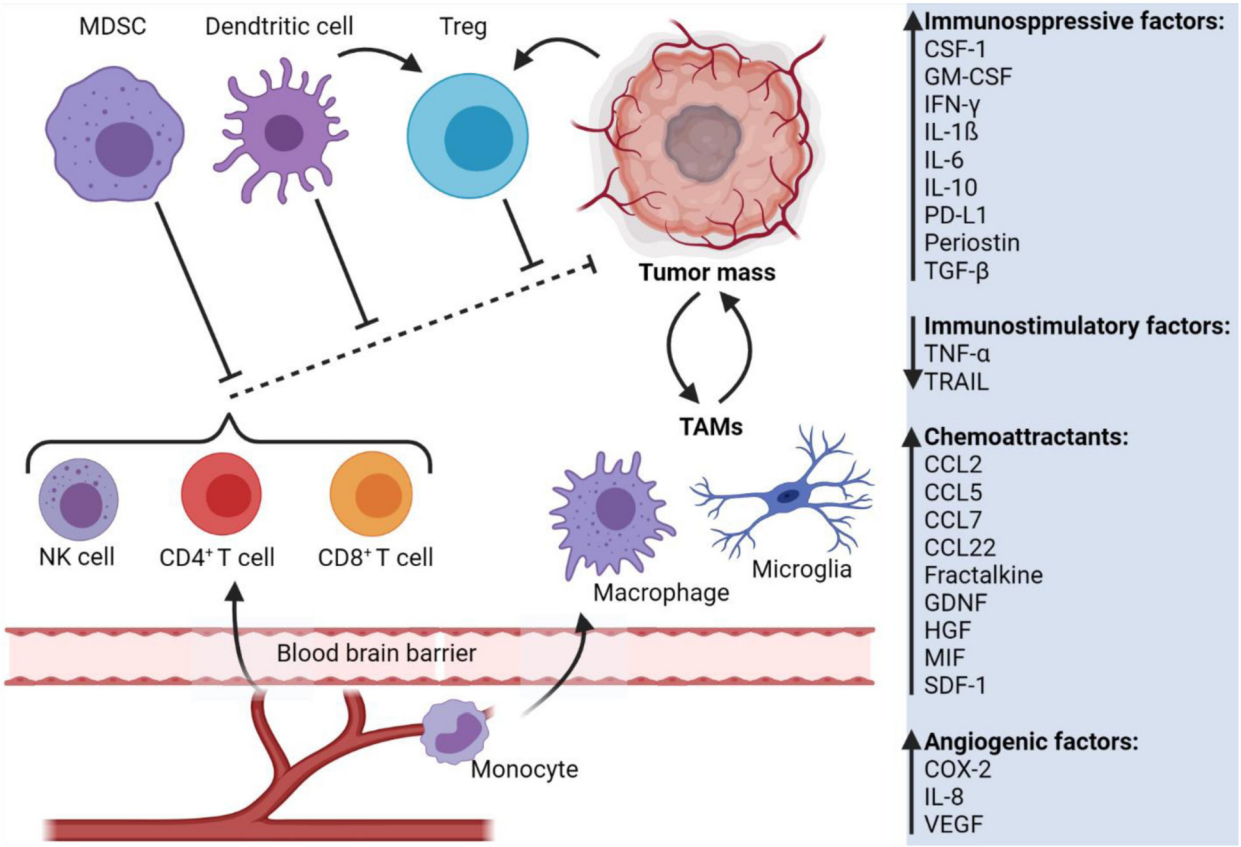

Figure 2: Immune cells attracted by chemokines, cross the disrupted blood-brain barrier to infiltrate the immunosuppressive glioblastoma environment. Brain resident microglia and invading macrophages, differentiated from attracted monocytes, are referred to as TAMs. Infiltrating effector T cells ($CD4^+$, $CD8^+$) and NK cells are blocked in their tumoricidal functions through immunosuppressive molecules released by MDSCs, DCs and Tregs. A list of molecules known to be upregulated (immunosuppressive factors, chemoattractants, angiogenic factors) or downregulated (immunostimulatory factors) in the TME is given on the right. Please see list of abbreviations on page 42 for full names and [57,58] for further information. Figure created with BioRender.com.

Furthermore, predominantly low levels of oxygen (hypoxia) and a lowered pH are characteristics of the TME. Hypoxia leads to the stabilization of the transcription factor HIF1-α (hypoxia-inducible factor 1-alpha), resulting in the production and release of tumor-supportive molecules like growth factors, cytokines, and metalloproteases. These factors can promote angiogenesis[59] or monocyte recruitment[60]. Moreover, hypoxia itself has shown to trap macrophages by inhibiting chemotaxis[61] and induce a pro-tumoral phenotype in these cells[62]. Hypoxia, through HIF-1α signaling, also leads to an upregulation of glycolytic genes such as *SLC2A1* (coding fur glucose transporter type 1)[63], enabling tumor cells to switch their energy production towards anaerobic glycolysis. A higher rate of glycolytic energy production increases the production of lactate, which is released through monocarboxylate transporter as H^+-lactate into the extracellular space, hereby lowering the extracellular pH[64,65].

Although the TME is a known key regulator of tumor progression[66] and a recent publication demonstrates that distinct molecular GB profiles are correlated with differences in their microenvironment[45], the TME is not (yet) part of the WHO classification. Nevertheless, the interest in targeting the TME for tumor therapy is growing and clinical trials are already ongoing[67].

1.3 Tumor-associated microglia and macrophages

The human immune defense system is composed of innate and adaptative immune cells. Macrophages and microglia, are innate immune cells which represent the first line of defense[68]. Even if these cell types have comparable functions and share many features, they also have cell type specific characteristics. A reason for these differences could be found in the cellular origins: Microglia arise from the yolk sac[69], whereas macrophages originate from the prenatal yolk sac[70] or by differentiating from circulating monocytes[71].

Under healthy conditions the macrophage population in the CNS consists only of microglia, which make up 5-20% of the total glial cell population[72]. In case the BBB is disrupted, which can be caused by inflammation, disease, or cancer, the brain parenchyma can be infiltrated by circulating

immune cells[73]. Especially in GBs a high rate of myeloid cell infiltration is detected, probably explaining the high percentage of 30-50% of microglia and macrophages of the total tumor mass[47]. Studies focusing on the tumor mass composition give contradictory results about the percentage of microglia and macrophages, mainly because of difficulties to differentiate these cell types due to a lack of specific markers[74]. As a result, macrophages and microglia are often referred to as TAMs without further differentiation. On top of that, it has been reported that tumor-infiltrating monocytes, the precursors of macrophages, could persist in an undifferentiated state of self-renewal, adding another level of complexity[75]. Using a genetically engineered mouse model, it was demonstrated that peripheral macrophages represent the majority of TAMs in the tumor mass, and resident microglia form a minor TAM population[76]. However, since other studies describe different microglia/macrophage ratios this topic is still controversially discussed. These differences can probably be traced back to the used models and markers for cell type identification, however a time-dependent increase of the macrophage population has been detected in most of longitudinal studies (see [77] for a review).

Independent of their origin or localization, microglia and macrophages are characterized by a high plasticity and heterogeneity[78]. After stimulation by different types of molecules (e.g., growth factors, cytokines, microbial products, nucleotides) inflammatory response cascades are activated, finally leading to the clearance of pathogens or the stimulation of other immune cells, including neutrophils, innate lymphoid cells, and NK cells[79]. Besides pathogen elimination, the major task of macrophages and microglia is the maintenance of homeostasis, e.g., by phagocytic removal of apoptotic cells or self-limitation of inflammation during infections. This variety of functions is only possible due to the high range of phenotypic adaptations these cells can undergo. Depending on the environmental conditions macrophages and microglia adopt inflammatory states ranging from pro- to anti-inflammatory.

To allow a better characterization and understanding of the immune states of macrophages, artificial stimuli have been used to shift the cells *in vitro* towards a pro- or anti-inflammatory state. Macrophages treated with the pro-inflammatory interferon-γ (IFN–γ) and/or lipopolysaccharides

(LPS) represent the so called M1 population, whereas macrophages treated with the anti-inflammatory cytokines IL-4/IL13 represent the M2 population[79]. Although this categorization helps to investigate the functionality of TAMs, recent analyzes revealed a spectrum of activation states which is not covered by the M1/M2 nomenclature[80].

M1 macrophages initiate and sustain the inflammatory responses by secreting cytokines such as tumor necrosis factor-α (TNF-α), IL-6, and IFN-γ, and recruiting other immune cells to the inflamed tissue[79]. This inflammatory reaction is beneficial for example in the killing of invading bacteria or abnormal cells, but it also induces collateral damage to the surrounding healthy tissue [e.g., through the release of reactive oxygen species (ROS)]. To prevent serious damage macrophages are subjected to strong regulatory mechanisms finally introducing an anti-inflammatory phenotype and thereby dampening the inflammation. However, if the pro-inflammatory reactions of macrophages are going to be dysregulated or overstimulated, it can have severe pathological consequences as seen in chronic inflammatory and autoimmune diseases (see [81] for a review). In other situations, the inflammatory response of macrophages is suppressed and therefore not strong enough to eliminate the threat. This phenomenon can be observed in TAMs, acquiring an anti-inflammatory phenotype, though being close to pathogenic cells.

Influenced by the tumor cells, most infiltrating TAMs become tumor-supportive and promote tumor growth, invasion, angiogenesis, and metastasis[82]. By secreting anti-inflammatory cytokines such as IL-6, IL-10 and TGF-β they also contribute to an immunosuppressive microenvironment[83]. Finally, the tumor-supportive activities of TAMs lead to a sooner and higher tumor cell migration and an increased invasiveness of the tumor cells as shown in murine models[84,85]. Likewise, studies using human samples revealed a correlation between the presence of TAMs and poor prognoses or an increase in tumor aggressiveness[86,87]. How GB cells polarize TAMs towards the tumor-supportive phenotype is still barely known, but several factors including cytokines, exosomes, and metabolites were already identified to influence the inflammatory state of TAMs[88–90]. Importantly, it has been shown that the tumor-supportive state of TAMs can be suppressed *in vitro* through artificial stimuli, resulting in anti-tumor activities in *in vitro* models[91–93].

Moreover, it was found that macrophages showing different phenotypes coexist within the same TAM population, also in human samples[94–96]. Importantly, it seems that the distribution of pro- and anti-tumoral TAMs is not random, but determined though spatial conditions[95,97]. Further studies of human material showed that anti-inflammatory (M2) macrophages were correlated with unfavorable prognoses[98]. Looking at standard GB treatment approaches it was shown that surgical resection or TMZ treatment increase the anti-inflammatory phenotype of TAMs[99]. Moreover, radiation therapy renders the tumor more aggressive, which could be caused by a selection of M2 macrophages which are more resistant towards radiation than M1 macrophages[100]. This selection could explain why recurrent tumors mostly arise near the irradiated area[101]. Besides, TAMs were described to be involved in tumor resistance towards TMZ and anti-angiogenic treatments[58].

Thus, the removal of tumor-supportive TAMs or their reprogramming towards a pro-inflammatory/tumoricidal state represent interesting and promising therapeutic approaches which are already tested in clinical trials (please see [58,96] for detailed compilations). Especially the influence of intracellular metabolic pathways on the inflammatory status of immune cells, a process called immunometabolism, is gathering more and more attention. Even if the knowledge in this field is still limited (see chapter 1.4), the potential of manipulating metabolic pathways to directly stimulate immune cells and use them as therapeutic tools is immense.

1.4 Immunometabolism of macrophages

The cellular energy metabolism is based on adenosine triphosphate (ATP), which can be produced by two major pathways: the glycolytic pathway and the oxidative phosphorylation (OXPHOS) pathway. The ATP yield per glucose molecule is higher using OXPHOS (36 molecules ATP) compared to glycolysis (2 molecules ATP), but OXPHOS is oxygen-dependent and therefore not always possible. Moreover, besides ATP the glycolysis pathway generates other metabolic intermediates which are needed for various cellular processes (e.g., synthesis of amino acids or fatty acids). Interestingly, especially cancer cells do normally not use OXPHOS for their energy production (even in presence of oxygen), instead they perform aerobic glycolysis, a phenomenon called the Warburg Effect[102]. This shift in energy metabolism, representing one hallmark

of cancer[103], requires high levels of glucose but allows rapid energy production and the generation of intermediates used for the biosynthesis of amino acids, nucleotides, and lipids which are necessary for cell growth[104].

But not only tumor cells adapt their metabolism, also macrophages change their energy production, depending on their phenotype. Factors influencing macrophage metabolism are various and include intrinsic as well as extrinsic signals. First studies demonstrated that pro-inflammatory activation of murine macrophages through *Corynebacterium ovis* infection leads to an increased rate of glycolysis and a decreased oxygen consumption[105]. Further analyses revealed a broken tricarboxylic acid (TCA) cycle, caused by upregulation of *ACOD1* [coding for cis-aconitate decarboxylase (CAD)], producing itaconate, which in turn inhibits succinate dehydrogenase (SDH), finally leading to an accumulation of succinate[106]. Rising levels of succinate enhance the production of ROS and inhibit prolyl hydroxylases (PHDs)[107]. The inhibition of PHDs stabilizes transcription factor HIF1-α[108], which in turn upregulates the level of the pro-inflammatory cytokine IL-1β[109] and the expression of glycolytic proteins[110]. A consequence of dysfunctional OXPHOS is an increased leakage of electrons in the mitochondrial electron transport chain (ETC), finally leading to the generation of ROS through reverse electron transport (RET)[111]. Moreover, pro-inflammatory/M1 macrophages upregulate the expression of inducible nitric oxide synthase (iNOS) to produce nitric oxide (NO) from arginine. NO plays an important role as antimicrobial molecule and in killing cancer cells[112]. Furthermore, glycolysis, pentose phosphate pathway (PPP), acetylation and fatty acid synthesis (FAS) are upregulated, whereas fatty acid oxidation (FAO) and OXPHOS pathway are downregulated. The impairment of the TCA cycle promotes the intracellular accumulation of citrate and succinate, which is used as an indicator of a pro-inflammatory phenotype (see Figure 3)[106,113,114].

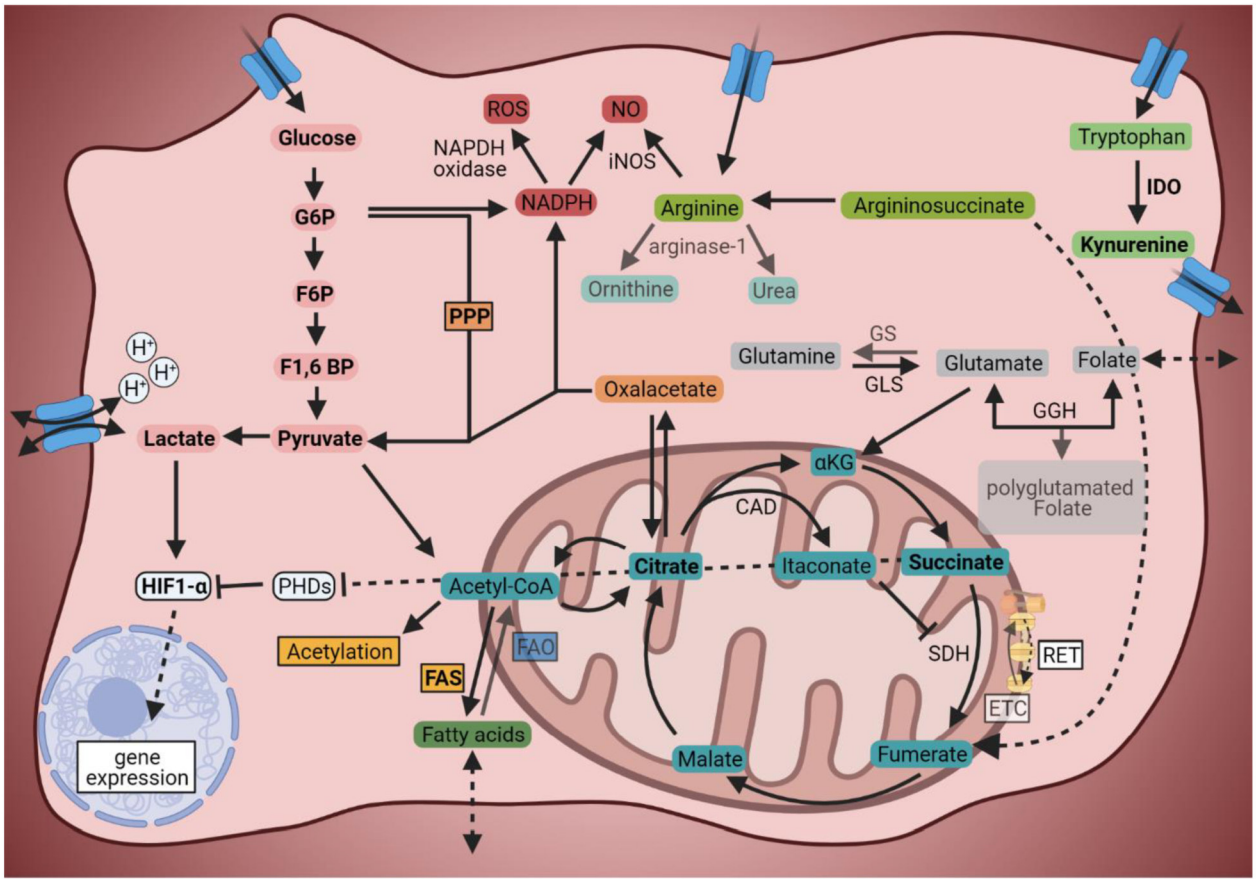

Figure 3: Metabolic adaptations of pro-inflammatory stimulated macrophages. As a consequence of increased glycolysis, the cellular lactate production increases. Together with H^+ lactate can be exported via monocarboxylate transporters, thereby lowering the extracellular pH. Moreover, lactate stabilizes transcription factor HIF1-α, promoting the transcription of glycolytic and inflammatory genes. Increased expression of iNOS and generation of NADPH through the PPP are used to produce ROS and NO. High levels of citrate promote the production of itaconate, which blocks SDH and thereby leads to an accumulation of succinate. This increase of succinate stabilizes HIF1-α through inhibition of PHDs and leads to a reversed electron transport chain, further increasing ROS production. The synthesis of fatty acids is important for the production of prostaglandins[115], whereas acetylation of histones regulates pro-inflammatory gene expression[114]. Furthermore, GLS and *GGH* are upregulated, maintaining the availability of free glutamate, probably to replenish α-KG. Grayed objects represent lower levels compared to unstimulated macrophages. Objects in bold represent enhanced levels compared to unstimulated macrophages. Please see list of abbreviations on page 42 for full names. Figure created with BioRender.com.

On the contrary, anti-inflammatory/M2 polarized macrophages use arginase-1 to metabolize arginine to urea and ornithine, thereby promoting wound healing and cell proliferation[116]. Moreover, OXPHOS, FAO, and glutamine metabolism are upregulated, whereas the PPP is downregulated (see Figure 4)[106]. Glutamine synthetase (GS) seems to play a major role in this metabolic alterations, since it has been shown that GS is increased in M2 macrophages, whereas its inhibition

promotes the M1 phenotype[117]. Our own studies on pro- (LPS + Polyinosinic:polycytidylic acid) or anti-inflammatory (IL-4 + IL-10) stimulated human macrophages confirmed the upregulation of GS through anti-inflammatory cytokines, but moreover, we could show the upregulation of glutaminase (GLS), converting glutamine to glutamate, after pro-inflammatory treatment[118]. Furthermore, we identified another glutamate-related enzyme, gamma-glutamyl hydrolase (GGH), to be connected to the inflammatory status of macrophages. Based on our observations, higher levels of GGH correspond to the pro-inflammatory phenotype, whereas lower levels are related to the anti-inflammatory phenotype. Interestingly, GGH is also involved in folate metabolism and it has been shown that M2 macrophages and TAMs show an increased expression of folate receptor ß, leading to an enhanced folate uptake[119].

It has to be mentioned that species-dependent variations in macrophage phenotypes exist[120] and that most common immunometabolic markers, like iNOS or *Arg1*, are validated only in the murine system. Nevertheless, our understanding of immunometabolism is still growing and there is increasing evidence that polarization of immune cells requires metabolic adaptations.

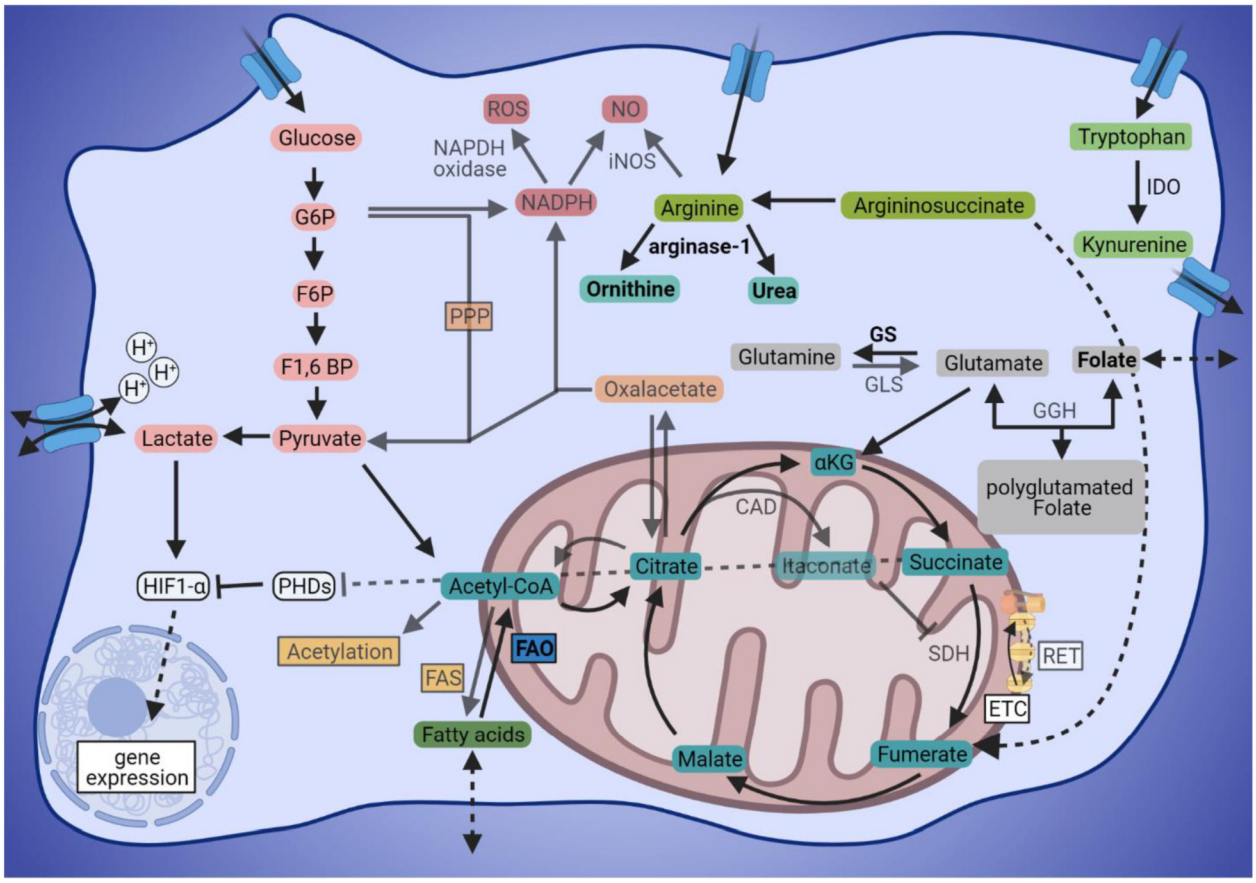

Figure 4: Metabolic adaptations of anti-inflammatory stimulated macrophages. In anti-inflammatory macrophages an intact TCA cycle generates NAD and FAD, which are necessary for ATP production via OXPHOS. PPP metabolism is downregulated, and fatty acids are predominantly oxidized to fuel the TCA cycle. Moreover, the expression of arginase-1 converts arginine into ornithine and urea. Furthermore, higher levels of GS and downregulation of *GLS* promote the availability of glutamine and increase glutamine metabolism. Lower levels of *GGH* probably decrease the availability of free glutamate and support the intracellular retainment of folate, which is further promoted by an increased folate uptake. Grayed objects represent lower levels compared to unstimulated macrophages. Objects in bold represent enhanced levels compared to unstimulated macrophages. Please see list of abbreviations on page 42 for full names. Figure created with BioRender.com.

By manipulating the metabolic pathways described above it should be possible to reprogram macrophages towards a specific phenotype. It has already been demonstrated that reprogramming the glucose metabolism leads to shift in macrophage phenotype[121]. However, the situation is much more complex considering TAMs since these cells are massively influenced by neighboring cells and the conditions in the tumor environment.

1.5 Macrophages in the tumor microenvironment

Signaling molecules produced in tumor environments (e.g., glucose, glutamine, lactate, protons) impact the polarization fate and immunosuppressive functions of TAMs, thus possibly resulting in immune tolerance and treatment resistance in GB (see [122] for a review). The exact mechanisms regulating TAM immunometabolism need further investigations. However, based on current knowledge, TAMs undergo metabolic alterations correlated to the M2 phenotype, but also contain elements of the M1 phenotype (see Figure 5).

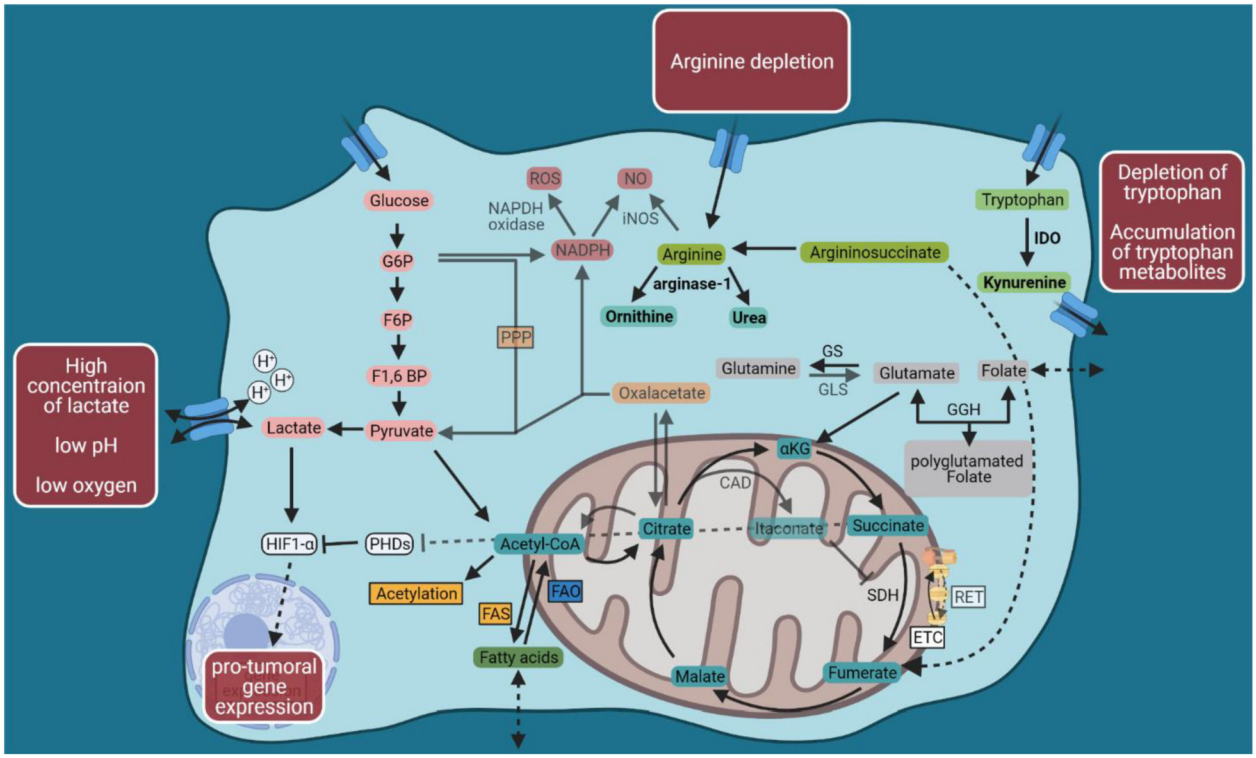

Figure 5: Metabolic adaptations of tumor-associated macrophages in the glioblastoma environment. In the tumor environment, low oxygen concentration and high levels of lactate, accompanied by a low pH, are dominant. Lactate, which is released in high amounts by tumor cells, is also produced by TAMs through glycolysis. The metabolic alterations of TAMs resemble those of macrophages after anti-inflammatory stimulation (see Figure 4) but also show elements of macrophages after pro-inflammatory stimulation (see Figure 3). Especially the intact TCA cycle and the expression of arginase-1 support the anti-inflammatory phenotype accompanied by tumor-supportive gene expression and inhibition of cytotoxic T cells. Moreover, the upregulation of IDO results in the depletion of extracellular tryptophan and the accumulation of tryptophan metabolites (e.g., kynurenine), both shown to inhibit cytotoxic T cells. Grayed objects represent lower levels compared to unstimulated macrophages. Objects in bold represent enhanced levels compared to unstimulated macrophages. Please see list of abbreviations on page 42 for full names. Figure created with BioRender.com.

The conditions macrophages and other tumor infiltrating immune cells have to face are unique for each tumor and by far different from the conditions that can be reconstituted in the laboratory. Nevertheless, researchers were able to identify and characterize some factors influencing the inflammatory phenotype of TAMs: High rates of aerobic glycolysis in tumor cells lead to an increased production of lactate, which can be exported via monocarboxylate transporters and accumulate in the extracellular space[123]. Importantly, high levels of lactate support the immunosuppressive phenotype of TAMs through HIF1-α and the expression of vascular endothelial growth factor and arginase-1[123]. Moreover, the extracellular space is acidified, resulting in pH values of solid cancers ranging from 6.0 to 6.5[124], enhancing the pro-tumoral phenotype of TAMs[125]. As TAMs seem to depend on glycolysis, probably to refill metabolic intermediates and avoid damages induced by ROS, environmental acidification and lactate accumulation are further promoted. Furthermore, especially in brain tumors, an abundancy of glutamate and glutamine is detectable. Glutamate, being released in high amounts by (brain) tumor cells[126–128] promotes tumor growth and correlates negatively with the overall survival[129]. Interestingly, higher levels of glutamine uptake and metabolism have been described[130] in TAMs and it has been shown that depletion of glutamine prevents acquisition of a tumor-supportive phenotype[106].

Of major importance, especially for tumor progression and therapy, is the fact that TAMs also alter the immune functions of other immune cells. The depletion of extracellular arginine through the upregulation of arginase-1 impairs the function of T-cell receptors[131] and the differentiation of T-cells[132]. Furthermore, depletion of tryptophan or accumulation of tryptophan metabolites by indoleamine 2,3-dioxygenase (IDO) inhibit cytotoxic T cells and thereby supports the tumoral immune resistance[133].

1.6 Novel macrophage-based therapeutic strategies

At the beginning of tumor formation, immune cells, including macrophages and T cells, are likely to react to and eliminate the tumor cells. This is successful in most cases, but once a tumor could establish itself it starts to modify the TME which is changing the phenotypes of surrounding immune cells towards a pro-tumoral and immune-suppressive state. As a result, the presence of TAMs in the TME mostly correlates with disease progression and a poor prognosis. Only in colorectal cancer a higher abundance of TAMs is associated with a higher overall survival[134]. These observations are in line with the predominantly tumor-supportive phenotype of TAMs. It has to be mentioned that tumor-supportive TAMs also decrease the efficacy of novel therapeutics like immune checkpoint inhibitors[135]. Besides, macrophages can be involved in tumor generation by promoting a mutagenic environment (through the release of ROS[136]) or by secreting factors important for *de novo* carcinogenesis (e.g., TNF-α[137]).

Since TAM populations are mixed populations containing cells showing pro- or anti-inflammatory phenotypes and it is not yet possible to target them separately, total elimination pf TAMs or blocking TAM recruitment could be possible ways to impede tumor growth. In a murine model genetic ablation of CSF-1 was used to specifically block the attraction of macrophages to the tumor side, leading to a decreased invasiveness and thereby demonstrating the pro-tumoral role of macrophages[138]. The receptor of CSF-1 (CSF-1R) is mostly expressed in monocytes and macrophages[139], enabling a cell type dependent targeting. Hence, small molecules targeting CSF-1R (like BLZ945 or PLX3397) can be used to specifically induce cell death[140] or inhibit chemotactic recruitment[141]. In a phase II study in patients with recurrent glioblastoma, PLX3397 treatment was tolerated, and PLX3397 was able to pass the BBB; nevertheless, PLX3397 treatment did not show improvement in the 6-month progression-free survival when compared with radio- and chemotherapy[142]. Interestingly, using *in silico* modelling it was demonstrated that patients would only benefit from microglia depletion if treatment would be applied at early stages of tumor development[143].

More promising approaches are the targeted reprogramming of macrophages using nanoparticles or viruses shifting the cells towards a tumor-suppressive phenotype[144,145]. These strategies not only combat the tumor-supportive functions of TAMs, but they also stimulate their tumoricidal activities, finally transforming the TME into a pro-inflammatory milieu. Hereby, the anti-tumor activities of other immune cells (e.g., T- or NK cells) are promoted whereas the negative effects of a total macrophage ablation (loss of their supportive and protective functions) are avoided. Interestingly, TAMs express high levels of the immune checkpoint molecules PD-L1, PD-L2 and PD-1[146], the latter one shown to inhibit tumor phagocytosis[147]. Inhibition of PD-1 on TAMs reduces tumor growth and prolongs survival in murine cancer models[147], speaking in favor of combining immune checkpoint therapy with macrophage reprogramming. The fact that macrophages are also able to induce antibody-dependent cellular cytotoxicity[148] points out why more attention should be paid to these cells in (personalized) antibody-based tumor therapies.

2 Present investigations

2.1 Aims

At the present state, glioblastoma treatments can only marginally improve the overall survival of patients, but no therapy leads to a complete cure. The current strategy focuses mostly on targeting the tumor cells, failing to account for other (cellular and non-cellular) constituents of the tumor[149]. Hence, to achieve a complete elimination of tumors, new therapeutic strategies are in great demand. Unfortunately, novel promising approaches like immunotherapy show major limitations: In 2018, only 43.6% of cancer patients were eligible for immunotherapy, and the predicted immunotherapy response rate was 12.46% with significant variability among cancers[150]. It should be noted that response rates strongly vary with patient characteristics and tumor pathology. Especially in the case of Glioblastoma the blood-brain barrier and the immune-suppressive environment represent major limitations for immunotherapeutic approaches. Moreover, the mutational load, a predictive factor for immune checkpoint therapy[151], is low in GB[152]. This low mutual burden also represents an obstacle for the identification and targeting of tumor specific antigens for (personalized) immunotherapy[153]. Fortunately, the identification and targeting of tumor specific antigens is making rapid progress, also due to major technological improvements (next generation sequencing, etc.)[153]. Anyway, there is still no breakthrough in modulating the tumor environment from “cold” (inflammatory inactive) to “hot” (inflammatory active), being mandatory for a successful immunotherapy[154]. Thus, therapeutic strategies inducing an inflammatory shift are needed.

First steps in the development of strategies suitable for the induction of an inflammatory active TME are the identification of possible targets and their validation using *in vitro* and *in vivo* settings. Unfortunately, the acquisition and availability of sample material (e.g., tumor biopsies) or the transferability of animal models to the human system represent major obstacles in biomedical science. The scarcity of primary sample material and primary cells (like macrophages) restricts the number or type of feasible experiments. A possible way to circumvent this issue is the use of less cells/material per experiment. However, the reduction of cell numbers is not as trivial as it

sounds. Besides getting less analyzable cellular material (e.g., DNA or RNA), it has to be demonstrated that a small cell population behaves the same way as a big population does. In **Publication I** *"Assessing the reliability of gene expression measurements in very-low-numbers of human monocyte-derived macrophages"* (see page 48) we focus on this topic and prove that a downscaling of cell numbers for experimental approaches is possible, at least in our setup. This result enabled us to continue working with less cells and thereby to start with the investigation of the influence of metabolism on the inflammatory status of human monocyte-derived macrophages.

In **Publication II** *"Metabolic and inflammatory reprogramming of macrophages by ONC201 translates in a pro-inflammatory environment even in presence of glioblastoma cells"* (see page 62) we evaluated the possibility of manipulating the energy metabolism of macrophages (as regulatory immune cells) to create a pro-inflammatory tumor environment. The idea is that this shift will not only reactivate the tumor-suppressive function of TAMs, but it will also restrict the activity of regulatory T cells and hereby promote the tumoricidal functions of $CD4^+$ and $CD8^+$ T cells. Hence, the induction of an inflammatory active TME represents a promising strategy for glioblastoma therapy and creates the basis for other therapeutic approaches.

We based our experiments on human macrophages derived from monocytes, which were isolated from the blood of healthy donors. By taking advantage of this procedure, we were independent of cellular human material (e.g., biopsies), but still able to conduct our research on primary cells. Moreover, we avoided "impurities" due to the presence of other cell types, like microglia, and were sure about the macrophage origin. These conditions allowed us to analyze specifically the type of cells which would represent the majority of GB infiltrating immune cells. Importantly, the high relevance of macrophages for other diseases and other types of cancer strengthens the point of developing macrophage-based therapies. Besides, the relatively easy accessibility, isolation and differentiation of monocytes (the precursors of macrophages) would allow *ex vivo* manipulations of huge cell numbers followed by non-invasive re-infusion. The high susceptibility of monocytes/macrophages to chemoattractants promotes the infiltration of affected organs/tissues and thereby supports locally targeted therapy.

2.2 Publication I

The publication *"Assessing the reliability of gene expression measurements in very-low-numbers of human monocyte-derived macrophages"*[118] addresses the question of the feasibility to reduce the number of primary macrophages in an experimental setup without affecting the outcome of this experiment (Figure 6).

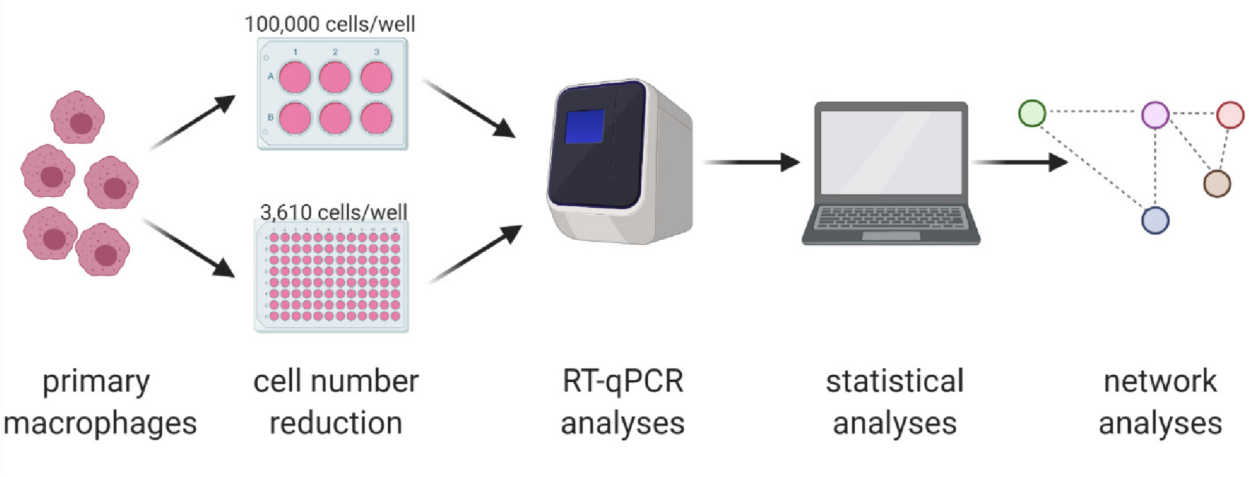

Figure 6: Graphical abstract of *"Assessing the reliability of gene expression measurements in very-low-numbers of human monocyte-derived macrophages"*. Please see text or publication (page 48) for further information. Figure created with BioRender.com.

If possible, the reduction of cellular material would allow an expanded analysis of limited material, like tumor biopsies, which would be beneficial for research, diagnostic and therapy. By stimulating primary macrophages from various donors towards a pro- or anti-inflammatory phenotype and analyzing their gene expression, we created an experimental system that is very prone to changes, and also sensitive enough to detect them. Our experiments revealed that it is possible to reduce the number of macrophages from 100,000 to 3,610 cells without affecting the experimental results. We further suppose that the results of our work can be transferred to other cell types and analyses. The outcome of our work is the basis for researchers, especially when working with limited material, to perform experiments with less cells and thereby increase the number of possible experiments or analyses.

Furthermore, we detected a network of inflammatory genes and identified GGH (an enzyme involved in folate and glutamate metabolism) as a possible regulator of the inflammatory status of macrophages. We hypothesize that GGH influence the phenotype of macrophages through the regulation of intracellular folate and glutamate levels. Indeed, GGH catalyzes the hydrolysis of polyglutamate sidechains from polyglutamylated folate. Thereby it increases the level of free glutamate and decreases the level of folic acid by enabling it to pass the cell membrane, which is not possible for polyglutamylated folate. Interestingly, both metabolites have been shown to be involved in epigenetic modifications of macrophages through DNA methylation (glutamate via α-ketoglutarate)[155–157]. Based on the fact that DNA methylations are important regulators of the inflammatory state of macrophages[158], GGH is probably influencing the phenotype of immune cells via balancing the intracellular levels of folate and glutamate. However, other substrates of GGH probably exist, but further investigations are needed at this point. Since our study is the first showing a connection between the inflammatory state of macrophages and GGH, more research is needed to reveal its way of function and corresponding effects on immune cells.

2.3 Publication II

The work described in *"Metabolic and inflammatory reprogramming of macrophages by ONC201 translates in a pro-inflammatory environment even in presence of glioblastoma cells"*[159] focuses on the immunometabolism of macrophages as a possible lever to activate the pro-inflammatory phenotype of these cells (Figure 7).

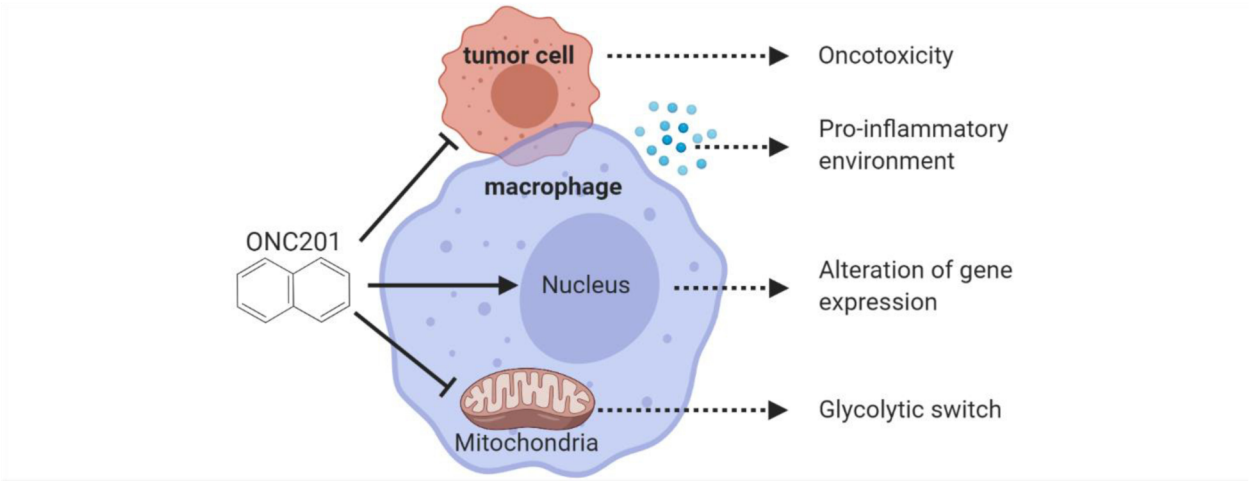

Figure 7: Graphical abstract of "*Metabolic and inflammatory reprogramming of macrophages by ONC201 translates in a pro-inflammatory environment even in presence of glioblastoma cells*". Please see text or publication (page 62) for further information. Figure created with BioRender.com.

Stimulating TAMs through alteration of metabolic pathways could be used to selectively target cells exhibiting a specific metabolic (and thereby inflammatory) phenotype. Finally, this approach would help to overcome glioblastoma induced immune suppression and reinforce immunotherapeutic treatments. The small molecule ONC201, which is capable of passing the blood-brain barrier and is currently under clinical investigation for tumor therapy[160], mediates the disruption of the OXPHOS pathway[161,162] and is therefore a promising candidate for a metabolism-based treatment. In **Publication II** we could demonstrate that macrophages and astrocytes are more resistant towards ONC201-induced cytotoxicity than the three tested glioblastoma cell lines. After treating macrophages, either in mono-cultures or co-cultures with GB cell lines, we performed extracellular flux measurements and could observe a severe loss of macrophage mitochondria integrity, accompanied by a switch of their ATP production from OXPHOS towards glycolysis. Gene and protein analyses revealed a gain in the pro-inflammatory phenotype of macrophages and the generation of a pro-inflammatory environment, even in the presence of glioblastoma cells. These results demonstrate the potential of metabolic manipulations to counteract the immunosuppressive effects of tumor cells and reactivate the tumor-suppressive functions of immune cells.

2.4 Concluding remarks and future perspectives

In **Publication I** we showed that it is possible to reduce the number of cells to a small fraction without losing information or biasing the results of gene expression analysis. As technological improvements will allow us to gather more and more information from low amounts of cellular material, it is essential to prove the reliability of these data. The opportunity to analyze even small cellular fractions with different approaches opens unforeseen scientific and diagnostic possibilities. Since, we were interested in establishing a cost-effective method being applicable in most laboratories equipped with standard devices, we focused our experiments on quantitative PCR. We have verified the usage of small sample sizes only using human monocyte-derived macrophages and reverse transcription quantitative PCR, but we hypothesize that our results are also valid for other species, cell types and types of analyses. Of course, other technologies like single-cell RNA sequencing can be used to analyze even smaller numbers of cells[163]. However, these approaches are much more money-consuming, also face technical limitations (e.g., the lack of detection of some RNAs) and require special devices and skills[164].

Our studies also pointed out GGH as a possible regulator of macrophage immunometabolism. Due to the fact that glutamatergic genes have already been described to be involved in the communication between glioblastoma cells and TAMs[130], manipulating glutamate metabolism to shape immune cell functions could be a promising approach. Supposed that GGH affects the polarization state of macrophages, targeting this enzyme would allow a specific immune cell activation. Our findings regarding the gene expression of glutamatergic genes fit well with other observations, like the identification of the protein-glutamine gamma-glutamyltransferase 2 as a marker for M2 macrophages[120], underlining the impact of glutamate/glutamine metabolism on the inflammatory state of TAMs[106]. Furthermore, the already described upregulation of folate import in anti-inflammatory macrophages and TAMs[119] increases the concentration of intracellular folate and thereby probably restricts GGH activity, underlining the role of GGH in macrophage immunometabolism. Anyway, before testing GGH as a target for tumor therapy, a deeper charac-

terization of this enzyme and its effects on immune cell functions is mandatory. Therefore, experiments analyzing the immune state of macrophages after manipulation of protein expression levels by overexpression or repression of translation are currently performed.

In **Publication II** another way of immunometabolic manipulation of immune cells was investigated. We used the small, blood-brain barrier permeable and oncotoxic molecule ONC201[165] to block the OXPHOS pathway in human monocyte-derived macrophages. By blocking OXPHOS we intended to force the cells towards a glycolytic energy production and thereby promote a pro-inflammatory phenotype. As revealed by our observations, this metabolic switch shifted not only the macrophages, but also their environment towards a pro-inflammatory state. Of special importance is the fact that even the presence of GB cells could not suppress these changes. Moreover, the detected loss of mitochondrial integrity in macrophages, preventing a reprogramming of these cells towards an anti-inflammatory state[166], speaks in favor of a long-lasting pro-inflammatory phenotype. Although we could not detect an increased oncotoxicity based on the metabolic reprogramming of macrophages, this study underlines the promising use of immunometabolic drugs for tumor therapy. It has to be mentioned that due to technical limitations no other immune cells were present in our system. Therefore, one can only speculate about possible ONC201-induced effects on other tumor-associated immune cells: On the one hand, the pro-inflammatory shift of the TME could boost the tumoricidal functions of NK and T cells and therefore be effective for tumor therapy. On the other hand, the presence of Tregs or MDSCs could suppress the immune-stimulatory effect induced by ONC201 and hence limit its efficacy. Anyway, our results speak in favor of testing ONC201 in combinatorial strategies like immune checkpoint therapies. It has been shown that the presence of TAMs and T cells in the TME is needed to unleash the full therapeutic potential of combined immune checkpoint therapies[145], underlining the strong interaction of these cells and clearly speaking against a complete elimination of TAMs.

Another important factor regarding a possible tumor therapy using ONC201 is its efficacy under hypoxia. ONC201 activates the mitochondrial caseinolytic protease P (ClpP), which promotes the degradation of respiratory chain proteins, finally leading to the impairment of oxidative phosphorylation and generation of ROS[161,167]. Our own data (not shown) indicates a reduced oncotoxic

activity of ONC201 under hypoxia (3% O_2), which could probably be explained by a lower generation of ROS under this conditions. Besides, ClpP activation increases the expression of cyclic AMP-dependent transcription factor ATF-4[161], regulating the expression of DNA damage-inducible transcript 3 protein, which is involved in triggering inflammation and apoptosis[168–170]. Our analyses on human macrophages revealed only an induction of inflammation in the examined period of six days, but apoptotic events could happen at a later timepoint. The apoptosis of macrophages could be a control-mechanism to limit inflammation and restore homeostasis. Interestingly, we observed a time-dependent upregulation of *DRD5* (coding for D(1B) dopamine receptor, which is known to inhibit NF-kB activation[171]), which could represent another way to restrict inflammatory events. As a next step to further examine these possible regulatory mechanisms, we are going to study the long-term effects of ONC201 in primary human macrophages. In case the inflammatory response of macrophages induced by ONC201 is tightly controlled, the administration of ONC201 could be used to induce a pro-inflammatory boost in the TME, which is temporally restricted and thereby limits long term side effects. To examine the consequences of this inflammatory boost, *ex vivo* or *in vivo* studies focusing on the interaction of macrophages with other immune cells will be needed.

Anyway, directing macrophages towards a pro- or anti-inflammatory state still represents a promising strategy for tumor therapy or the treatment of autoimmune diseases. Their key roles as regulators of immune cells and linkers between adaptive and innate immune system makes them an undeniable element for therapy and recovery. Cell type specific targeting, which could be achieved using appropriate nanoparticles[172], could be used to directly manipulate macrophages and use the natural regulatory mechanism of the human immune system to exploit its full potential as a therapeutic tool[173]. Especially for non-responders of immune checkpoint therapy this approach could open new perspectives. Nevertheless, possible side and long-term effects caused by the metabolic manipulation of immune cells (e.g., neurological damages induced by uncontrolled inflammation[81]) still need to be examined. In case of unwanted effects, strategies for a temporal, local and controlled inflammation need to be developed. A possible way to counteract overwhelming immune reactions is the administration of immunosuppressive drugs[174].

However, the growing number of clinical trials targeting TAMs[58,96] highlights the potential and the growing interest in novel, immune cell-based therapies and will hopefully allow us one day to understand and unleash the full potential of these cells.

3 References

1. Louis, D. N. *et al.* The 2007 WHO classification of tumours of the central nervous system. *Acta Neuropathol.* **114**, 97–109 (2007) doi: 10.1007/s00401-007-0243-4.

2. Louis, D. N. *et al.* The 2016 World Health Organization Classification of Tumors of the Central Nervous System: a summary. *Acta Neuropathol.* **131**, 803–820 (2016) doi: 10.1007/s00401-016-1545-1.

3. Ostrom, Q. T. *et al.* CBTRUS statistical report: Primary brain and other central nervous system tumors diagnosed in the United States in 2013-2017. *Neuro. Oncol.* **22**, IV1–IV96 (2020) doi: 10.1093/neuonc/noaa200.

4. Bailey, P. & Cushing, H. W. *A Classification of the Tumors of the Glioma Group on a Histo-genetic Basis, with a Correlated Study of Prognosis... With 108 Illustrations*. (JB Lippincott Company, 1926).

5. Bernstein, J. J. & Woodard, C. A. Glioblastoma cells do not intravasate into blood vessels. *Neurosurgery* **36**, 124–132 (1995) doi: 10.1227/00006123-199501000-00016.

6. Robert, M. C. & Wastie, M. E. Glioblastoma multiforme: A rare manifestation of extensive liver and bone metastases. *Biomed. Imaging Interv. J.* **4**, e3 (2008) doi: 10.2349/biij.4.1.e3.

7. Ohgaki, H. & Kleihues, P. Genetic pathways to primary and secondary glioblastoma. *Am. J. Pathol.* **170**, 1445–1453 (2007) doi: 10.2353/ajpath.2007.070011.

8. Ohgaki, H. & Kleihues, P. Population-Based Studies on Incidence, Survival Rates, and Genetic Alterations in Astrocytic and Oligodendroglial Gliomas. *J. Neuropathol. Exp. Neurol.* **64**, 479–489 (2005) doi: 10.1093/jnen/64.6.479.

9. Braganza, M. Z. *et al.* Ionizing radiation and the risk of brain and central nervous system tumors: A systematic review. *Neuro. Oncol.* **14**, 1316–1324 (2012) doi: 10.1093/neuonc/nos208.

10. Malmer, B., Henriksson, R. & Grönberg, H. Familial brain tumours - Genetics or environment? A nationwide cohort study of cancer risk in spouses and first-degree relatives of brain tumour patients. *Int. J. Cancer* **106**, 260–263 (2003) doi: 10.1002/ijc.11213.

11. Amirian, E. S. *et al.* Approaching a scientific consensus on the association between allergies and glioma risk: A report from the glioma international case-control study. *Cancer Epidemiol. Biomarkers Prev.* **25**, 282–290 (2016) doi: 10.1158/1055-9965.EPI-15-0847.

12. Davis, M. E. Glioblastoma: Overview of disease and treatment. *Clin. J. Oncol. Nurs.* **20**, 1–8 (2016) doi: 10.1188/16.CJON.S1.2-8.

13. Gupta, A. & Dwivedi, T. A simplified overview of World Health Organization classification update of central nervous system tumors 2016. *J. Neurosci. Rural Pract.* **8**, 629–641 (2017) doi: 10.4103/jnrp.jnrp_168_17.

14. Hartmann, C. *et al.* Patients with IDH1 wild type anaplastic astrocytomas exhibit worse prognosis

than IDH1-mutated glioblastomas, and IDH1 mutation status accounts for the unfavorable prognostic effect of higher age: Implications for classification of gliomas. *Acta Neuropathol.* **120**, 707–718 (2010) doi: 10.1007/s00401-010-0781-z.

15. Stupp, R. *et al.* Effects of radiotherapy with concomitant and adjuvant temozolomide versus radiotherapy alone on survival in glioblastoma in a randomised phase III study: 5-year analysis of the EORTC-NCIC trial. *Lancet Oncol.* **10**, 459–466 (2009) doi: 10.1016/S1470-2045(09)70025-7.

16. Lakomy, R. *et al.* Real-World Evidence in Glioblastoma: Stupp's Regimen After a Decade. *Front. Oncol.* **10**, 840 (2020) doi: 10.3389/fonc.2020.00840.

17. Lacroix, M. *et al.* A multivariate analysis of 416 patients with glioblastoma multiforme: Prognosis, extent of resection, and survival. *J. Neurosurg.* **95**, 190–198 (2001) doi: 10.3171/jns.2001.95.2.0190.

18. Young, R. M., Jamshidi, A., Davis, G. & Sherman, J. H. Current trends in the surgical management and treatment of adult glioblastoma. *Ann. Transl. Med.* **3**, (2015) doi: 10.3978/j.issn.2305-5839.2015.05.10.

19. Stummer, W. *et al.* Fluorescence-guided surgery with 5-aminolevulinic acid for resection of malignant glioma: a randomised controlled multicentre phase III trial. *Lancet Oncol.* **7**, 392–401 (2006) doi: 10.1016/S1470-2045(06)70665-9.

20. Sherriff, J. *et al.* Patterns of relapse in glioblastoma multiforme following concomitant chemoradiotherapy with temozolomide. *Br. J. Radiol.* **86**, (2013) doi: 10.1259/bjr.20120414.

21. Lee, J. H. *et al.* Human glioblastoma arises from subventricular zone cells with low-level driver mutations. *Nature* **560**, 243–247 (2018) doi: 10.1038/s41586-018-0389-3.

22. Hallaert, G. *et al.* Survival impact of incidental subventricular zone irradiation in IDH-wildtype glioblastoma. *Acta Oncol. (Madr).* (2021) doi: 10.1080/0284186X.2021.1893899.

23. Van Tellingen, O. *et al.* Overcoming the blood-brain tumor barrier for effective glioblastoma treatment. *Drug Resist. Updat.* **19**, 1–12 (2015) doi: 10.1016/j.drup.2015.02.002.

24. Postma, T. J. *et al.* Neurotoxicity of combination chemotherapy with procarbazine, CCNU and vincristine (PCV) for recurrent glioma. *J. Neurooncol.* **38**, 69–75 (1998) doi: 10.1023/A:1005909318270.

25. Diaz, R. J. *et al.* The role of bevacizumab in the treatment of glioblastoma. *J. Neurooncol.* **133**, 455–467 (2017) doi: 10.1007/s11060-017-2477-x.

26. Friedman, H. S. *et al.* Bevacizumab alone and in combination with irinotecan in recurrent glioblastoma. *J. Clin. Oncol.* **27**, 4733–4740 (2009) doi: 10.1200/JCO.2008.19.8721.

27. Kreisl, T. N. *et al.* Phase II trial of single-agent bevacizumab followed by bevacizumab plus irinotecan at tumor progression in recurrent glioblastoma. *J. Clin. Oncol.* **27**, 740–745 (2009) doi: 10.1200/JCO.2008.16.3055.

28. Nduom, E. K., Weller, M. & Heimberger, A. B. Immunosuppressive mechanisms in glioblastoma. *Neuro. Oncol.* **17**, vii9–vii14 (2015) doi: 10.1093/neuonc/nov151.

29. Dunn, G. P., Bruce, A. T., Ikeda, H., Old, L. J. & Schreiber, R. D. Cancer immunoediting: From immunosurveillance to tumor escape. *Nat. Immunol.* **3**, 991–998 (2002) doi: 10.1038/ni1102-991.

30. Ribas, A. & Wolchok, J. D. Cancer immunotherapy using checkpoint blockade. *Science* **359**, 1350–1355 (2018) doi: 10.1126/science.aar4060.

31. Filley, A. C., Henriquez, M. & Dey, M. Recurrent glioma clinical trial, CheckMate-143: The game is not over yet. *Oncotarget* **8**, 91779–91794 (2017) doi: 10.18632/oncotarget.21586.

32. Razavi, S. M. *et al.* Immune Evasion Strategies of Glioblastoma. *Front. Surg.* **3**, 11 (2016) doi: 10.3389/fsurg.2016.00011.

33. Magee, D. E. *et al.* Adverse event profile for immunotherapy agents compared with chemotherapy in solid organ tumors: a systematic review and meta-analysis of randomized clinical trials. *Ann. Oncol.* **31**, 50–60 (2020) doi: 10.1016/j.annonc.2019.10.008.

34. Patel, A. P. *et al.* Single-cell RNA-seq highlights intratumoral heterogeneity in primary glioblastoma. *Science* **344**, 1396–1401 (2014) doi: 10.1126/science.1254257.

35. Bonavia, R., Inda, M. D. M., Cavenee, W. K. & Furnari, F. B. Heterogeneity maintenance in glioblastoma: A social network. *Cancer Res.* **71**, 4055–4060 (2011) doi: 10.1158/0008-5472.CAN-11-0153.

36. Soeda, A. *et al.* The evidence of glioblastoma heterogeneity. *Sci. Rep.* **5**, 7979 (2015) doi: 10.1038/srep07979.

37. Quail, D. F. & Joyce, J. A. Microenvironmental regulation of tumor progression and metastasis. *Nat. Med.* **19**, 1423–1437 (2013) doi: 10.1038/nm.3394.

38. Bussard, K. M., Mutkus, L., Stumpf, K., Gomez-Manzano, C. & Marini, F. C. Tumor-associated stromal cells as key contributors to the tumor microenvironment. *Breast Cancer Res.* **18**, 84 (2016) doi: 10.1186/s13058-016-0740-2.

39. Tamura, R. *et al.* Difference in Immunosuppressive Cells Between Peritumoral Area and Tumor Core in Glioblastoma. *World Neurosurg.* **120**, e601–e610 (2018) doi: 10.1016/j.wneu.2018.08.133.

40. Franceschi, E. *et al.* Treatment options for recurrent glioblastoma: Pitfalls and future trends. *Expert Rev. Anticancer Ther.* **9**, 613–619 (2009) doi: 10.1586/ERA.09.23.

41. McLendon, R. *et al.* Comprehensive genomic characterization defines human glioblastoma genes and core pathways. *Nature* **455**, 1061–1068 (2008) doi: 10.1038/nature07385.

42. Verhaak, R. G. W. *et al.* Integrated Genomic Analysis Identifies Clinically Relevant Subtypes of Glioblastoma Characterized by Abnormalities in PDGFRA, IDH1, EGFR, and NF1. *Cancer Cell* **17**, 98–110 (2010) doi: 10.1016/j.ccr.2009.12.020.

43. Phillips, H. S. *et al.* Molecular subclasses of high-grade glioma predict prognosis, delineate a pattern of disease progression, and resemble stages in neurogenesis. *Cancer Cell* **9**, 157–173 (2006) doi: 10.1016/j.ccr.2006.02.019.

44. Huse, J. T., Phillips, H. S. & Brennan, C. W. Molecular subclassification of diffuse gliomas: Seeing order in the chaos. *Glia* **59**, 1190–1199 (2011) doi: 10.1002/glia.21165.

45. Wang, Q. *et al.* Tumor Evolution of Glioma-Intrinsic Gene Expression Subtypes Associates with Immunological Changes in the Microenvironment. *Cancer Cell* **32**, 42-56.e6 (2017) doi: 10.1016/j.ccell.2017.06.003.

46. Venkatesh, H. S. *et al.* Neuronal activity promotes glioma growth through neuroligin-3 secretion. *Cell* **161**, 803–816 (2015) doi: 10.1016/j.cell.2015.04.012.

47. Hambardzumyan, D., Gutmann, D. H. & Kettenmann, H. The role of microglia and macrophages in glioma maintenance and progression. *Nat. Neurosci.* **19**, 20–27 (2016) doi: 10.1038/nn.4185.

48. Chang, A. L. *et al.* CCL2 Produced by the Glioma Microenvironment Is Essential for the Recruitment of Regulatory T Cells and Myeloid-Derived Suppressor Cells. *Cancer Res.* **76**, 5671–5682 (2016) doi: 10.1158/0008-5472.CAN-16-0144.

49. Jordan, J. T. *et al.* Preferential migration of regulatory T cells mediated by glioma-secreted chemokines can be blocked with chemotherapy. *Cancer Immunol. Immunother.* **57**, 123–131 (2008) doi: 10.1007/s00262-007-0336-x.

50. Elliott, L. H., Brooks, W. H. & Roszman, T. L. Activation of immunoregulatory lymphocytes obtained from patients with malignant gliomas. *J. Neurosurg.* **67**, 231–236 (1987) doi: 10.3171/jns.1987.67.2.0231.

51. Humphries, W., Wei, J., Sampson, J. H. & Heimberger, A. B. The Role of Tregs in Glioma-Mediated Immunosuppression: Potential Target for Intervention. *Neurosurg. Clin. N. Am.* **21**, 125–137 (2010) doi: 10.1016/j.nec.2009.08.012.

52. Raychaudhuri, B. *et al.* Myeloid derived suppressor cell infiltration of murine and human gliomas is associated with reduction of tumor infiltrating lymphocytes. *J. Neurooncol.* **122**, 293–301 (2015) doi: 10.1007/s11060-015-1720-6.

53. Wang, S. C., Hong, J. H., Hsueh, C. & Chiang, C. S. Tumor-secreted SDF-1 promotes glioma invasiveness and TAM tropism toward hypoxia in a murine astrocytoma model. *Lab. Investig.* **92**, 151–162 (2012) doi: 10.1038/labinvest.2011.128.

54. De, I. *et al.* CSF1 overexpression promotes high-grade glioma formation without impacting the polarization status of glioma-associated microglia and macrophages. *Cancer Res.* **76**, 2552–2560 (2016) doi: 10.1158/0008-5472.CAN-15-2386.

55. Lewis, C. E. & Pollard, J. W. Distinct role of macrophages in different tumor microenvironments. *Cancer Res.* **66**, 605–612 (2006) doi: 10.1158/0008-5472.CAN-05-4005.

56. Yoshimura, A. & Muto, G. TGF-β Function in Immune Suppression. in *Current topics in microbiology and immunology* vol. 350 127–147 (Curr Top Microbiol Immunol, 2010). doi: 10.1007/82_2010_87.

57. DeCordova, S. *et al.* Molecular Heterogeneity and Immunosuppressive Microenvironment in Glioblastoma. *Front. Immunol.* **11**, 1402 (2020) doi: 10.3389/fimmu.2020.01402.

58. Grégoire, H. *et al.* Targeting Tumor Associated Macrophages to Overcome Conventional Treatment Resistance in Glioblastoma. *Front. Pharmacol.* **11**, 368 (2020) doi: 10.3389/fphar.2020.00368.

59. Bonapace, L. *et al.* Cessation of CCL2 inhibition accelerates breast cancer metastasis by promoting angiogenesis. *Nature* **515**, 130–133 (2014) doi: 10.1038/nature13862.

60. Simons, M., Gordon, E. & Claesson-Welsh, L. Mechanisms and regulation of endothelial VEGF receptor signalling. *Nat. Rev. Mol. Cell Biol.* **17**, 611–625 (2016) doi: 10.1038/nrm.2016.87.

61. Grimshaw, M. J. & Balkwill, F. R. Inhibition of monocyte and macrophage chemotaxis by hypoxia and inflammation - a potential mechanism. *Eur. J. Immunol.* **31**, 480–489 (2001) doi: 10.1002/1521-4141(200102)31:2<480::AID-IMMU480>3.0.CO;2-L.

62. Raggi, F. *et al.* Regulation of human Macrophage M1-M2 Polarization Balance by hypoxia and the Triggering receptor expressed on Myeloid cells-1. *Front. Immunol.* **8**, 1097 (2017) doi: 10.3389/fimmu.2017.01097.

63. Robey, I. F., Lien, A. D., Welsh, S. J., Baggett, B. K. & Gillies, R. J. Hypoxia-inducible factor-1α and the glycolytic phenotype in tumors. *Neoplasia* **7**, 324–330 (2005) doi: 10.1593/neo.04430.

64. Swietach, P., Vaughan-Jones, R. D., Harris, A. L. & Hulikova, A. The chemistry, physiology and pathology of pH in cancer. *Philos. Trans. R. Soc. B Biol. Sci.* **369**, 20130099 (2014) doi: 10.1098/rstb.2013.0099.

65. Halestrap, A. P. & Price, N. T. The proton-linked monocarboxylate transporter (MCT) family: Structure, function and regulation. *Biochem. J.* **343**, 281–299 (1999) doi: 10.1042/0264-6021:3430281.

66. Quail, D. F. & Joyce, J. A. The Microenvironmental Landscape of Brain Tumors. *Cancer Cell* **31**, 326–341 (2017) doi: 10.1016/j.ccell.2017.02.009.

67. Strepkos, D., Markouli, M., Klonou, A., Piperi, C. & Papavassiliou, A. G. Insights in the immunobiology of glioblastoma. *J. Mol. Med.* **98**, 1–10 (2020) doi: 10.1007/s00109-019-01835-4.

68. Davies, L. C., Jenkins, S. J., Allen, J. E. & Taylor, P. R. Tissue-resident macrophages. *Nat. Immunol.* **14**, 986–995 (2013) doi: 10.1038/ni.2705.

69. Ginhoux, F. *et al.* Fate mapping analysis reveals that adult microglia derive from primitive macrophages. *Science* **330**, 841–845 (2010) doi: 10.1126/science.1194637.

70. Perdiguero, E. G. & Geissmann, F. The development and maintenance of resident macrophages. *Nat. Immunol.* **17**, 2–8 (2016) doi: 10.1038/ni.3341.

71. Shi, C. & Pamer, E. G. Monocyte recruitment during infection and inflammation. *Nat. Rev. Immunol.* **11**, 762–774 (2011) doi: 10.1038/nri3070.

72. Hugh Perry, V. A revised view of the central nervous system microenvironment and major histocompatibility complex class II antigen presentation. *J. Neuroimmunol.* **90**, 113–121 (1998) doi: 10.1016/S0165-5728(98)00145-3.

73. Lanz, T. V. *et al.* Protein kinase Cβ as a therapeutic target stabilizing blood-brain barrier disruption in experimental autoimmune encephalomyelitis. *Proc. Natl. Acad. Sci. U. S. A.* **110**, 14735–14740 (2013) doi: 10.1073/pnas.1302569110.

74. Badie, B. & Schartner, J. M. Flow Cytometric Characterization of Tumor-associated Macrophages in Experimental Gliomas. *Neurosurgery* **46**, 957–962 (2000) doi: 10.1097/00006123-200004000-00035.

75. Lin, J. Da *et al.* Single-cell analysis of fate-mapped macrophages reveals heterogeneity, including stem-like properties, during atherosclerosis progression and regression. *JCI insight* **4**, e124574 (2019) doi: 10.1172/jci.insight.124574.

76. Chen, Z. *et al.* Cellular and molecular identity of tumor-associated macrophages in glioblastoma. *Cancer Res.* **77**, 2266–2278 (2017) doi: 10.1158/0008-5472.CAN-16-2310.

77. Brandenburg, S., Blank, A., Bungert, A. D. & Vajkoczy, P. Distinction of microglia and macrophages in glioblastoma: Close relatives, different tasks? *Int. J. Mol. Sci.* **22**, 194 (2021) doi: 10.3390/ijms22010194.

78. Yin, J., Valin, K. L., Dixon, M. L. & Leavenworth, J. W. The Role of Microglia and Macrophages in CNS Homeostasis, Autoimmunity, and Cancer. *J. Immunol. Res.* **2017**, 5150678 (2017) doi: 10.1155/2017/5150678.

79. Locati, M., Curtale, G. & Mantovani, A. Diversity, Mechanisms, and Significance of Macrophage Plasticity. *Annu. Rev. Pathol. Mech. Dis.* **15**, 123–147 (2020) doi: 10.1146/annurev-pathmechdis-012418-012718.

80. Biswas, S. K. *et al.* A distinct and unique transcriptional program expressed by tumor-associated macrophages (defective NF-κB and enhanced IRF-3/STAT1 activation). *Blood* **107**, 2112–2122 (2006) doi: 10.1182/blood-2005-01-0428.

81. Wynn, T. A., Chawla, A. & Pollard, J. W. Macrophage biology in development, homeostasis and disease. *Nature* **496**, 445–455 (2013) doi: 10.1038/nature12034.

82. Qian, B. Z. & Pollard, J. W. Macrophage Diversity Enhances Tumor Progression and Metastasis. *Cell* **141**, 39–51 (2010) doi: 10.1016/j.cell.2010.03.014.

83. Charles, N. A., Holland, E. C., Gilbertson, R., Glass, R. & Kettenmann, H. The brain tumor microenvironment. *Glia* **59**, 1169–1180 (2011) doi: 10.1002/glia.21136.

84. Bettinger, I., Thanos, S. & Paulus, W. Microglia promote glioma migration. *Acta Neuropathol.* **103**,

351–355 (2002) doi: 10.1007/s00401-001-0472-x.

85. Markovic, D. S., Glass, R., Synowitz, M., Rooijen, N. van & Kettenmann, H. Microglia Stimulate the Invasiveness of Glioma Cells by Increasing the Activity of Metalloprotease-2. *J. Neuropathol. Exp. Neurol.* **64**, 754–762 (2005) doi: 10.1097/01.jnen.0000178445.33972.a9.

86. Caponegro, M. D., Moffitt, R. A. & Tsirka, S. E. Expression of neuropilin-1 is linked to glioma associated microglia and macrophages and correlates with unfavorable prognosis in high grade gliomas. *Oncotarget* **9**, 35655–35665 (2018) doi: 10.18632/oncotarget.26273.

87. Sørensen, M. D., Dahlrot, R. H., Boldt, H. B., Hansen, S. & Kristensen, B. W. Tumour-associated microglia/macrophages predict poor prognosis in high-grade gliomas and correlate with an aggressive tumour subtype. *Neuropathol. Appl. Neurobiol.* **44**, 185–206 (2018) doi: 10.1111/nan.12428.

88. Takenaka, M. C. *et al.* Control of tumor-associated macrophages and T cells in glioblastoma via AHR and CD39. *Nat. Neurosci.* **22**, 729–740 (2019) doi: 10.1038/s41593-019-0370-y.

89. Wei, J. *et al.* Osteopontin mediates glioblastoma-associated macrophage infiltration and is a potential therapeutic target. *J. Clin. Invest.* **129**, 137–149 (2019) doi: 10.1172/JCI121266.

90. Ubil, E. *et al.* Tumor-secreted Pros1 inhibits macrophage M1 polarization to reduce antitumor immune response. *J. Clin. Invest.* **128**, 2356–2369 (2018) doi: 10.1172/JCI97354.

91. Kees, T. *et al.* Microglia isolated from patients with glioma gain antitumor activities on poly (I:C) stimulation. *Neuro. Oncol.* **14**, 64–78 (2012) doi: 10.1093/neuonc/nor182.

92. Liu, M. *et al.* Metabolic rewiring of macrophages by CpG potentiates clearance of cancer cells and overcomes tumor-expressed CD47−mediated 'don't-eat-me' signal. *Nat. Immunol.* **20**, 265–275 (2019) doi: 10.1038/s41590-018-0292-y.

93. Guerriero, J. L. *et al.* Class IIa HDAC inhibition reduces breast tumours and metastases through anti-tumour macrophages. *Nature* **543**, 428–432 (2017) doi: 10.1038/nature21409.

94. Huang, Y. K. *et al.* Macrophage spatial heterogeneity in gastric cancer defined by multiplex immunohistochemistry. *Nat. Commun.* **10**, 3928 (2019) doi: 10.1038/s41467-019-11788-4.

95. Müller, S. *et al.* Single-cell profiling of human gliomas reveals macrophage ontogeny as a basis for regional differences in macrophage activation in the tumor microenvironment. *Genome Biol.* **18**, 234 (2017) doi: 10.1186/s13059-017-1362-4.

96. Pires-Afonso, Y., Niclou, S. P. & Michelucci, A. Revealing and harnessing tumour-associated microglia/macrophage heterogeneity in glioblastoma. *Int. J. Mol. Sci.* **21**, 689 (2020) doi: 10.3390/ijms21030689.

97. Caponegro, M. D. *et al.* A distinct microglial subset at the <scp>tumor–stroma</scp> interface of glioma. *Glia* glia.23991 (2021) doi: 10.1002/glia.23991.

98. Zhou, W. *et al.* Periostin secreted by glioblastoma stem cells recruits M2 tumour-associated

macrophages and promotes malignant growth. *Nat. Cell Biol.* **17**, 170–182 (2015) doi: 10.1038/ncb3090.

99. Hudson, A. L. *et al.* Glioblastoma recurrence correlates with increased APE1 and polarization toward an immuno-suppressive microenvironment. *Front. Oncol.* **8**, 314 (2018) doi: 10.3389/fonc.2018.00314.

100. Leblond, M. M. *et al.* M2 macrophages are more resistant than M1 macrophages following radiation therapy in the context of glioblastoma. *Oncotarget* **8**, 72597–72612 (2017) doi: 10.18632/oncotarget.19994.

101. Gupta, K. & Burns, T. C. Radiation-induced alterations in the recurrent glioblastoma microenvironment: Therapeutic implications. *Front. Oncol.* **8**, 503 (2018) doi: 10.3389/fonc.2018.00503.

102. Warburg, O. The metabolism of carcinoma cells 1. *J. Cancer Res.* **9**, 148–163 (1925) doi: 10.1158/jcr.1925.148.

103. Hanahan, D. & Weinberg, R. A. Hallmarks of cancer: The next generation. *Cell* **144**, 646–674 (2011) doi: 10.1016/j.cell.2011.02.013.

104. Heiden, M. G. V., Cantley, L. C. & Thompson, C. B. Understanding the warburg effect: The metabolic requirements of cell proliferation. *Science* **324**, 1029–1033 (2009) doi: 10.1126/science.1160809.

105. Hard, G. C. Some biochemical aspects of the immune macrophage. *Br. J. Exp. Pathol.* **51**, 97–105 (1970).

106. Jha, A. K. *et al.* Network integration of parallel metabolic and transcriptional data reveals metabolic modules that regulate macrophage polarization. *Immunity* **42**, 419–430 (2015) doi: 10.1016/j.immuni.2015.02.005.

107. Selak, M. A. *et al.* Succinate links TCA cycle dysfunction to oncogenesis by inhibiting HIF-α prolyl hydroxylase. *Cancer Cell* **7**, 77–85 (2005) doi: 10.1016/j.ccr.2004.11.022.

108. Bruick, R. K. & McKnight, S. L. A conserved family of prolyl-4-hydroxylases that modify HIF. *Science* **294**, 1337–1340 (2001) doi: 10.1126/science.1066373.

109. Tannahill, G. M. *et al.* Succinate is an inflammatory signal that induces IL-1β through HIF-1α. *Nature* **496**, 238–242 (2013) doi: 10.1038/nature11986.

110. Wang, T. *et al.* HIF1 α -Induced Glycolysis Metabolism Is Essential to the Activation of Inflammatory Macrophages. *Mediators Inflamm.* **2017**, 9029327 (2017) doi: 10.1155/2017/9029327.

111. Mills, E. L. *et al.* Succinate Dehydrogenase Supports Metabolic Repurposing of Mitochondria to Drive Inflammatory Macrophages. *Cell* **167**, 457-470.e13 (2016) doi: 10.1016/j.cell.2016.08.064.

112. Bogdan, C. Nitric oxide and the immune response. *Nat. Immunol.* **2**, 907–916 (2001) doi: 10.1038/ni1001-907.

113. Feingold, K. R. *et al.* Mechanisms of triglyceride accumulation in activated macrophages. *J. Leukoc. Biol.* **92**, 829–839 (2012) doi: 10.1189/jlb.1111537.

114. Lauterbach, M. A. *et al.* Toll-like Receptor Signaling Rewires Macrophage Metabolism and Promotes Histone Acetylation via ATP-Citrate Lyase. *Immunity* **51**, 997-1011.e7 (2019) doi: 10.1016/j.immuni.2019.11.009.

115. Infantino, V., Iacobazzi, V., Palmieri, F. & Menga, A. ATP-citrate lyase is essential for macrophage inflammatory response. *Biochem. Biophys. Res. Commun.* **440**, 105–111 (2013) doi: 10.1016/j.bbrc.2013.09.037.

116. Bronte, V. & Zanovello, P. Regulation of immune responses by L-arginine metabolism. *Nat. Rev. Immunol.* **5**, 641–654 (2005) doi: 10.1038/nri1668.

117. Palmieri, E. M. *et al.* Pharmacologic or Genetic Targeting of Glutamine Synthetase Skews Macrophages toward an M1-like Phenotype and Inhibits Tumor Metastasis. *Cell Rep.* **20**, 1654–1666 (2017) doi: 10.1016/j.celrep.2017.07.054.

118. Geiß, C., Alanis-Lobato, G., Andrade-Navarro, M. & Régnier-Vigouroux, A. Assessing the reliability of gene expression measurements in very-low-numbers of human monocyte-derived macrophages. *Sci. Rep.* **9**, 17908 (2019) doi: 10.1038/s41598-019-54500-8.

119. Puig-Kröger, A. *et al.* Folate receptor β is expressed by tumor-associated macrophages and constitutes a marker for M2 anti-inflammatory/regulatory Macrophages. *Cancer Res.* **69**, 9395–9403 (2009) doi: 10.1158/0008-5472.CAN-09-2050.

120. Martinez, F. O. *et al.* Genetic programs expressed in resting and IL-4 alternatively activated mouse and human macrophages: similarities and differences. *Blood* **121**, e57–e69 (2013) doi: 10.1182/blood-2012-06-436212.

121. Haschemi, A. *et al.* The Sedoheptulose Kinase CARKL Directs Macrophage Polarization through Control of Glucose Metabolism. *Cell Metab.* **15**, 813–826 (2012) doi: 10.1016/j.cmet.2012.04.023.

122. Chen, D., Zhang, X., Li, Z. & Zhu, B. Metabolic regulatory crosstalk between tumor microenvironment and tumor-associated macrophages. *Theranostics* **11**, 1016–1030 (2020) doi: 10.7150/THNO.51777.

123. Colegio, O. R. *et al.* Functional polarization of tumour-associated macrophages by tumour-derived lactic acid. *Nature* **513**, 559–563 (2014) doi: 10.1038/nature13490.

124. Webb, B. A., Chimenti, M., Jacobson, M. P. & Barber, D. L. Dysregulated pH: A perfect storm for cancer progression. *Nat. Rev. Cancer* **11**, 671–677 (2011) doi: 10.1038/nrc3110.

125. Bohn, T. *et al.* Tumor immunoevasion via acidosis-dependent induction of regulatory tumor-associated macrophages. *Nat. Immunol.* **19**, 1319–1329 (2018) doi: 10.1038/s41590-018-0226-8.

126. Ye, Z. C. & Sontheimer, H. Glioma cells release excitotoxic concentrations of glutamate. *Cancer Res.* **59**, 4383–4391 (1999).

127. de Groot, J. & Sontheimer, H. Glutamate and the biology of gliomas. *Glia* **59**, 1181–1189 (2011) doi: 10.1002/glia.21113.

128. Seidlitz, E. P., Sharma, M. K., Saikali, Z., Ghert, M. & Singh, G. Cancer cell lines release glutamate into the extracellular environment. *Clin. Exp. Metastasis* **26**, 781–787 (2009) doi: 10.1007/s10585-009-9277-4.

129. Takano, T. *et al.* Glutamate release promotes growth of malignant gliomas. *Nat. Med.* **7**, 1010–1015 (2001) doi: 10.1038/nm0901-1010.

130. Choi, J., Stradmann-Bellinghausen, B., Yakubov, E., Savaskan, N. E. & Regnier-Vigouroux, A. Glioblastoma cells induce differential glutamatergic gene expressions in human tumor-associated microglia/macrophages and monocyte-derived macrophages. *Cancer Biol. Ther.* **16**, 1205–1213 (2015) doi: 10.1080/15384047.2015.1056406.

131. Rath, M., Müller, I., Kropf, P., Closs, E. I. & Munder, M. Metabolism via arginase or nitric oxide synthase: Two competing arginine pathways in macrophages. *Front. Immunol.* **5**, 532 (2014) doi: 10.3389/fimmu.2014.00532.

132. Geiger, R. *et al.* L-Arginine Modulates T Cell Metabolism and Enhances Survival and Anti-tumor Activity. *Cell* **167**, 829-842.e13 (2016) doi: 10.1016/j.cell.2016.09.031.

133. Munn, D. H. & Mellor, A. L. Indoleamine 2,3 dioxygenase and metabolic control of immune responses. *Trends Immunol.* **34**, 137–143 (2013) doi: 10.1016/j.it.2012.10.001.

134. Zhang, Q. wen *et al.* Prognostic Significance of Tumor-Associated Macrophages in Solid Tumor: A Meta-Analysis of the Literature. *PLoS One* **7**, e50946 (2012) doi: 10.1371/journal.pone.0050946.

135. Cassetta, L. & Kitamura, T. Targeting tumor-associated macrophages as a potential strategy to enhance the response to immune checkpoint inhibitors. *Front. Cell Dev. Biol.* **6**, 38 (2018) doi: 10.3389/fcell.2018.00038.

136. Canli, Ö. *et al.* Myeloid Cell-Derived Reactive Oxygen Species Induce Epithelial Mutagenesis. *Cancer Cell* **32**, 869-883.e5 (2017) doi: 10.1016/j.ccell.2017.11.004.

137. Moore, R. J. *et al.* Mice deficient in tumor necrosis factor-α are resistant to skin carcinogenesis. *Nat. Med.* **5**, 828–831 (1999) doi: 10.1038/10552.

138. Lin, E. Y., Nguyen, A. V., Russell, R. G. & Pollard, J. W. Colony-stimulating factor 1 promotes progression of mammary tumors to malignancy. *J. Exp. Med.* **193**, 727–739 (2001) doi: 10.1084/jem.193.6.727.

139. Stanley, E. R. & Chitu, V. CSF-1 receptor signaling in myeloid cells. *Cold Spring Harb. Perspect. Biol.* **6**, a021857 (2014) doi: 10.1101/cshperspect.a021857.

140. Pyonteck, S. M. *et al.* CSF-1R inhibition alters macrophage polarization and blocks glioma progression. *Nat. Med.* **19**, 1264–1272 (2013) doi: 10.1038/nm.3337.

141. Coniglio, S. J. *et al.* Microglial stimulation of glioblastoma invasion involves epidermal growth factor

receptor (EGFR) and colony stimulating factor 1 receptor (CSF-1R) signaling. *Mol. Med.* **18**, 519–527 (2012) doi: 10.2119/molmed.2011.00217.

142. Butowski, N. *et al.* Orally administered colony stimulating factor 1 receptor inhibitor PLX3397 in recurrent glioblastoma: An Ivy Foundation Early Phase Clinical Trials Consortium phase II study. *Neuro. Oncol.* **18**, 557–564 (2016) doi: 10.1093/neuonc/nov245.

143. Wu, Y., Lu, Y., Chen, W., Fu, J. & Fan, R. In silico experimentation of glioma microenvironment development and anti-tumor therapy. *PLoS Comput. Biol.* **8**, e1002355 (2012) doi: 10.1371/journal.pcbi.1002355.

144. Wang, Y. *et al.* Polymeric nanoparticles enable reversing macrophage in tumor microenvironment for immunotherapy. *Biomaterials* **112**, 153–163 (2017) doi: 10.1016/j.biomaterials.2016.09.034.

145. Saha, D., Martuza, R. L. & Rabkin, S. D. Macrophage Polarization Contributes to Glioblastoma Eradication by Combination Immunovirotherapy and Immune Checkpoint Blockade. *Cancer Cell* **32**, 253-267.e5 (2017) doi: 10.1016/j.ccell.2017.07.006.

146. Xiang, X., Wang, J., Lu, D. & Xu, X. Targeting tumor-associated macrophages to synergize tumor immunotherapy. *Signal Transduct. Target. Ther.* **6**, 75 (2021) doi: 10.1038/s41392-021-00484-9.

147. Gordon, S. R. *et al.* PD-1 expression by tumour-associated macrophages inhibits phagocytosis and tumour immunity. *Nature* **545**, 495–499 (2017) doi: 10.1038/nature22396.

148. Johnson, W. J., Bolognesi, D. P. & Adams, D. O. Antibody-dependent cytolysis (ADCC) of tumor cells by activated murine macrophages is a two-step process: Quantification of target binding and subsequent target lysis. *Cell. Immunol.* **83**, 170–180 (1984) doi: 10.1016/0008-8749(84)90236-3.

149. Le Rhun, E. *et al.* Molecular targeted therapy of glioblastoma. *Cancer Treat. Rev.* **80**, 101896 (2019) doi: 10.1016/j.ctrv.2019.101896.

150. Haslam, A. & Prasad, V. Estimation of the Percentage of US Patients With Cancer Who Are Eligible for and Respond to Checkpoint Inhibitor Immunotherapy Drugs. *JAMA Netw. open* **2**, e192535 (2019) doi: 10.1001/jamanetworkopen.2019.2535.

151. Rizvi, N. A. *et al.* Mutational landscape determines sensitivity to PD-1 blockade in non–small cell lung cancer. *Science* **348**, 124–128 (2015) doi: 10.1126/science.aaa1348.

152. Alexandrov, L. B. *et al.* Signatures of mutational processes in human cancer. *Nature* **500**, 415–421 (2013) doi: 10.1038/nature12477.

153. Nejo, T., Yamamichi, A., Almeida, N. D., Goretsky, Y. E. & Okada, H. Tumor antigens in glioma. *Semin. Immunol.* **47**, 101385 (2020) doi: 10.1016/j.smim.2020.101385.

154. Trinchieri, G. Cancer Immunity: Lessons from Infectious Diseases. *J. Infect. Dis.* **212**, S67–S73 (2015) doi: 10.1093/infdis/jiv070.

155. Kawakami, K. *et al.* Low expression of γ-glutamyl hydrolase mRNA in primary colorectal cancer with the CpG island methylator phenotype. *Br. J. Cancer* **98**, 1555–1561 (2008) doi:

10.1038/sj.bjc.6604346.

156. Kim, S. E. *et al.* γ-Glutamyl hydrolase modulation significantly influences global and gene-specific DNA methylation and gene expression in human colon and breast cancer cells. *Genes Nutr.* **10**, 1–17 (2015) doi: 10.1007/s12263-014-0444-0.

157. Liu, P. S. *et al.* α-ketoglutarate orchestrates macrophage activation through metabolic and epigenetic reprogramming. *Nat. Immunol.* **18**, 985–994 (2017) doi: 10.1038/ni.3796.

158. Kapellos, T. S. & Iqbal, A. J. Epigenetic control of macrophage polarisation and soluble mediator gene expression during inflammation. *Mediators Inflamm.* **2016**, (2016) doi: 10.1155/2016/6591703.

159. Geiß, C., Witzler, C., Poschet, G., Ruf, W. & Régnier-Vigouroux, A. Metabolic and inflammatory reprogramming of macrophages by ONC201 translates in a pro-inflammatory environment even in presence of glioblastoma cells. *Eur. J. Immunol.* (2021) doi: 10.1002/eji.202048957.

160. Ralff, M. D., Lulla, A. R., Wagner, J. & El-Deiry, W. S. ONC201: A new treatment option being tested clinically for recurrent glioblastoma. *Transl. Cancer Res.* **6**, S1239–S1243 (2017) doi: 10.21037/tcr.2017.10.03.

161. Ishizawa, J. *et al.* Mitochondrial ClpP-Mediated Proteolysis Induces Selective Cancer Cell Lethality. *Cancer Cell* **35**, 721-737.e9 (2019) doi: 10.1016/j.ccell.2019.03.014.

162. Greer, Y. E. *et al.* ONC201 kills breast cancer cells in vitro by targeting mitochondria. *Oncotarget* **9**, 18454–18479 (2018) doi: 10.18632/oncotarget.24862.

163. Haque, A., Engel, J., Teichmann, S. A. & Lönnberg, T. A practical guide to single-cell RNA-sequencing for biomedical research and clinical applications. *Genome Med.* **9**, 75 (2017) doi: 10.1186/s13073-017-0467-4.

164. Hwang, B., Lee, J. H. & Bang, D. Single-cell RNA sequencing technologies and bioinformatics pipelines. *Exp. Mol. Med.* **50**, 1–14 (2018) doi: 10.1038/s12276-018-0071-8.

165. Ishida, C. T. *et al.* Metabolic reprogramming by dual AKT/ERK inhibition through imipridones elicits unique vulnerabilities in glioblastoma. *Clin. Cancer Res.* **24**, 5392–5406 (2018) doi: 10.1158/1078-0432.CCR-18-1040.

166. Van den Bossche, J. *et al.* Mitochondrial Dysfunction Prevents Repolarization of Inflammatory Macrophages. *Cell Rep.* **17**, 684–696 (2016) doi: 10.1016/j.celrep.2016.09.008.

167. Nouri, K., Feng, Y. & Schimmer, A. D. Mitochondrial ClpP serine protease-biological function and emerging target for cancer therapy. *Cell Death Dis.* **11**, 1–12 (2020) doi: 10.1038/s41419-020-03062-z.

168. Oyadomari, S. & Mori, M. Roles of CHOP/GADD153 in endoplasmic reticulum stress. *Cell Death Differ.* **11**, 381–389 (2004) doi: 10.1038/sj.cdd.4401373.

169. Goodall, J. C. *et al.* Endoplasmic reticulum stress-induced transcription factor, CHOP, is crucial for dendritic cell IL-23 expression. *Proc. Natl. Acad. Sci. U. S. A.* **107**, 17698–17703 (2010) doi:

10.1073/pnas.1011736107.

170. Nakayama, Y. *et al.* Molecular mechanisms of the LPS-induced non-apoptotic ER stress-CHOP pathway. *J. Biochem.* **147**, 471–483 (2010) doi: 10.1093/jb/mvp189.

171. Wu, Y. *et al.* Dopamine Uses the DRD5-ARRB2-PP2A Signaling Axis to Block the TRAF6-Mediated NF-κB Pathway and Suppress Systemic Inflammation. *Mol. Cell* **78**, 42-56.e6 (2020) doi: 10.1016/j.molcel.2020.01.022.

172. Zhang, F. *et al.* Genetic programming of macrophages to perform anti-tumor functions using targeted mRNA nanocarriers. *Nat. Commun.* **10**, (2019) doi: 10.1038/s41467-019-11911-5.

173. Poltavets, A. S., Vishnyakova, P. A., Elchaninov, A. V., Sukhikh, G. T. & Fatkhudinov, T. K. Macrophage Modification Strategies for Efficient Cell Therapy. *Cells* **9**, 1535 (2020) doi: 10.3390/cells9061535.

174. Allison, A. C. Immunosuppressive drugs: the first 50 years and a glance forward. *Immunopharmacology* **47**, 63–83 (2000) doi: 10.1016/S0162-3109(00)00186-7.

Acronyms and Abbreviations

ATP	Adenosine triphosphate
BBB	Blood-brain barrier
CAD	Cis-aconitate decarboxylase
CCL	C-C motif chemokine
ClpP	Caseinolytic protease P
CNS	Central nervous system
COX-2	Cyclooxygenase-2
CSF-1	Macrophage colony-stimulating factor 1
CSF-1R	Macrophage colony-stimulating factor 1 receptor
CTLA-4	Cytotoxic T-lymphocyte protein 4
DNA	Deoxyribonucleic acid
ETC	Electron transport chain
F1,6BP	Fructose 1,6-bisphosphate
F6P	Fructose 6-phosphate
FAD	Flavin adenine dinucleotide
FAO	Fatty acid oxidation
FAS	Fatty acid synthesis
G6P	Glucose 6-phosphate
GB	Glioblastoma
GDNF	Glial cell line-derived neurotrophic factor
GGH	Gamma-glutamyl hydrolase
GLS	Glutaminase
GM-CSF	Granulocyte-macrophage colony-stimulating factor
GS	Glutamine synthetase
HGF	Hepatocyte growth factor
HIF1-α	Hypoxia-inducible factor 1-alpha
IDO	Indoleamine 2,3-dioxygenase
IFN-γ	Interferon-γ
IL	Interleukin
iNOS	Inducible Nitric oxide synthase
LPS	Lipopolysaccharide
MDSC	Myeloid-derived suppressor cell
MIF	Macrophage migration inhibitory factor
NAD	Nicotinamide adenine dinucleotide
NO	Nitric oxide

OXPHOS	Oxidative phosphorylation
PCR	Polymerase chain reaction
PD-1	Programmed cell death protein 1
PD-L1	Programmed cell death 1 ligand 1
PD-L2	Programmed cell death 1 ligand 2
PHD	Prolyl hydroxylase
PPP	Pentose phosphate pathway
RET	Reverse electron transport
RNA	Ribonucleic acid
ROS	Reactive oxygen species
SDF-1	Stromal cell-derived factor 1
SDH	Succinate dehydrogenase
TAMs	Tumor-associated microglia/macrophages
TCA	Tricarboxylic acid
TGF-ß	Transforming growth factor ß
TME	Tumor microenvironment
TMZ	Temozolomide
TNF-α	Tumor necrosis factor-α
TRAIL	Tumor necrosis factor ligand superfamily member 10
Treg	Regulatory T cell
VEGF	Vascular endothelial growth factor A
WHO	World Health Organization
α-KG	α-ketoglutarate

List of figures

Publication I

scientific reports

Article | Open Access | Published: 29 November 2019

Assessing the reliability of gene expression measurements in very-low-numbers of human monocyte-derived macrophages

Carsten Geiß, Gregorio Alanis-Lobato, Miguel Andrade-Navarro & Anne Régnier-Vigouroux

Scientific Reports **9**, Article number: 17908 (2019)

SCIENTIFIC REPORTS
nature research

OPEN

Assessing the reliability of gene expression measurements in very-low-numbers of human monocyte-derived macrophages

Carsten Geiß[1], Gregorio Alanis-Lobato[2,3], Miguel Andrade-Navarro[3] & Anne Régnier-Vigouroux[1*]

Tumor-derived primary cells are essential for *in vitro* and *in vivo* studies of tumor biology. The scarcity of this cellular material limits the feasibility of experiments or analyses and hence hinders basic and clinical research progress. We set out to determine the minimum number of cells that can be analyzed with standard laboratory equipment and that leads to reliable results, unbiased by cell number. A proof-of-principle study was conducted with primary human monocyte-derived macrophages, seeded in decreasing number and constant cell density. Gene expression of cells stimulated to acquire opposite inflammatory states was analyzed by quantitative PCR. Statistical analysis indicated the lack of significant difference in the expression profile of cells cultured at the highest (100,000 cells) and lowest numbers (3,610 cells) tested. Gene Ontology, pathway enrichment and network analysis confirmed the reliability of the data obtained with the lowest cell number. This statistical and computational analysis of gene expression profiles indicates that low cell number analysis is as dependable and informative as the analysis of a larger cell number. Our work demonstrates that it is possible to employ samples with a scarce number of cells in experimental studies and encourages the application of this approach on other cell types.

The use of primary cells in basic and clinical research is of upmost importance and interest because it facilitates the analysis of a biological material whose physiological properties (e.g. morphology, phenotype, function) are much less compromised than those of established, immortalized cell lines[1]. However, experimenting with these cells entails some restrictions due to (i) their properties (e.g. the (epi)genetic uniqueness of each donor), (ii) technical (e.g. differences resulting from the preparation of each sample) and (iii) practical issues (e.g. limited amount of material). This is a recurrent question in cancer research where researchers must deal not only with the high heterogeneity of the biological tissues of interest but also with problems associated with their physical availability and accessibility. This is the case, for instance, with the cellular material that can be obtained from biopsies of glioblastoma. Those brain tumors are characterized by a high level of molecular and cellular heterogeneity, which largely contribute to their resistance to therapy[2,3]. Tumor-associated microglia/macrophages (TAMs) constitute one subpopulation of glioblastoma cells that efficiently support tumor growth[4,5] and, as such, represent attractive therapeutic targets[6]. Targeting these cells for therapeutic purposes necessitates a thorough knowledge of their properties. This knowledge has tremendously increased in the last few years thanks to experimental work performed with human primary microglia/macrophages[7–14]. However, the study of these highly plastic cells still poses experimental challenges. For instance, the patient to patient variability in terms of amount and quality of cells isolated from glioblastoma resections limits the extent and range of assays. Furthermore, discrete cellular phenotypic or functional profiles might vary with the location of the cells in the tumor or with their origin (resident microglia versus infiltrating macrophages). This heterogeneity and its biological significance typically cancel out in the analysis of cells pooled from the whole tumor. Two approaches might be considered to circumvent

[1]Institute of Developmental Biology and Neurobiology, Faculty of Biology, Johannes Gutenberg University of Mainz, Johann-Joachim-Becher-Weg 13, 55128, Mainz, Germany. [2]Human Embryo and Stem Cell Laboratory, The Francis Crick Institute, 1 Midland Road, London, NW1 1AT, UK. [3]Institute of Organismic and Molecular Evolution, Faculty of Biology, Johannes Gutenberg University of Mainz, Hans-Dieter-Hüsch-Weg 15, 55128, Mainz, Germany. *email: vigouroux@uni-mainz.de

Multiple well plate	Area/well (cm^2)	Seeded cell number/well	µl medium/ well
6 well	8,87	100,000	4,000
12 well	3,90	44,000	1,760
24 well	1,90	21,400	860
48 well	1,00	11,300	450
96 well	0,32	3,610	140

Table 1. Seeding conditions of monocyte-derived macrophages in vessels of different size. To keep the cell density identical, the cell number per vessel was calculated by dividing the vessel area by the reference vessel area (8,87 cm^2) and multiplying the result by the standard cell number (100,000).

these limitations: the use of single-cell analysis or the use of a very low number of cells. Both would have to comply with the requirement of full reliability in the data generated by each setup.

Single cell profiling, namely single cell-RNA sequencing, combined with bioinformatics, is becoming a mainstream methodology to characterize the transcriptome of individual cells. A recent publication has reported profiles of TAMs freshly isolated from brain tumor biopsies, indicating the feasibility of this approach for such heterogeneous tumors[15]. The measurement of gene expression in single cells however has a number of experimental pitfalls such as the so-called "dropout event" or lack of detection of some RNAs[16,17]. More worryingly, highly plastic cells such as microglia or macrophages are expected to exhibit temporal fluctuation in gene expression. This transcriptional burst is covered in the transcriptome analysis of cell populations but not in a single cell analysis. As a consequence, different intermediate transcriptional states of TAMs - that would be part of a longitudinal and regional TAM signature - will be lost in a single cell analysis and hidden in the analysis of a large number of cells but will be kept in the analysis of a small number of cells. These intermediate states potentially represent relevant therapeutic targets, making the analysis of a limited number of reactive cells -such as cells of the immune system- more relevant than that of individual cells. The limitations and reliability of this approach have not been systematically determined yet. Reducing cell numbers might increase the variability in gene expression according to the law of large numbers. The response of highly plastic cells to the same external stimuli might as well differ according to their number. Thus, what is the minimum number of cells that we can analyze and that will lead to results that are not significantly different from those obtained with a more standard number of cells?

To answer this question, we investigated how much we can reduce the number of cells without affecting the gene expression profile analyzed by standard procedures that they would exhibit when analyzed at a higher cell number. As a cellular model, we used human primary monocyte-derived macrophages (MDMs). Besides representing the precursors of macrophages that infiltrate tumors, these cells offer the advantages of being easily isolated from various donors (biological variation) and having a well-characterized response to inflammatory stimuli[18,19]. In order to simulate *in vivo* conditions in which macrophages are exposed to multiple pro- and/or anti-inflammatory stimuli, we treated MDMs with two Toll-like receptor (TLR) ligands or with two cytokines to polarize them towards a defined pro- or anti-inflammatory status, respectively. Cells were seeded in decreasing amount but at the same density in multi-well plates with various diameters. Following treatment, the resulting macrophage states were characterized by RT-qPCR. Gene expression levels in cells seeded at the highest cell number were compared with levels in cells seeded at the lower cell numbers. Statistical analyses were carried out to assess the degree of change between the two conditions and to select the lowest possible number of cells that maintains sensitivity of and reliability in the gene expression measurements. Finally, we performed functional enrichment and network analyses with these data as a means to understand the biological processes and molecular interactions that are perturbed under changing conditions.

Results

Decreasing the number of cells does not affect the expression level of a selected set of genes. In order to determine the lowest number of cells that enables a reliable detection of gene expression, comparable to that detected in high cell numbers, we first analyzed mRNA levels of a small set of genes in MDMs after 24 h of treatment with lipopolysaccharide (LPS) and polyinosinic-polycytidylic acid (poly(I:C)) (hereinafter referred to as M(LPS/IC)). LPS, a ligand of TLR-4, and poly(I:C), a ligand of TLR-3, are pro-inflammatory molecules that trigger tumoricidal activities of macrophages and TAMs[8,18]. Cells from the same macrophage preparation were seeded at various numbers but at constant density in vessels of decreasing size (see Table 1). The highest number of cells we tested, referred to as standard number of cells, was 100,000 cells seeded in one well of a 6-well plate. The lowest vessel we tested was the well of a 96-well plate in which 3,610 cells were seeded. We did not assay a lower number of cells because it would be impractical for any type of molecular analysis using standard methodologies and equipment.

We first assessed whether the applied stimulus affects cell viability. As shown in Fig. 1, there were no significant changes in cell viability after 24 h of stimulation at any seeded cell number. We next analyzed and compared the expression of a set of 6 genes in cells seeded at the standard number (6-well plate) and at the lowest number (96-well plate). RNA extraction and RT-qPCR were performed with technical replicates consisting of individual wells of the 6-well plates and a pool of two wells of the 96-well plates. After 24 h of pro-inflammatory treatment with the LPS/poly(I:C) combination, cells seeded at the highest number (100,000 cells per well in 6-well plates) exhibited the expected profile. Gene expression of *IL1B* and *SLC1A2* was upregulated[18,20], that of *CD163* and *CD206* was downregulated[18,21], whereas that of *GAPDH* (our unpublished observations) and *GLUL*[22] were not altered (Fig. 2A). An expression profile similar to that of the standard condition was observed for cells seeded at the lowest number (Fig. 2B). The statistical analysis of

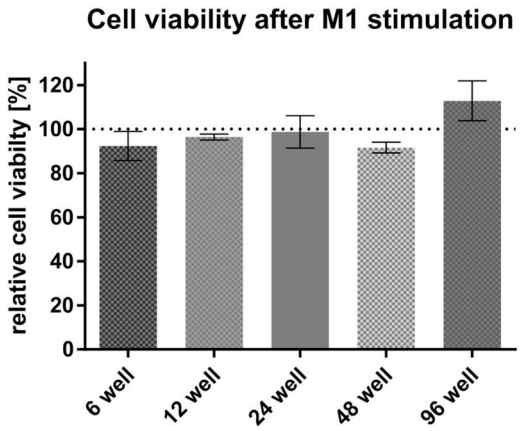

Figure 1. Viability of human MDMs 24 h after treatment with LPS and poly(I:C). Data are expressed as viability of treated cells relative to viability of untreated cells. Values are means ± SD of at least three technical replicates. Statistical analysis was performed using a two-tailed t-test. Calculated p-values: 6 well, untreated vs M1: 0.1683; 12 well, untreated vs M1: 0.6438; 24 well, untreated vs M1: 0.8825; 48 well, untreated vs M1: 0.1370; 96 well, untreated vs M1: 0.1180.

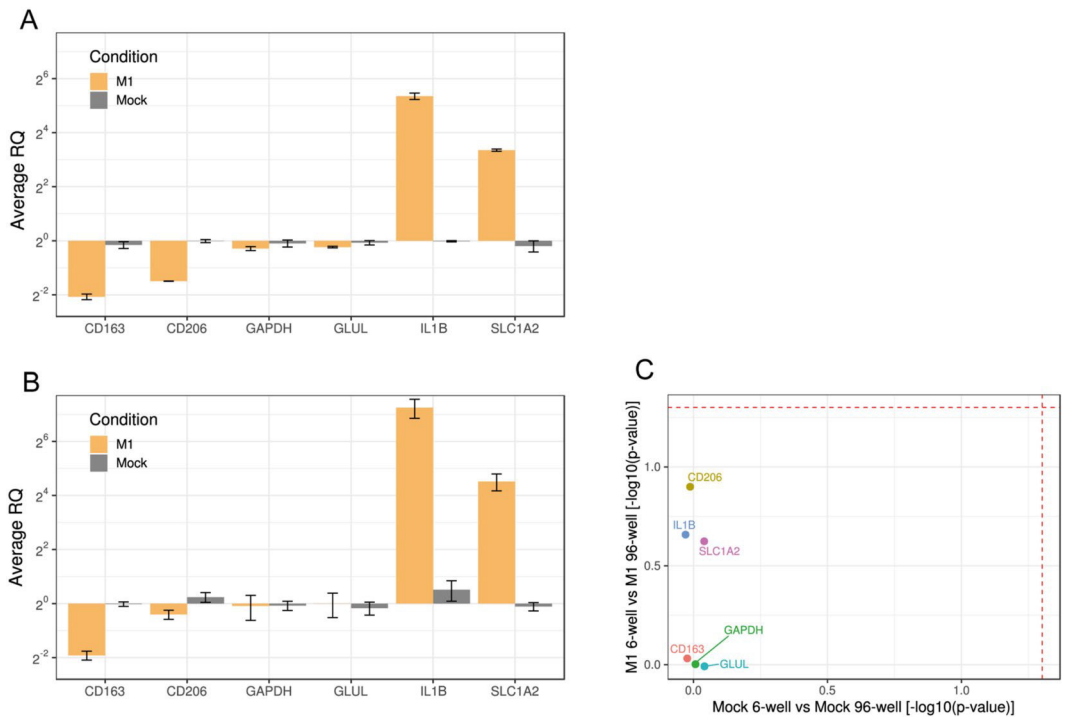

Figure 2. Relative gene expression of human MDMs seeded in 6-well or 96-well plates, 24 h after M(LPS/IC) stimulation (M1) or absence of stimulation (Mock). (**A**) qPCR analysis of 6-well samples. (**B**) qPCR analysis of 96-well samples. M1 values are relative to mock which is normalized to 1. Average RQs of three technical replicates ± SD are shown. Technical replicates: individual wells of a 6-well plate, pool of two wells of a 96-well plate. Reference genes: *SDHA*, *HPRT1*. (**C**) Scatter plot showing the statistical comparison between seeding conditions for matched treatments. Dashed lines correspond to the significance level $\alpha = 0.05$.

these data (see the Materials and Methods) did not show significant differences between the standard condition and the lowest cell number (Fig. 2C). From these results we concluded that it is possible to decrease the number of cultured cells to a minimum of 3,610 cells per well of a 96-well plate without inducing significant changes in the expression of a panel of genes. In the next experiments, gene expression levels were analyzed and compared in cells seeded in the standard condition (6-well plates) and cells seeded at the lowest number (96-well plates).

Different stimuli induce the expected gene expression profile independently of cell number. We next analyzed gene expression in MDMs treated with an anti-inflammatory stimulus and compared it with the MDM response to the pro-inflammatory stimulus. These stimuli are expected to induce distinct

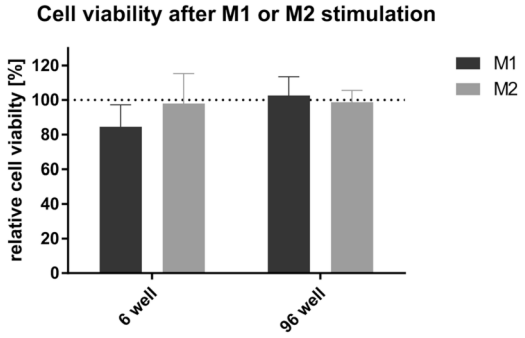

Figure 3. Cell viability of human MDMs 24 h after stimulation with LPS and poly(I:C) (black) or IL-4 and IL-10 (grey). All values are means ± SD of at least three independent experiments. Statistical analysis was performed using the Kruskal-Wallis method. Comparison of M(LPS/IC) vs M(IL-4/IL-10) vs untreated cells revealed no significant differences.

pro-inflammatory and anti-inflammatory phenotypes that should translate into the opposite expression profile of the inflammatory genes *IL1B*, *CD163* and *CD206*[18,21]. Cells from individual preparations of MDMs were seeded in 6- and 96-well plates and were left untreated or were incubated for 24 h with the pro-inflammatory M(LPS/IC) stimulus or with the anti-inflammatory combination of the interleukin-4 (IL-4) and interleukin-10 (IL-10) (M(IL-4/IL-10)) stimuli. After having excluded possible cytotoxic effects of the M(IL-4/IL-10) stimuli (Fig. 3), gene expression was analyzed by RT-qPCR. Consistent with our observations (see Fig. 2), M(LPS/IC) stimulation induced the expected pro-inflammatory profile. That is, upregulation of the pro-inflammatory *IL1B* and downregulation of the anti-inflammatory *CD163* and *CD206*, both in MDMs seeded at the standard and at the lowest number of cells (Fig. 4). M(IL-4/IL-10) stimulation did not alter the level of *IL1B* or *CD163* expressed by untreated macrophages, suggesting a basal anti-inflammatory status of these cultured MDMs for which the expression of these genes could not be modulated further by the IL-4/IL-10 stimulus. It did, however, increase the level of *CD206* expression, indicating that MDMs were responsive to the anti-inflammatory stimulus. This expression profile was observed both for cells seeded at the standard and lower numbers (Fig. 4A,B). The statistical analysis of these data did not show significant differences between the standard condition and the lower cell numbers (Fig. 4C,D). These results confirm that it is possible to decrease the number of cultured cells to a minimum of 3,610 cells without inducing significant changes in gene expression, independently of the type of stimulus to which the cells were subjected.

Analysis of a larger set of genes confirms the similarity of the gene expression profiles in standard and low numbers of MDMs. To further demonstrate that the gene expression profile detected in the low number of cells is similar to the profile detected in a larger number of the same cells, we extended our analysis to a broader spectrum of 28 genes. We included genes whose expression is regulated during inflammation and that code for: proteins involved in the immune response (e.g. TGFß, TNF), (metabolic) enzymes (e.g. arginase, dipeptidyl peptidase 4) and metabolite transporters (e.g. EAAT2, xCT). Selection of these genes was based on reported data, as well as on our own unpublished observations (see Table 2 for the complete list of genes). MDMs were seeded in 6-well plates and in 96-well plates and were either left untreated or were treated with the M(LPS/IC) or the M(IL-4/IL-10) stimulus for 24 h. Extracted RNA was then analyzed by quantitative RT-qPCR. Analysis of 28 genes with RT-qPCR requires more RNA than the amount that it is possible to extract from 3,610 cells. This analysis was therefore conducted with technical replicates consisting of a pool of thirty-two wells of the 96-well plates. The robustness of the qPCR was increased by including three instead of two reference genes (*SDHA*, *18 S* and *GAPDH*; see Materials and Methods). With the exception of five genes (*ARG1*, *IFNG*, *IL4*, *IL6*, *IL13*), all the genes listed in Table 2 were detectable in all tested conditions. The same profile was observed in both setups (Fig. 5A,B). The statistical analysis of these data confirmed that there were no significant differences between the two setups (Fig. 5C). These results indicate that we can perform an unbiased evaluation of the expression of a few genes of interest in a low number of cells.

Gene ontology and pathway enrichment analysis of dysregulated genes. We finally examined the validity of our approach through a bioinformatics analysis in order to determine and compare pathways altered in treated MDMs seeded at the standard and low numbers. The rationale was that both seeding conditions should result in similar sets of differentially expressed genes and that these genes should be involved in biological processes related to the induced pro- or anti-inflammatory responses. For that purpose, we further analyzed the data generated by the PCR array and determined the genes whose expression showed significant changes after treatment with the M(LPS/IC) and the M(IL-4/IL-10) stimuli. Volcano plots were generated for each differential gene expression analysis (see Materials and Methods): untreated versus M(LPS/IC), untreated versus M(IL-4/IL10) and M(LPS/IC) versus M(IL-4/IL-10), in both setups (Fig. 6). Only genes whose change in expression was at least 1.5-fold larger than the standard condition are indicated by name in Fig. 6. Among those genes, *CD206*, *IL1B*, *SHPK*, *VEGFA* and *GGH* displayed the most robust profile of expression, being identified in each condition and setup. Also note that regardless of the seeding condition (6-well or 96-well plates), the differential gene expression analysis led to similar gene lists.

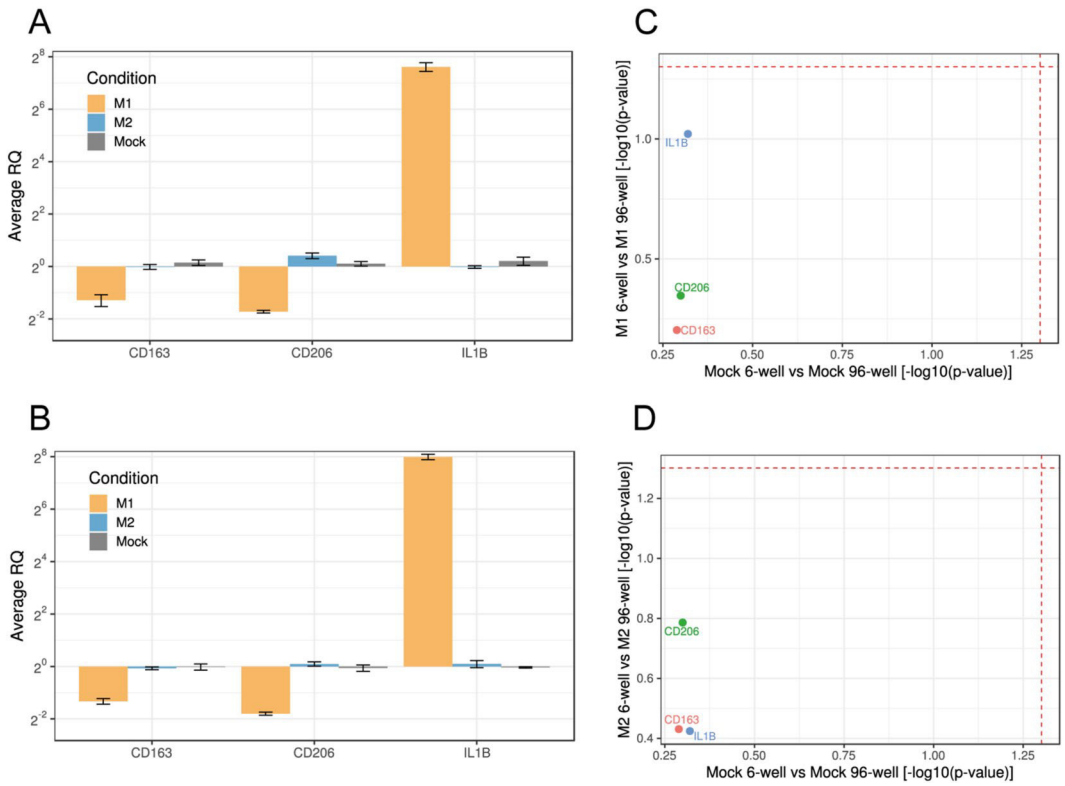

Figure 4. Relative gene expression of human MDMs seeded in 6-well or 96-well plates, 24 h after stimulation with LPS and poly(I:C) (M1), IL4 and IL-10 (M2) or absence of stimulation (Mock). (**A**) qPCR analysis of 6-well samples. (**B**) qPCR analysis of 96-well samples. M1 and M2 values are relative to mock which is normalized to 1. Average RQs of three technical replicates ± SD are shown. Technical replicates: individual wells of a 6-well plate, pool of two wells of a 96-well plate. Reference genes: *SDHA*, *HPRT1*. (**C,D**) Scatter plots showing the statistical comparison between seeding conditions for matched treatments (C = M1, D = M2). Dashed lines correspond to the significance level $\alpha = 0.05$.

We then searched for the biological processes and pathways associated with genes differentially expressed in the M(LPS/IC) and M(IL-4/IL-10) macrophages. GO and pathway enrichment analysis using the Reactome database are shown for the 6-well and 96-well plate setups (Fig. 7). Both seeding conditions led to very similar GO terms and Reactome pathways. Indeed, more than 50% of the GO terms and pathways were shared by both conditions whereas other GO terms and pathways presented high similarity. For instance, the upregulated GO terms "positive regulation of neuroinflammatory response" and "lipopolysaccharide-mediated signaling pathway" were found exclusively in the standard condition and the low cell condition, respectively. These two terms obviously refer to the same biological process that is inflammation, which we expect to be induced in M(LPS/IC) macrophages. Similarly, the GO terms "phagocytic cup" and "membrane raft" were found exclusively in the standard condition and the low number of cells condition respectively and refer both to membrane dynamics. These differences are most likely to be explained by the still "low" number of genes we analyzed and would disappear by increasing the number of tested genes. We thus can conclude that, when we use a low number of cells and identify genes of interest, we can trust that the enriched pathways are of value.

The results of the GO and pathway enrichment analysis prompted us to perform a network analysis with genes from the low cell number setup. This included all genes showing at least a 1.5-fold up- or downregulation in the M(LPS/IC) vs M(IL-4/IL-10) stimulated macrophages: *CD206*, *SHPK*, *GLS*, *GGH*, *CD163*, *GLUL*, *SLC7A11*, *CD14*, *SLC1A2*, *TNF*, *IL1B* (see Fig. 6F). Since genes coding for interacting proteins tend to be co-regulated, we examined the protein interaction network around the proteins coded by those dysregulated genes to point to affected pathways. A reference protein-protein interaction network was constructed using high-quality interactions from the HIPPIE database (see Materials and Methods)[23]. Based on this network, subnetworks containing only the proteins coded by the up- or down-regulated genes and their one-level neighbors (i.e. the proteins that directly interact with them) were built (Fig. 8). This network analysis revealed a connection between gamma-glutamyl hydrolase (GGH), which is upregulated after M(LPS/IC) stimulation, and other pro-inflammatory markers such as TNF. The possible relevance of this metabolic enzyme to the inflammatory status and functions of tumor-associated macrophages is discussed below.

Target gene (associated protein)	Assay ID
18s	Hs99999901_s1
SDHA (Succinate dehydrogenase (ubiquinone) flavoprotein subunit, mitochondrial)	Hs00188166_m1
HPRT1 (Hypoxanthine-guanine phosphoribosyltransferase)	Hs02800695_m1
IL1B (Interleukin-1 beta)	Hs01555410_m1
CD163 (Scavenger receptor cysteine-rich type 1 protein M130)	Hs00174705_m1
CD206 (Macrophage mannose receptor 1)	Hs00267207_m1
GAPDH (Glyceraldehyde-3-phosphate dehydrogenase)	Hs02758991_g1
GLUL (Glutamine synthetase)	Hs01013056_g1
SLC1A2 (Glutamine synthetase)	Hs01102423_m1
SLC7A11 (Cystine/glutamate transporter)	Hs00921938_m1
SLC1A5 (Neutral amino acid transporter B(0))	Hs01056542_m1
SLC3A2 (4F2 cell-surface antigen heavy chain)	Hs00374243_m1
GLS (Glutaminase kidney isoform, mitochondrial)	Hs01014020_m1
GGH (Gamma-glutamyl hydrolase)	Hs00914163_m1
OAT (Ornithine aminotransferase, mitochondrial)	Hs00236852_m1
CHORDC1 (Cysteine and histidine-rich domain-containing protein 1)	Hs00854389_g1
DPP4 (Dipeptidyl peptidase 4)	Hs00897386_m1
G6PD (Glucose-6-phosphate 1-dehydrogenase)	Hs00166169_m1
ARG1 (Arginase-1)	Hs00163660_m1
ARG2 (Arginase-2, mitochondrial)	Hs00982833_m1
IL4 (Interleukin-4)	Hs00174122_m1
IL6 (Interleukin-6)	Hs00174131_m1
IL10 (Interleukin-10)	Hs00961622_m1
IL13 (Interleukin-13)	Hs00174379_m1
TNF (Tumor necrosis factor)	Hs00174128_m1
IFNG (Interferon gamma)	Hs00989291_m1
TGFB1 (Transforming growth factor beta-1 proprotein)	Hs00998133_m1
CD14 (Monocyte differentiation antigen CD14)	Hs02621496_s1
VEGFA (Vascular endothelial growth factor A)	Hs00900055_m1
SLC2A1 (Solute carrier family 2, facilitated glucose transporter member 1)	Hs00892681_m1
PKM (Pyruvate kinase PKM)	Hs00761782_s1
SHPK (Sedoheptulokinase)	Hs00950008_m1

Table 2. List of TaqMan® primers used for qPCR.

Discussion

In this study, we sought to determine the reliability and the limitations in analyzing low numbers of cells in terms of their gene expression. Indeed, a decrease in cell number could result in an increased variability in gene expression or force changes in their response to external stimuli. We demonstrate that gene expression analysis of a low number of cells is as reliable and informative as the analysis of a larger number of cells. We provide an experimental workflow to assess the reliability of gene expression measurements of a low cell number using RT-qPCR followed by the statistical and computational analysis of the gene expression profiles that we obtained. This experimental workflow is applied to human monocyte-derived macrophages and presents a valid framework for similar studies with other cell types.

We investigated a cellular experimental system that combines different sources of variability: the genetic background of healthy blood donors which is reflected in each of the macrophage preparations used for the study; the stimuli applied to the cells; and finally, the inherent heterogeneity of an *in vitro* culture of primary cells. We kept the seeding density of the cells constant in order to ensure that we would assess the effect of cell number and not that of cell density. Given that our standard number was 100,000 cells/well seeded in a 6-well plate, the size of the smallest vessel available for cell culture, the 96-well plate, imposed a constraint of 3,610 cells on the lowest number of seeded cells. We did not observe statistical differences in the profile of a given set of genes expressed by macrophages from the same preparation and seeded at 3,610 or 100,000 cells. This indicates that, in our experimental system, we can lower the number of macrophages to 3,610 without the risk of introducing an artefactual variability factor. A practical consequence is that more experiments can be conducted with the same batch of cells by using less cells per experiment. In the case of cells isolated from a tissue and that can only be extracted in limited amounts, such as tumor-associated macrophages, our results suggest that 3,610 cells would be sufficient to obtain statistically reliable gene expression measurements. This low number of cells is indeed not meant to be used for the analysis of a large number of parameters (e.g. number of genes) because of the physical limit it imposes on the quantity of material to be analyzed (e.g. RNA). As reported in Figs. 2 and 4, assessing the expression of seven to eight genes (including two reference genes) with our RT-qPCR protocol required pooling

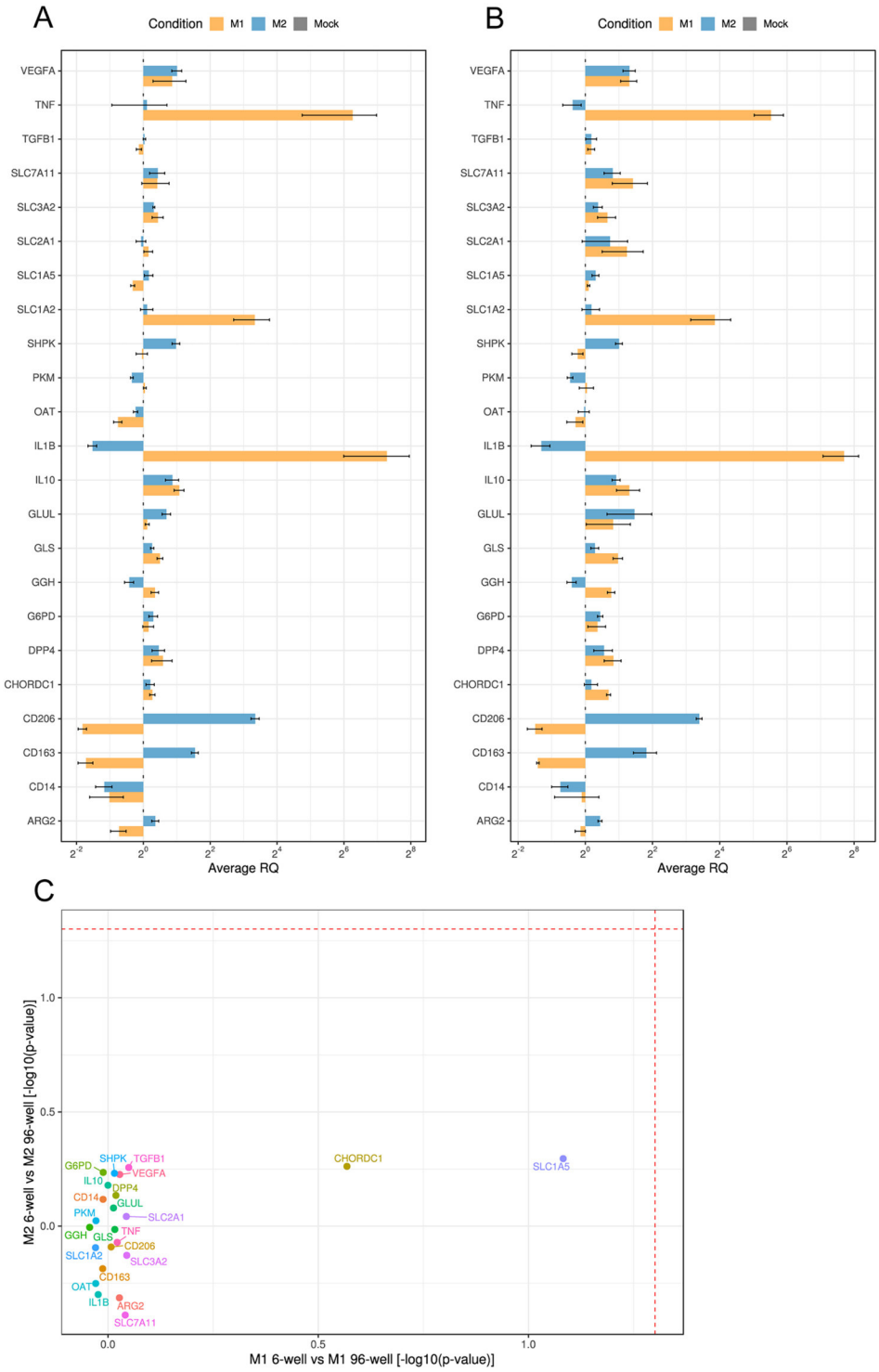

Figure 5. Relative gene expression of human MDMs seeded in 6-well and 96-well plates, 24 h after M(LPS/IC) stimulation (M1), M(IL-4/IL-10) stimulation (M2), or absence of stimulation (Mock). (**A**) Average RQ values of 6-well samples. (**B**) Average RQ values of 96-well samples. M1 and M2 values are relative to mock which is normalized to 1. Bars represent means of monoplicates of 3 independent experiments ± SEM. Technical replicates: individual wells of a 6-well plate, pool of thirty-two wells of a 96-well plate. Reference genes: *SDHA*, *18S*, *GAPDH*. (**C**) Scatter plot showing the statistical comparison between seeding conditions for matched treatments in M(LPS/IC) and M(IL-4/IL-10) stimulated macrophages. Dashed lines correspond to the significance level $\alpha = 0.05$.

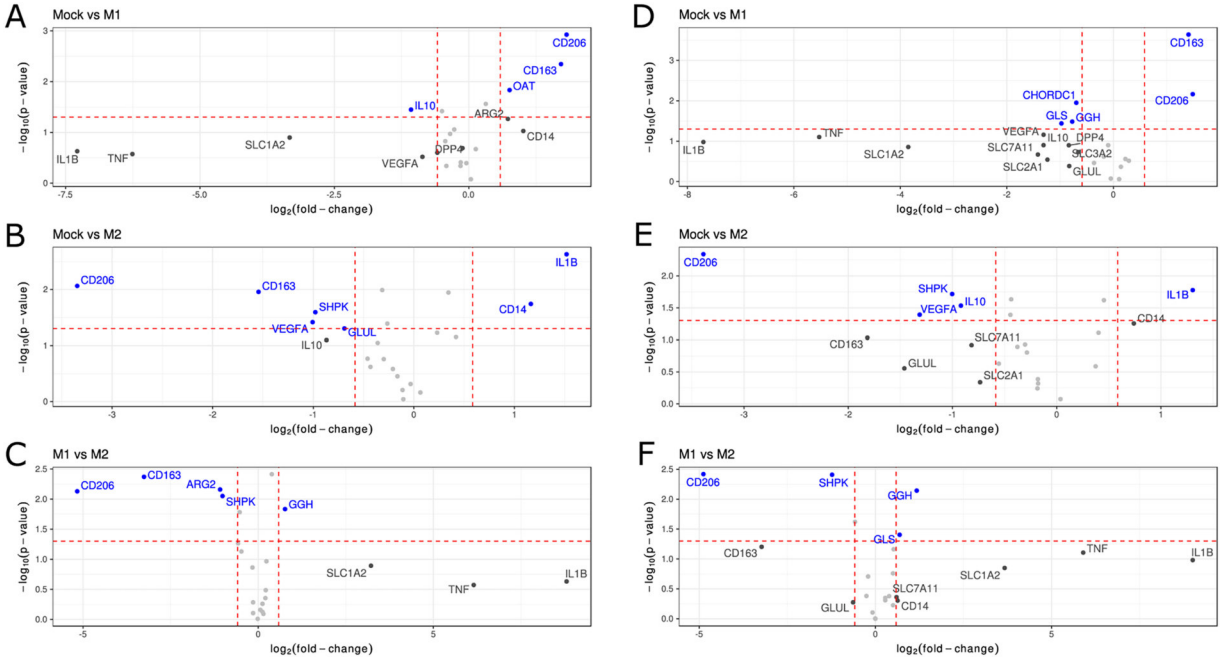

Figure 6. Volcano plots showing the results of the differential gene expression analysis. Only genes that display the strongest alteration in expression in both the 6-well and 96-well setups are indicated by names. Genes whose change in expression was at least 1.5-fold larger than the standard condition and had an associated p-value of at most 0.05 are highlighted in blue. Genes for which only the first condition is met are shown in gray. (**A**–**C**) Data from the 6-well plate analysis. (**D**–**F**) Data from the 96-well plate analysis. Mock = untreated cells, M1 = M(LPS/IC) macrophages, M2 = M(IL-4/IL-10) macrophages.

material from two wells of cells seeded at the lowest number. Although we *de facto* analyzed the RNA extracted from 7,220 cells, these cells were cultured separately and thus represent cellular replicates. Our study highlights that working with a low cell number certainly imposes a limit on the quantity but not on the quality of the parameters (genes, in this study) analyzed.

The robustness of our analysis was tested by applying two different types of inflammatory stimuli to these very plastic cells that are well characterized for their swift response to any modification of the extracellular milieu. The stimuli we selected trigger different signaling pathways and activate different transcription factors, resulting in two very different molecular and functional profiles of macrophages. The gene expression profiles obtained after the pro- or the anti-inflammatory activation were evaluated using a restricted set of genes. This evaluation was confirmed in the analysis of a larger set of genes and showed the expected changes in the expression levels of specific genes in both setups (standard versus low number of cells). We thus detected the upregulation of *TNF*, *SLC1A2* and *IL1B* after M(LPS/IC) stimulation or the upregulation of *CD163*, *CD206* and *SHPK*[24] after M(IL4/IL10) stimulation. Moreover, we observed a remarkable similarity in the expression profiles of all genes displayed by both low and standard numbers of cells after the pro- or the anti-inflammatory activation. It thus appears that notwithstanding the use of a very sensitive type of cells (macrophages), the usual sources of technical (such as the batch effect) or biological variation (such as cell heterogeneity or plasticity) neither had an impact on the analysis of the low number of cells we determined nor did they compromise its reproducibility. This leads us to the assumption that this approach could be valid for other types of cells and could be used whenever the cellular material is limited.

Statistical analyses and network analyses with gene expression data of the larger set of genes provided further evidence for the reliability of the data obtained from the low number of cells. Indeed, similar lists of differentially expressed genes and enriched pathways were obtained from both setups. Interestingly, the investigation of dysregulated genes from a protein network perspective suggested interaction between two metabolic enzymes, the gamma-glutamyl hydrolase (GGH) and the glutaminase (GLS), with the pro-inflammatory cytokine TNF, which are all upregulated after M(LPS/IC) stimulation. GGH is a critical enzyme in the regulation of folates. It is responsible for the intracellular cleavage of the poly g-glutamates[25], releasing glutamate as one reaction product. GLS is involved in glutamate/glutamine metabolism which is highly relevant to the inflammatory status of macrophages[26,27]. Whether and how these proteins interact and what functional meaning it would have for the immunometabolism of macrophages is worth investigating.

In closing, this study has focused on only one cell type, human macrophages, and one target of analysis, mRNA, as a proof of principle. We have used standard RT-qPCR and laboratory equipment to measure gene expression in these very plastic primary cells seeded at high and low cell numbers. The statistical and computational analysis of the gene expression profiles we have obtained in different conditions of cell seeding and treatment prove our hypothesis that the analysis of a low number of cells is not only reliable, but also informative.

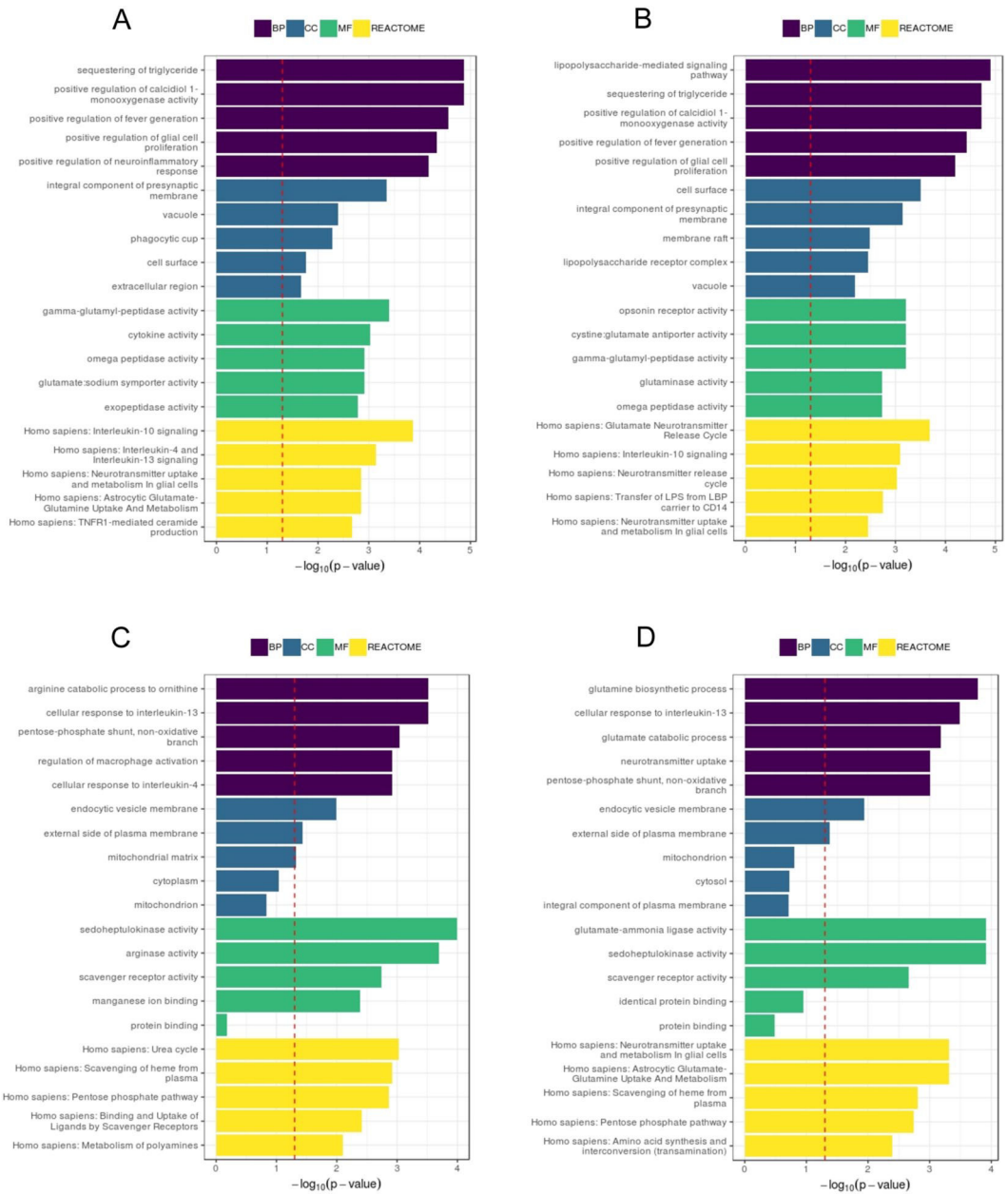

Figure 7. GO and pathway enrichment analysis of data generated from the 6-well and 96-well plate setups. Comparison of the M(LPS/IC) versus M(IL-4/IL-10) macrophages. (**A**) Upregulated terms in the 6-well setup. (**B**) Upregulated terms in the 96-well setup. (**C**) Downregulated terms in the 6-well setup. (**D**) Downregulated terms in the 96-well setup. BP, Biological Process; MF, Molecular Function; CC, Cellular Component.

Having shown the soundness of our approach in this experimental framework, we hope this work will motivate further studies on different types of cells. Indeed, our study is of relevance for a wide range of biologists and biomedical scientists who could adapt the experimental workflow we provide to their own experimental needs and questions.

Materials and Methods

Ethics statement. Buffy coats were purchased from the Transfusion Center of the University Medical Center of the Johannes Gutenberg University (Mainz, Germany) and were obtained from anonymized healthy blood donors. All buffy coats used in this study are residual biological materials made available by the Transfusion Center to scientists on a randomized basis. Blood samples are collected and processed in accordance with the relevant German guidelines and regulations. Personal data is neither collected nor shared for this material.

Monocyte isolation and differentiation into MDMs. Buffy coats were isolated from whole blood of healthy donors collected in CPD bags at the Transfusion Center (University Medical Center of the Johannes

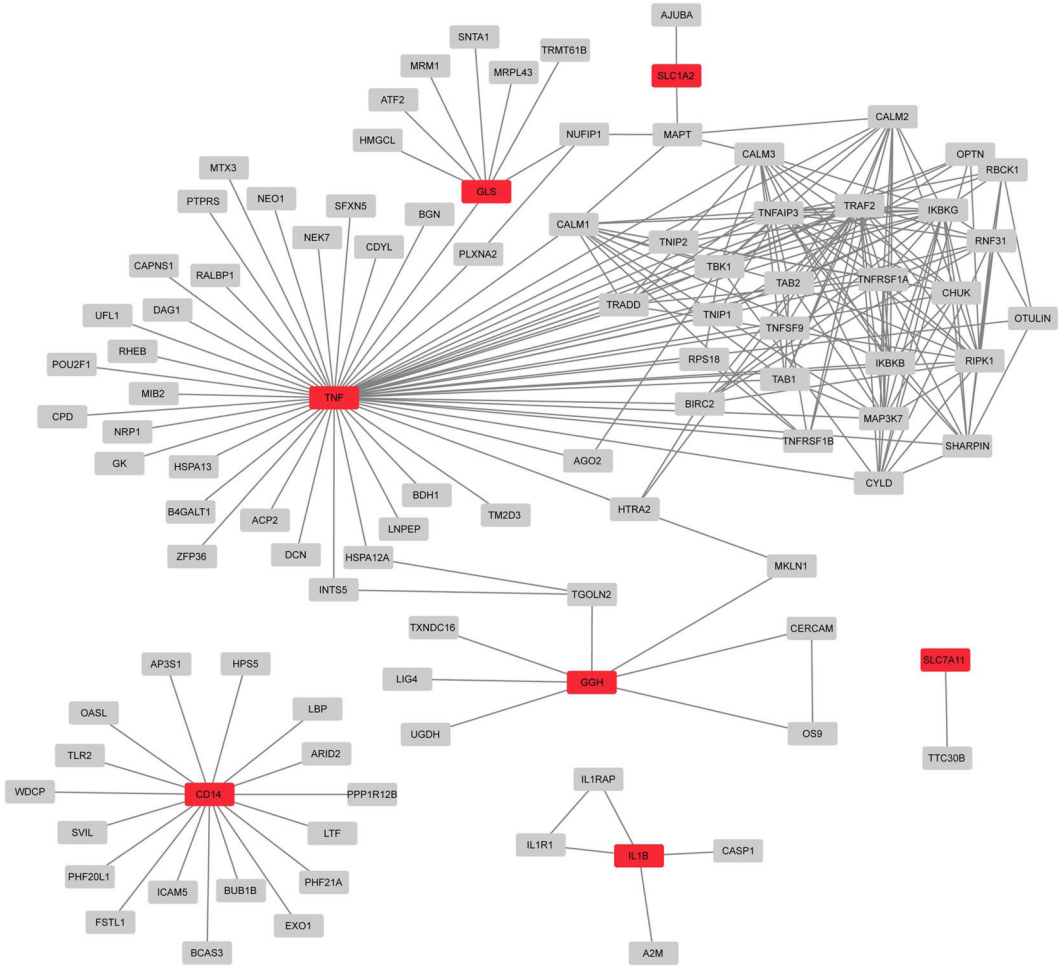

Figure 8. Direct protein-protein interaction partners (gray nodes) of proteins coded by differentially expressed genes (red nodes) according to the M1 vs M2 comparison from the low cell number setup.

Gutenberg University). Briefly, after an initial centrifugation without a density gradient, the pelleted erythrocytes and the top plasma layer were transferred into new bags, leaving the interface (buffy coat) in the original bag. Each unit (approx. 460 ml) of whole blood yielded an approx. 60 ml buffy coat.

Peripheral blood mononuclear cells (PBMC) were isolated from buffy coats as follows. The total volume of each buffy coat was filled up with sterile PBS to a final volume of 120 ml. Afterwards, 10 ml Ficoll®-Paque PREMIUM 1.073 (GE Healthcare) were overlaid with 30 ml of the diluted blood and centrifuged (40 min, 400 rcf, RT, without brake). The PBMC containing layer was isolated and centrifuged again (5 min, 450 rcf, RT). The cell pellet was resuspended in 10 ml erythrocyte lysis buffer (0.15 mM NH_4Cl, 10 mM $KHCO_3$, 0.1 mM EDTA, pH 7.2–7.4), incubated for 5 min on ice and centrifuged (5 min, 450 rcf, 4 °C). The pellet was resuspended in PBS, centrifuged (15 min, 200 rcf, RT), resuspended again in PBS and centrifuged (10 min, 450 rcf, RT). Finally, the pellet was resuspended in 1x NB complete medium [10 ng/ml basic fibroblast growth factor (PeproTech), 20 ng/ml epidermal growth factor (PeproTech), B27™ supplement (Gibco) in Neurobasal™-A medium (Gibco)] and cells distributed on 10 cm Petri dishes (Sarstedt). After 2.5 h of incubation (37 °C, 5% CO_2), supernatants were collected and replaced by cDMEM [DMEM (Sigma), 10% heat-inactivated FCS (Sigma), 2 mM L-Glutamine (Gibco), 50 µg/ml Gentamicin (Gibco)] containing 20 ng/ml macrophage-colony stimulating factor (M-CSF, Biolegend) for cell differentiation into MDMs. The collected supernatant was distributed on new 10 cm Petri dishes and incubated overnight (37 °C, 5% CO_2) for a second round of cell attachment. The next day, supernatants were replaced by cDMEM containing 20 ng/ml M-CSF. All dishes were incubated for one week in cDMEM containing M-CSF and cultured for another week in cDMEM without M-CSF prior to experiments. At the end of these two weeks, cells displayed the typical morphology of macrophages and flow cytometry indicated that more than 94% of the cells expressed the CD11b protein (data not shown). Average yield is 8×10^6–1×10^7 macrophages per preparation.

***In vitro* culture and stimulation.** Each independent experiment was conducted with cells from one preparation. Monocyte-derived macrophages were seeded in tissue culture vessels of different size (tissue culture plates, Greiner), adapting cell number to vessel area in order to keep the cell density identical (Table 1). The smallest

vessel we could assay was the well of a 96-well plate, hence the lowest number of cells to be tested was 3,610 cells. Cells were seeded in cDMEM and incubated for 24 h (37 °C, 5% CO_2) to let cells attach and recover from scraping/trypsinisation. Afterwards medium was removed and replaced by low serum-containing cDMEM (1% FCS) supplemented or not with the inflammatory stimuli. Cells were thus left untreated or treated for another 24 h (37 °C, 5% CO_2) before analysis. Low serum-containing cDMEM was used in order to decrease potential side effects of FCS components during MDMs treatment (e.g. competition with stimuli). Treatment consisted of: 10 µg/ml polyinosinic-polycytidylic acid (InvivoGen) combined with 10 ng/ml lipopolysaccharide (Sigma Aldrich) as pro-inflammatory stimulus; 10 ng/ml Interleukin-4 (BioLegend) combined with 10 ng/ml Interleukin-10 (BioLegend) as anti-inflammatory stimulus. As recommended in[28], macrophages are described according to the stimuli they were treated with: M(LPS/IC) and M(IL-4/IL-10). For space reasons, M(LPS/IC) and M(IL-4/IL-10) labels appear in graphs and legends as M1 and M2 respectively.

Determination of cell viability. After 24 h of treatment, PrestoBlue™ Cell viability reagent (ThermoFisher) was added directly to the wells in the culture medium according to manufacturers' instructions. After 30 min of incubation at 37 °C (5% CO_2) fluorescence was measured at a multiplate reader (TECAN Infinite® 200 PRO) and cell viability calculated as described in the manufacturers' protocol.

Total RNA isolation, cDNA transcription and gene expression profiling. Isolation of total RNA was performed using RNeasy Mini Kit (Qiagen) according to manufacturers' instructions. After PrestoBlue incubation, cells were washed with 1xPBS and lysed in Buffer RLT (containing 1% ß-mercaptoethanol). All following steps were conducted as described in the manufacturers' protocol. RNA concentration and quality were determined using a Nanodrop 2200 (ThermoFisher). Only samples showing a 260/280 nm ratio between 1.8 and 2.1 were selected for cDNA transcription which was performed with the Omniscript RT Kit (Qiagen) and random hexamers (Life Technologies). Quantitative PCR (qPCR) analysis was done using TaqMan® primers and a StepOnePlus System (Applied Biosystems). Briefly, for each well of the 96-well qPCR plate (Sarstedt), 10 µl of TaqMan™ Universal PCR Master Mix (ThermoFisher) were mixed with 5 ng cDNA and 1 µl of the appropriate primer (Table 2). All measurements were performed using three technical replicates. The PCR array was conducted with a customized TaqMan® gene expression array plate (ThermoFisher) using the same conditions as mentioned above, without technical replicates. Relative quantification (RQ) of gene expression were determined using the $2^{-\Delta\Delta Ct}$ method[29]. To ensure the robustness of the PCR analyses, we included two reference genes when measurements were performed with technical triplicates (data reported in Figs. 2 and 4) and three reference genes when measurements were performed without technical replicates (data reported in Fig. 5). The reference genes were determined among a set of four candidates (*18S*, *SDHA*, *HPRT1*, *GAPDH*) using the geNorm algorithm[30]. *SDHA* and *HPRT1* were identified as the most stable genes in PCR conducted with technical triplicates. *SDHA* and *18 S*, followed by *GAPDH* were identified as the most stable genes in PCR conducted without technical replicates; *HPRT1* had to be dismissed because of technical issues.

Statistical comparison between seeding conditions. To compare the RQ of gene expression between seeding in 6- and 96-well plates, we employed a two-tailed t-test under the null hypothesis that there were no differences in expression between conditions. These tests were performed for matched treatments, i.e. mock 6-well vs mock 96-well, M1 6-well vs M1 96-well and M2 6-well vs M2 96-well. The resulting p-values were corrected for multiple comparisons using the Benjamini-Hochberg method.

Differential gene expression, functional enrichment and network analyses. We identified differentially expressed genes between treatments (mock vs M1, mock vs M2, M1 vs M2) using log2-fold changes accompanied by p-values computed via t-tests. This was done separately for the 6- and 96-well seeding conditions. Genes with absolute log2-fold changes $\geq$1.5 were considered to be up- or down-regulated. These genes were subjected to Gene Ontology (GO) and Reactome pathway enrichment analyses using the R package FunEnrich[31]. In addition, we constructed a protein-protein interaction network with the direct interactors of the genes showing at least a 1.5-fold up- or down-regulation in the M1 vs M2 stimulated macrophages. For this, we used experimentally validated protein-protein interaction data from version 2.2 of the Human Integrated Protein-Protein Interaction rEference (HIPPIE)[23]. Only interactions with confidence scores above the upper quartile of the score distribution were considered.

Data availability

The datasets used and/or analyzed during the current study are available from the corresponding author on reasonable request.

Received: 5 August 2019; Accepted: 14 November 2019;
Published online: 29 November 2019

References

1. Pan, C., Kumar, C., Bohl, S., Klingmueller, U. & Mann, M. Comparative proteomic phenotyping of cell lines and primary cells to assess preservation of cell type-specific functions. *Mol. Cell. Proteomics* **8**, 443–50 (2009).
2. Ohgaki, H. & Kleihues, P. The definition of primary and secondary glioblastoma. *Clin. Cancer Res.* **19**, 764–72 (2013).
3. Dirkse, A. *et al*. Stem cell-associated heterogeneity in Glioblastoma results from intrinsic tumor plasticity shaped by the microenvironment. *Nat. Commun.* **10**, 1787 (2019).
4. Li, W. & Graeber, M. B. The molecular profile of microglia under the influence of glioma. *Neuro. Oncol.* **14**, 958 (2012).

5. Hambardzumyan, D., Gutmann, D. H. & Kettenmann, H. The role of microglia and macrophages in glioma maintenance and progression. *Nat. Neurosci.* **19**, 20–7 (2016).
6. Mantovani, A., Marchesi, F., Malesci, A., Laghi, L. & Allavena, P. Tumour-associated macrophages as treatment targets in oncology. *Nat. Rev. Clin. Oncol.* **14**, 399–416 (2017).
7. Hussain, S. F., Yang, D., Suki, D., Grimm, E. & Heimberger, A. B. Innate immune functions of microglia isolated from human glioma patients. *J. Transl. Med.* **4**, 15 (2006).
8. Kees, T. *et al.* Microglia isolated from patients with glioma gain antitumor activities on poly (I:C) stimulation. *Neuro. Oncol.* **14**, 64–78 (2012).
9. Durafourt, B. A. *et al.* Comparison of polarization properties of human adult microglia and blood-derived macrophages. *Glia* **60**, 717–727 (2012).
10. Sarkar, S. *et al.* Therapeutic activation of macrophages and microglia to suppress brain tumor-initiating cells. *Nat. Neurosci.* **17**, 46–55 (2014).
11. Gabrusiewicz, K. *et al.* Glioblastoma-infiltrated innate immune cells resemble M0 macrophage phenotype. *JCI insight* **1** (2016).
12. Szulzewsky, F. *et al.* Human glioblastoma-associated microglia/monocytes express a distinct RNA profile compared to human control and murine samples. *Glia* **64**, 1416–1436 (2016).
13. Szebeni, G. J., Vizler, C., Kitajka, K. & Puskas, L. G. Inflammation and Cancer: Extra- and Intracellular Determinants of Tumor-Associated Macrophages as Tumor Promoters. *Mediators Inflamm.* **2017**, 9294018 (2017).
14. Yang, M., McKay, D., Pollard, J. W. & Lewis, C. E. Diverse Functions of Macrophages in Different Tumor Microenvironments. *Cancer Res.* **78**, 5492–5503 (2018).
15. Müller, S. *et al.* Single-cell profiling of human gliomas reveals macrophage ontogeny as a basis for regional differences in macrophage activation in the tumor microenvironment. *Genome Biol.* **18**, 234 (2017).
16. Ning, L. *et al.* Current challenges in the bioinformatics of single cell genomics. *Front. Oncol.* **4**, 7 (2014).
17. Haque, A., Engel, J., Teichmann, S. A. & Lönnberg, T. A practical guide to single-cell RNA-sequencing for biomedical research and clinical applications. *Genome Med.* **9**, 75 (2017).
18. Martinez, F. O. & Gordon, S. The M1 and M2 paradigm of macrophage activation: time for reassessment. *F1000Prime Rep.* **6**, 1–13 (2014).
19. Schultze, J. L. & Schmidt, S. V. Molecular features of macrophage activation. *Semin. Immunol.* **27**, 416–23 (2015).
20. Chretien, F. *et al.* Expression of excitatory amino acid transporter-2 (EAAT-2) and glutamine synthetase (GS) in brain macrophages and microglia of SIVmac251-infected macaques. *Neuropathol. Appl. Neurobiol.* **28**, 410–417 (2002).
21. East, L. & Isacke, C. M. The mannose receptor family. *Biochim. Biophys. Acta - Gen. Subj.* **1572**, 364–386 (2002).
22. Palmieri, E. M. *et al.* Pharmacologic or Genetic Targeting of Glutamine Synthetase Skews Macrophages toward an M1-like Phenotype and Inhibits Tumor Metastasis. *Cell Rep.* **20**, 1654–1666 (2017).
23. Alanis-Lobato, G., Andrade-Navarro, M. A. & Schaefer, M. H. HIPPIE v2.0: enhancing meaningfulness and reliability of protein-protein interaction networks. *Nucleic Acids Res.* **45**, D408–D414 (2017).
24. Haschemi, A. *et al.* The Sedoheptulose Kinase CARKL Directs Macrophage Polarization through Control of Glucose Metabolism. *Cell Metab.* **15**, 813 (2012).
25. McGuire, J. J. & Coward, J. K. In *Folates and Pterins. Chemistry and Biochemistry of* Folates (eds Blakley, R. L. & Benkovic, S. J.) 135–190 (Wiley, 1984).
26. Gras, G., Porcheray, F., Samah, B. & Leone, C. The glutamate-glutamine cycle as an inducible, protective face of macrophage activation. *J. Leukoc. Biol.* **80**, 1067–1075 (2006).
27. Jha, A. K. *et al.* Network Integration of Parallel Metabolic and Transcriptional Data Reveals Metabolic Modules that Regulate Macrophage Polarization. *Immunity* **42**, 419–430 (2015).
28. Murray, P. J. *et al.* Macrophage activation and polarization: nomenclature and experimental guidelines. *Immunity* **41**, 14–20 (2014).
29. Livak, K. J. & Schmittgen, T. D. Analysis of Relative Gene Expression Data Using Real-Time Quantitative PCR and the $2-\Delta\Delta CT$ Method. *Methods* **25**, 402–408 (2001).
30. Vandesompele, J. *et al.* Accurate normalization of real-time quantitative RT-PCR data by geometric averaging of multiple internal control genes. *Genome Biol.* **3**, RESEARCH0034 (2002).
31. FunEnrich R package. Available at, https://github.com/galanisl/FunEnrich. (Accessed: 24th June 2019) (2019).

Acknowledgements

The authors would like to thank Norah Fogarty (The Francis Crick Institute, London) for proofreading the article. Support from the Impulsfonds Forschungsinitiative Rheinland-Pfalz from the Johannes Gutenberg University: "Deciphering cell identity and function using single-cell data analysis".

Author contributions

Conception and design of the work: C.G., A.R.-V., G.A.-L. and M.A.-N. Experimental work and acquisition of data: C.G. Analysis of data: C.G. and G.A.-L. Interpretation of data: C.G., G.A.-L. and A.R.-V. Drafting of the manuscript: C.G. and A.R.-V. Critical revision for important intellectual content: C.G., A.R.-V., G.A.-L. and M.A.-N. All authors read and approved the final manuscript.

Competing interests

The authors declare no competing interests.

Additional information

Correspondence and requests for materials should be addressed to A.R.-V.

Publication II

Research Article | Basic | Open Access

Metabolic and inflammatory reprogramming of macrophages by ONC201 translates in a pro-inflammatory environment even in presence of glioblastoma cells

Carsten Geiß, Claudius Witzler, Gernot Poschet, Wolfram Ruf, Anne Régnier-Vigouroux

First published: 13 January 2021 | https://doi.org/10.1002/eji.202048957

 DOI: 10.1002/eji.202048957 Eur. J. Immunol. 2021. 51: 1246–1261

European Journal of Immunology

Immunomodulation and immune therapies

Research Article

Metabolic and inflammatory reprogramming of macrophages by ONC201 translates in a pro-inflammatory environment even in presence of glioblastoma cells

Carsten Geiß[1], *Claudius Witzler*[2], *Gernot Poschet*[3], *Wolfram Ruf*[2] *and Anne Régnier-Vigouroux*[1]

[1] Institute of Developmental Biology and Neurobiology, Johannes Gutenberg University, Mainz, Germany
[2] Center for Thrombosis and Hemostasis, Johannes Gutenberg University Medical Center, Mainz, Germany
[3] Centre for Organismal Studies, University of Heidelberg, Heidelberg, Germany

Tumor-associated macrophages facilitate tumor progression and resistance to therapy. Their capacity for metabolic and inflammatory reprogramming represents an attractive therapeutic target. ONC201/TIC10 is an anticancer molecule that antagonizes the dopamine receptor D2 and affects mitochondria integrity in tumor cells. We examined whether ONC201 induces a metabolic and pro-inflammatory switch in primary human monocyte-derived macrophages that reactivates their antitumor activities, thus enhancing the onco-toxicity of ONC201. Contrary to glioblastoma cells, macrophages exhibited a low ratio of dopamine receptors D2/D5 gene expression and were resistant to ONC201 cytotoxicity. Macrophages responded to ONC201 with a severe loss of mitochondria integrity, a switch to glycolytic ATP production, alterations in glutamate transport, and a shift towards a pro-inflammatory profile. Treatment of macrophages–glioblastoma cells co-cultures with ONC201 induced similar alterations in glutamatergic and inflammatory gene expression profiles of macrophages. It induced as well metabolic changes and a pro-inflammatory switch of the co-culture milieu. However, these changes did not translate into increased onco-toxicity. This study provides the first evidence that ONC201 affects macrophage immunometabolism and leads to a pro-inflammatory tumor environment. This speaks in favor of implementing ONC201 in combinatorial therapies and warrants further investigation of the mechanisms of action of ONC201 in macrophages and other immune cells.

Keywords: glioblastoma · immunometabolism · ONC201 · tumor-associated macrophages · tumor microenvironment

Additional supporting information may be found online in the Supporting Information section at the end of the article.

Introduction

Macrophages are very plastic cells that react to external signals by a fast reprogramming at the genetic and metabolic

Correspondence: Anne Régnier-Vigouroux
e-mail: vigouroux@uni-mainz.de

levels, thus facilitating an adequate answer to a changing environment [1]. Macrophages responding to pathogens or pro-inflammatory molecules activate a transcriptional program leading to an increased expression of pro-inflammatory genes and a switch from mitochondrial oxidative phosphorylation (OXPHOS) to glycolysis. Macrophages involved in tissue homeostasis and repair exhibit an anti-inflammatory profile and rely mostly on OXPHOS [2]. Macrophages present in solid tumors undergo reprogramming toward a "homeostatic" profile [3]. As a result, these tumor-associated macrophages (TAM) lose their cytotoxic capacities and gain tumor-supportive functions that largely contribute to tumor growth [4]. Considering their involvement in tumor biology and their capacity to rapidly change their transcriptional and functional profiles, TAMs represent a promising target for cancer therapy.

Glioblastoma, the most aggressive form of brain tumors, host a large number of blood-derived macrophages [5]. Together with microglia, the brain resident macrophages, they constitute a subpopulation of cells that actively promote tumor growth [6]. Various in vitro and in vivo strategies have addressed the feasibility to mitigate the tumor-supportive functions of these cells [7]. We demonstrated that human microglia/macrophages isolated from freshly resected glioblastoma could be reprogrammed by stimulating their Toll-like receptor 3 and consequently exerted anti-proliferative, anti-migratory, and cytotoxic activities, in vitro. This reprogramming however was inhibited by co-cultured glioblastoma cells, indicating the difficulty to translate such an approach to therapy [8]. An alternative strategy would consist in targeting the energy metabolism of macrophages. Metabolic adaptation is part of their plasticity and goes together with changes in their inflammatory profiles and functions [4]. TAMs are exposed to metabolic conditions shaped by tumor cells that exhibit strong metabolic alterations [9]. In glioblastoma, such a metabolic condition consists i.a. in elevated concentrations of extracellular glutamate [10] resulting from changes in the glutamate metabolism of the tumor cells [11]. We have reported alterations in the expression of glutamatergic genes in human tumor-associated microglia/macrophages and monocyte-derived macrophages exposed to tumor cells [12]. Moreover, recent data, including our own, suggest a connection between the glutamate metabolism and the inflammatory status of macrophages [13, 14].

Considering the potent role of metabolism on the inflammatory and functional status of macrophages and the metabolic changes occurring in tumor cells, metabolic reprogramming represents an extremely attractive therapeutic strategy. Recently, the small molecule ONC201/TIC10 has emerged as a very valuable drug in cancer therapy and has been included in clinical trials for glioblastoma [15–18]. ONC201 works as an antagonist of the dopamine receptor D2 (DRD2) [19] and as a ligand for the mitochondrial ClpP protein [20, 21]. Moreover it induces TRAIL [22] through activation of the transcription factor ATF4 [23]. Recent studies report that ONC201 affects mitochondria integrity[24] and induces a metabolic reprogramming in glioblastoma cells *in vitro*, leading to anti-proliferative and anti-migratory effects [25, 26]. This toxicity seems to be tumor cell-specific since human astrocytes [25] or monocyte-derived macrophages [27] have been reported to be ONC201 resistant at doses that killed tumor cells. However, ONC201 certainly affects the metabolism of these non-transformed cells present in and around the tumor mass. The impact of these alterations on the efficacy of ONC201 glioblastoma therapy has still to be elucidated.

Based on current data, we hypothesized that ONC201 has the potential to exert its activity in glioblastoma not only by targeting tumor cells, but also by inducing a metabolic switch in TAMs. This would invoke their pro-inflammatory activities, supporting and/or enhancing ONC201 cytotoxicity to tumor cells. To test this hypothesis, we first characterized the response of human monocyte-derived macrophages to ONC201 by analyzing their resistance to the drug, alterations in their glutamate- and energy-metabolism, and their inflammatory status. We then treated co-cultures of monocyte-derived macrophages and tumor cells from three different glioblastoma-derived cell lines with ONC201. We evaluated the degree of ONC201 cytotoxicity on both cell types and monitored inflammatory and metabolic changes in macrophages and the co-culture environment. With this study, we provide, to the best of our knowledge, the first analysis of the effects of ONC201 on the immunometabolism of monocyte-derived macrophages and its relevance to glioblastoma therapy.

Results

Macrophages are resistant to ONC201 and show a low *DRD2/DRD5* ratio

The sensitivity of human primary monocyte-derived macrophages (thereafter referred to as macrophages) to ONC201, was tested and compared to the sensitivity of three human glioblastoma (GB) cell lines. Normal human astrocytes were included as non-transformed counterpart of GB cells. We treated cells with increasing concentrations of ONC201 and monitored their viability (Figure 1A; Supporting Information Figure S1A). As expected, ONC201 induced a strong time- and concentration-dependent cytotoxic effect on the three GB cell lines. It had a lower effect on astrocytes, detectable from day 3 and only at the highest doses (50% viable cells at 2.5 μM and 5.0 μM). Macrophages were very resistant, with 80% or more viable cells at the latest time point and highest drug concentration.

Macrophage low sensitivity to ONC201 cytotoxicity might be related to their expression of the dopamine receptors D2 (DRD2) and D5 (DRD5). The ratio of DRD2/DRD5 gene expression is reported to be an indicator of tumor cell sensitivity to ONC201 [28]. Therefore, we examined DRD2 and DRD5 gene expression in untreated cells and calculated the corresponding ratio (Figure 1B). Astrocytes expressed very low levels of both receptors and were used for normalization of the data. Each GB cell line expressed higher levels of DRD2 than macrophages and astrocytes which showed comparable levels. Astrocytes (non-normalized data, not shown) and GB cells also expressed a higher level of *DRD2* than *DRD5*, whereas the contrary was observed

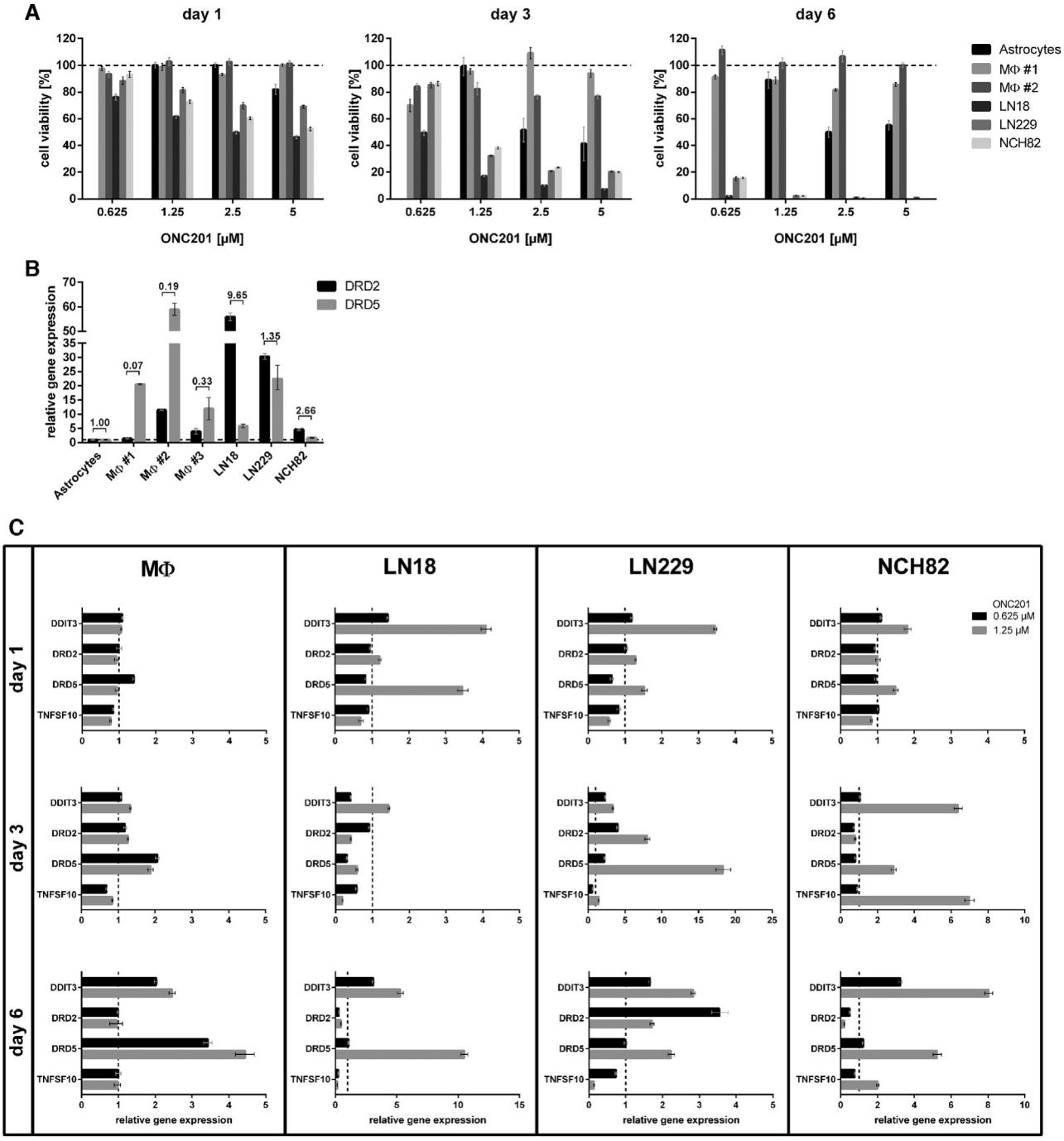

Figure 1. Sensitivity of primary astrocytes, primary macrophages and glioblastoma cell lines to ONC201. (A) Cell viability of the primary cells and GB cell lines LN18, LN229, NCH82 was determined using PrestoBlue reagent after treatment with ONC201. Note that astrocytes were not tested at 0.625 μM. Values are normalized to the respective DMSO treated controls (dashed line). Two different preparations of primary macrophages (MΦ #1, MΦ #2) were used. Data are given as mean ± SEM of ten technical replicates from one experiment. (B) Ratio of the relative gene expression levels of *DRD2* and *DRD5* in primary macrophages and GB cells. Values are normalized to the expression in primary astrocytes (dashed line). Three different preparations of primary macrophages (MΦ #1, MΦ #2, MΦ #3) were used. Data are given as mean ± SEM of three technical replicates from one experiment. (C) Relative gene expression levels of *DDIT-3*, *DRD2*, *DRD5*, and *TNFSF10* in primary macrophages and GB cells after ONC201 treatment. Values are normalized to the gene expression of the respective DMSO-treated controls (dashed line). Data are given as mean ± SEM of three technical replicates. Macrophages: data are from one experiment representative of three independent experiments (each performed with one macrophage preparation). GB cells, one experiment. Relative gene expression in (B) and (C) was determined by qPCR as described in *Materials and methods*.

for macrophages. In line with published observations, a comparison of the calculated *DRD2/DRD5* ratios with the cells' sensitivity to ONC201 indicated that sensitivity positively correlated with this ratio. Thus, macrophages, the most resistant cells, exhibited the lowest *DRD2/DRD5* ratio whereas the most ONC201-sensitive LN18 cells showed the highest *DRD2/DRD5* ratio. In conclusion, macrophages, as well as astrocytes, are more resistant to ONC201 than GB cells. This resistance correlates with their expression of a low *DRD2/DRD5* ratio.

The titration experiment (Figure 1A) indicated that ONC201 concentrations up to 1.25 μM induced a negligible cytotoxicity in macrophages and astrocytes but were highly toxic to the three GB cell lines. Since higher ONC201 concentrations did not trigger a dramatic increase of GB cell death, further characterization of ONC201 activity on macrophages was performed with concentrations of 0.625 and 1.25 μM ONC201.

ONC201 increases *DDIT-3* and *DRD5* expression in macrophages and GB cells

Macrophage low sensitivity to ONC201 could also reflect a deficiency of ONC201 in triggering signaling pathways in these cells. As an antagonist of DRD2, ONC201 induces early activation of the integrated stress response, leading to upregulation of DDIT-3 (DNA damage-inducible transcript 3 protein—also known as CHOP) and of TNFSF10 (Tumor necrosis factor ligand superfamily member 10 - also known as TRAIL) [23, 29]. Silencing of *DRD2* is reported to lead to an increase in *DRD5* expression [30], an interesting observation regarding the opposed effects of the signaling cascades activated by both receptors [31]. We examined *DDIT-3*, *DRD2*, *DRD5*, and *TNFSF10* expressions at three time points after ONC201 addition to the cells (Figure 1C). In macrophages, an increased *DRD5* expression was detected at day 3 and enhanced at day 6. Changes in *DDIT-3* expression were weak at day 3 but a clear increase was detectable at day 6. Changes in *DRD2* and *TNFSF10* expression levels were minimal. Contrary to its effect on macrophages, ONC201 affected gene expression levels in each GB cell line at an earlier time point and in a concentration-dependent manner. At day 1, ONC201 increased *DDIT-3* and *DRD5* expression in each GB cell line, with only minor changes in *DRD2*and decreased *TNFSF10* expression in two of the three GB lines. From day 3 on, *DDIT-3* and *DRD5* expression continued to increase whereas *DRD2* expression decreased in LN18 and NCH82 cells and increased in LN229 cells. The expected induction of *TNFSF10* expression was observed only in NCH82 cells. Altogether, this gene expression analysis indicates that macrophages, similar to GB cells, react to ONC201 by activating the integrated stress response (*DDIT-3* increase) and by modulating the expression of *DRD5*.

ONC201 inhibits OXPHOS in macrophages and induces loss of mitochondrial integrity

We next assessed ONC201 effects on macrophage metabolism. In a first step, we determined the total ATP production rate after treatment with the highest ONC201 concentration (5 μM). ONC201 induced a time-dependent reduction of mitochondrial ATP production and an increase of glycolytic ATP production, starting at day 3 (Figure 2A). We next analyzed the mitochondria status after three days of treatment with increasing ONC201 concentrations. Each tested ONC201 concentration led to increased proton leakage and strong reductions of the maximal and basal respiration, the non-mitochondrial oxygen consumption, the ATP production, and the coupling efficiency (Figure 2B, Supporting Information Figure S2). Reduction of mitochondrial ATP production was dose-dependent whereas the increase in glycolytic ATP production did not significantly change at each ONC201 concentration tested (Figure 2C). In conclusion, ONC201 induces a time- and concentration-dependent switch to glycolysis, concomitant to a severe loss of mitochondrial integrity in macrophages. These results suggest that ONC201 might activate the mitochondrial caseinolytic protease P (ClpP) and its signaling [20, 21] in macrophages.

ONC201 affects glutamate transport in macrophages and GB cells

To further investigate the effects of ONC201 on macrophage energy metabolism, we examined the expression profile of genes coding for transporters of glucose and glutamate. Both are critical metabolites of the TCA cycle and glutamate is specifically relevant in the context of glioblastoma. We analyzed *SLC2A1*, coding for glucose transporter type 1, as an indicator for glucose uptake; *SLC7A11*, coding for the Cystine/glutamate transporter, exporting glutamate in exchange for cystine and known to be upregulated through ATF4 [32]; and *SLC1A2* coding for a major transporter for glutamate uptake (Excitatory amino acid transporter 2) that likely counteracts the effects of *SLC7A11* on glutamate transport. As shown in Figure 3A, expression of *SLC2A1* was not or only slightly affected, suggesting that ONC201 did not impact glucose import in macrophages and GB cells. This lack of effect might reflect a high basal level of the receptor expression as a consequence of culture in high glucose conditions, thus prohibiting further upregulation of *SLC2A1*. On the contrary, ONC201 affected the gene expression of the two glutamate transporters, though to various extents, in both cell types. *SLC1A2* expression increased in LN18 from day 1 on, but decreased in all other cells at day 6. The most striking effect was observed on *SLC7A11*. ONC201 treatment increased its expression in each cell type. This increase, together with *DDIT-3* increase, are clear hints of ATF4 activation by ONC201.

To assess the relevance of altered *SLC1A2* and *SLC7A11* expressions to glutamate transport, we determined the amount of extracellular glutamate in the cell supernatants. Untreated macrophages accumulated much less extracellular glutamate than the three GB cells (Supporting Information Table S1). As shown in Figure 3B, macrophages responded to treatment with a significant ONC201-concentration-dependent increase of extracellular glutamate at day 6. GB cells on the contrary displayed an increased

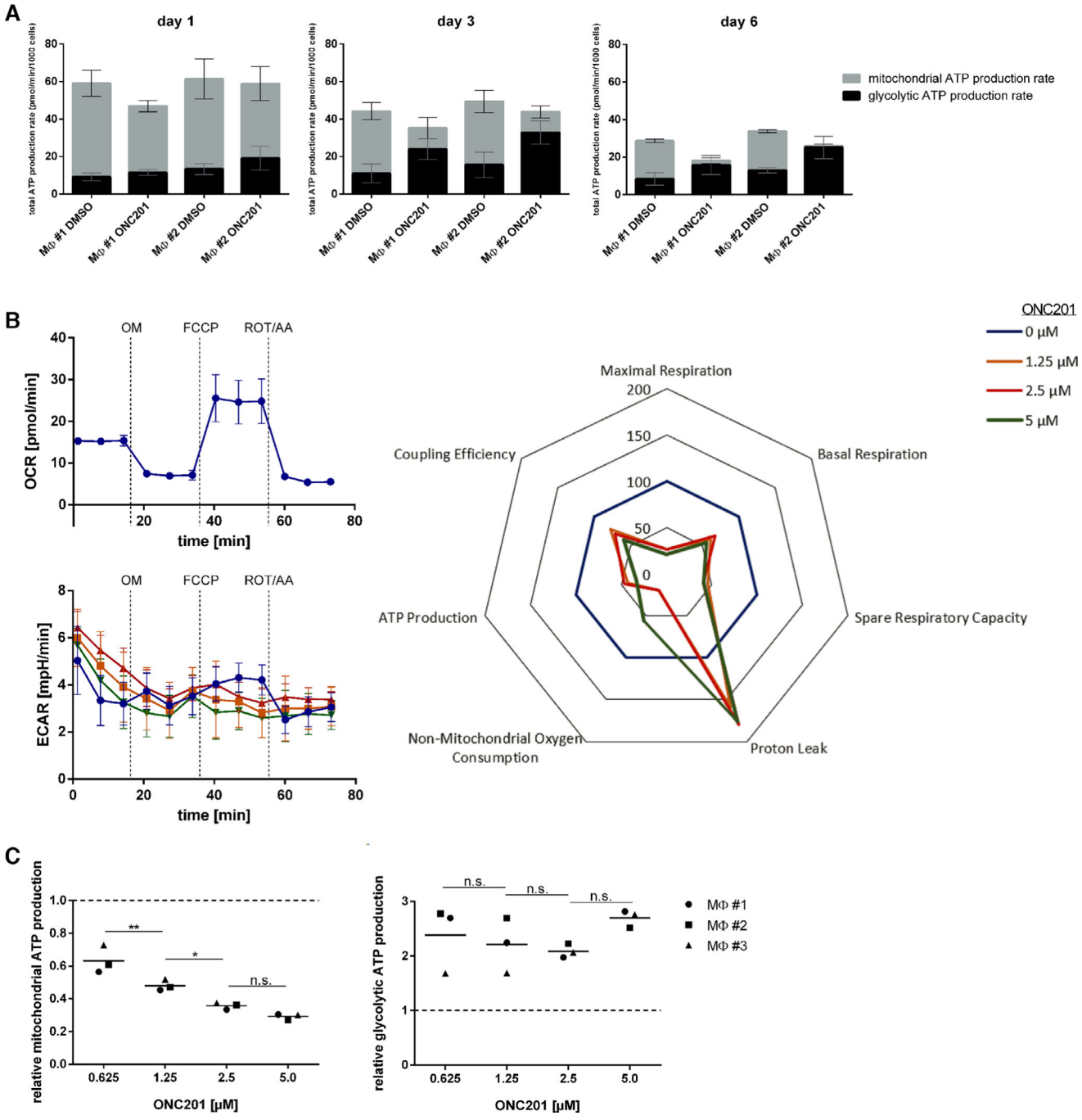

Figure 2. ONC201 reduces mitochondrial integrity and increases glycolytic ATP production rate. ATP production rates were determined by extracellular flux analysis using the Real-Time ATP Rate assay. (A) Mitochondrial and glycolytic ATP production rates of two independent macrophage preparations (MΦ #1, MΦ #2) after treatment with 5 µM ONC201. Data are given as mean ± SEM of four technical replicates from one experiment. (B) Mito Stress Tests: macrophages were treated with indicated doses of ONC201 for three days. Left: OCR and ECAR were calculated based on extracellular flux analysis of these cells sequentially treated with oligomycin (OM), FCCP, and rotenone (ROT) plus antimycin A (AA). Right: Calculated mitochondrial parameters are shown relative to those in DMSO treated macrophages. Data are given as mean ± SEM of four technical replicates and are from one experiment representative of two independent experiments. (C) Relative mitochondrial (left) and glycolytic (right) ATP production by macrophages after three days of treatment with ONC201. Data are from three independent experiments (macrophage preparations MΦ #1, MΦ #2, MΦ #3). Values are normalized to the respective DMSO-treated controls (dashed line) and represent the mean of two independent measurements for each biological sample run in four technical replicates. $^{*}p \leq 0.05$, $^{**}p \leq 0.01$, n.s. = non-significant (two-way ANOVA corrected for multiple comparisons using Tukey test).

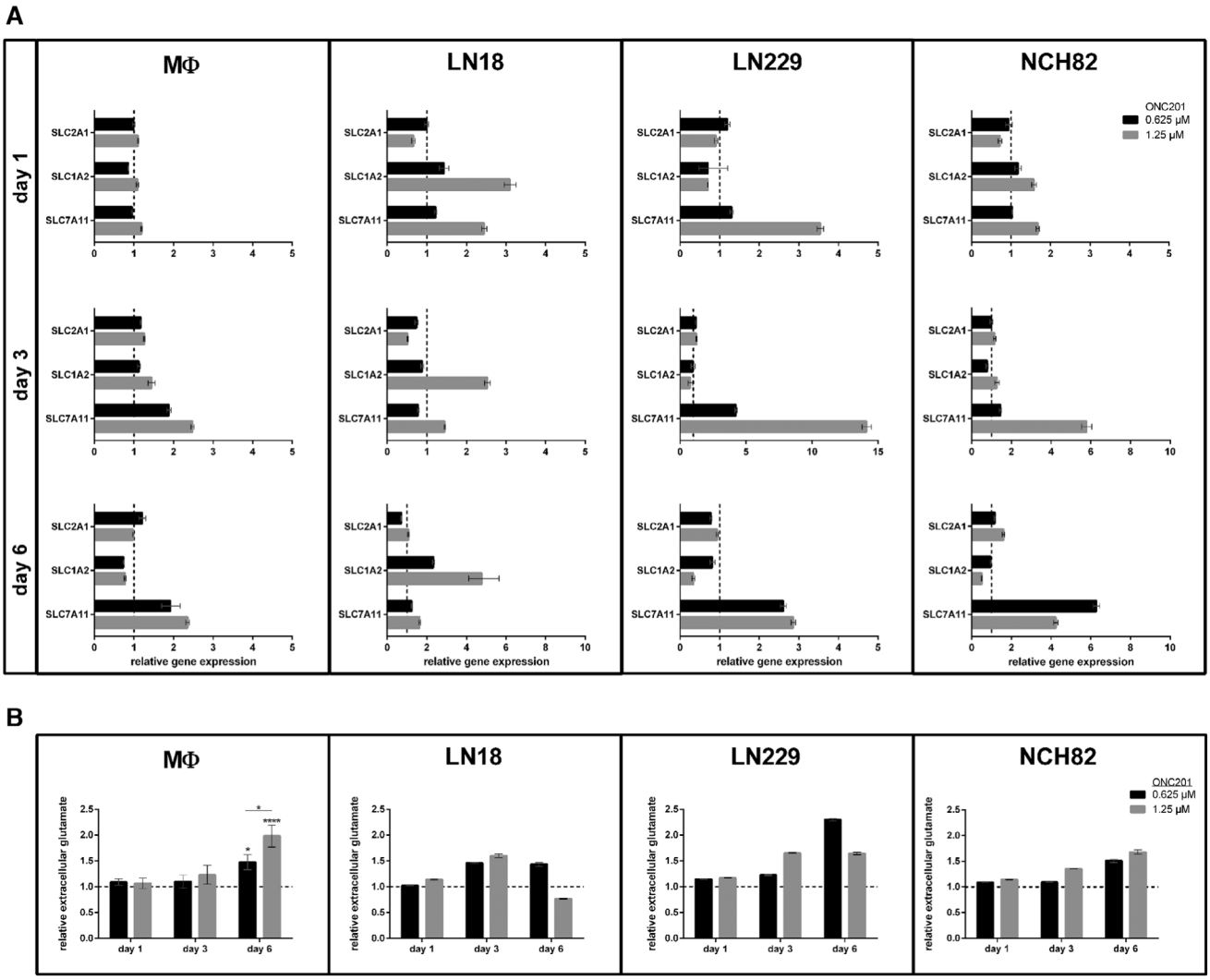

Figure 3. ONC201 induces changes in extracellular glutamate concentrations and expression of metabolic genes. (A) Relative expression levels of *SLC2A1*, *SLC1A2*, and *SLC7A11* were determined by qPCR in ONC201-treated macrophages and GB cells. Values are normalized to the gene expression of the respective DMSO-treated controls (dashed line). Data are given as mean ± SEM of three technical replicates. Macrophages, two independent experiments; GB cells, one experiment. (B) Extracellular glutamate concentrations of macrophages and GB cells treated with ONC201 were determined with the Glutamate-Glo™ Assay. Data are given as mean ± SEM of two technical replicates. Macrophages, six independent experiments; GB cells, one experiment $^{*}p \leq 0.05$, $^{****}p \leq 0.0001$ (two-way ANOVA corrected for multiple comparisons using Tukey test).

amount of glutamate from day 3 of treatment on. The results are in line with the increased expression of *SLC7A11* and the partly decreased expression of *SLC1A2*. Note that the high rate of cytotoxicity in GB cells (Figure 1) possibly explains their lower glutamate concentrations at day 6. Altogether, these data indicate that ONC201 affects glutamate transport in macrophages and enhances its dysregulation in GB cells.

ONC201 induces a pro-inflammatory phenotype in macrophages

Macrophages switching to glycolysis are reported to adopt a pro-inflammatory profile [2]. We characterized the inflammatory status of ONC201-treated macrophages by investigating the expression levels of the pro-inflammatory genes *IL1B* (Interleukin-1ß) and *TNF* (Tumor necrosis factor) and of the anti-inflammatory genes *CD163* (Scavenger receptor cysteine-rich type 1 protein M130) and *CD206* (Macrophage mannose receptor 1). As shown in Figure 4A, *IL1B* expression significantly increased after treatment with 1.25 µM ONC201 for 6 days; the same trend (though not significant, $P = 0.0503$) was observed with 0.625 µM ONC201. Expression levels of *TNF*, *CD163*, and *CD206* were not significantly affected at any time point tested. However, a dose-dependent trend could be detected at day 6 for these genes. *TNF* on the one hand side and *CD163* and *CD206* on the other hand side were more and less expressed, respectively. Together with alterations in *IL1B* expression, these results suggest the

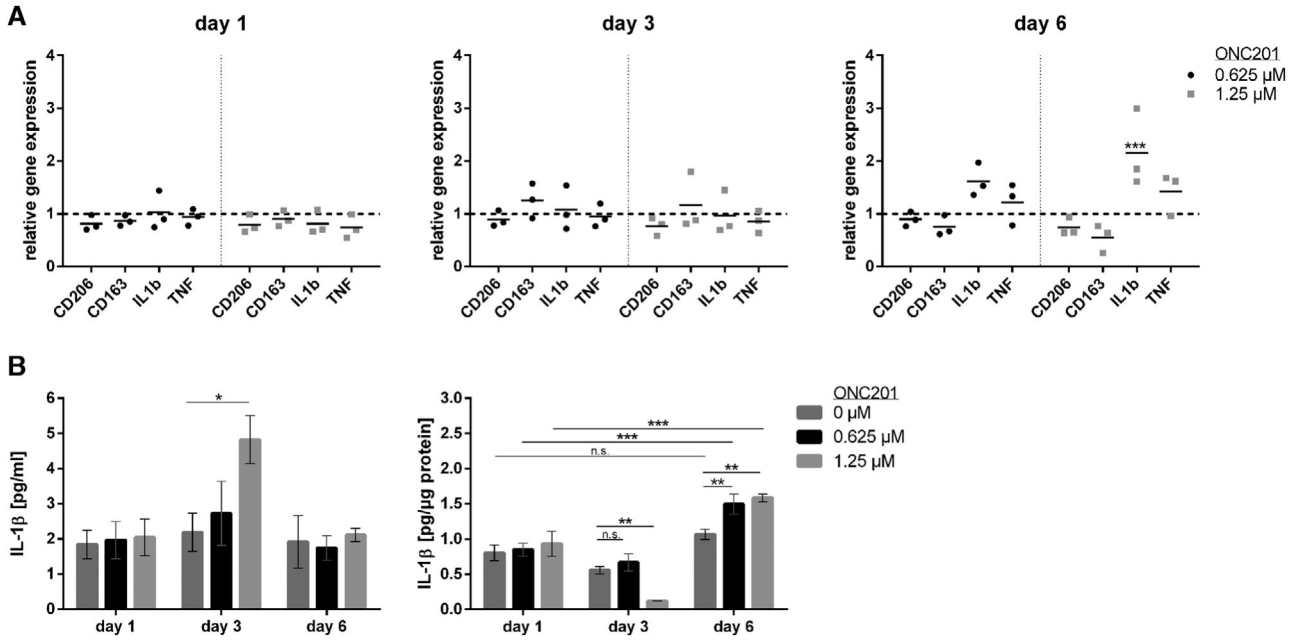

Figure 4. ONC201 induces a pro-inflammatory profile in macrophages. (A) Relative gene expression levels of *CD206*, *CD163*, *IL1B*, and *TNF* in ONC201-treated macrophages were determined by qPCR. Values are normalized to the gene expression of the respective DMSO-treated controls (dashed line). Data are given as mean ± SEM of three technical replicates and are from three independent experiments. (B) Quantification of IL-1ß in the supernatants (left) and cell homogenates (right) of ONC201-treated macrophages using the IL-1ß Human ProQuantum Immunoassay Kit. Values of intracellular IL-1ß are normalized to the total amount of protein used for analysis. Data are given as mean ± SEM of three technical replicates and are from three independent experiments. $^{*}p \leq 0.05$, $^{**}p \leq 0.01$, $^{***}p \leq 0.001$ (two-way ANOVA corrected for multiple comparisons using Tukey test).

acquisition of a pro-inflammatory profile. It is worth mentioning that treatment of macrophages with ONC201 in the presence of pro- or anti-inflammatory molecules induced a time-dependent shift towards a pro-inflammatory profile (Supporting Information Figure S3).

To confirm the effect of ONC201 on *IL1B* and *TNF* expressions, cells and supernatants were tested for the presence of the respective proteins (Figure 4B). TNF-α was detected neither in the supernatants nor in the cells. At day 3, treatment with 1.25 µM ONC201 led to an increased amount of extracellular IL-1ß that correlated with a decreased intracellular amount, suggesting IL-1ß release from an intracellular pool. At day 6, the intracellular level of IL-1ß increased significantly at both ONC201 concentrations while the extracellular level was back to day 1 levels. Furthermore, a comparison of the intracellular levels at day 1 and day 3 with those at day 6 in treated macrophages, indicates an increase in intracellular IL-1ß. Together with the increased gene expression observed in these conditions (Figure 4A), these data suggest not only a replenishment but also an increase of the intracellular IL-1ß pool in macrophages. To conclude, the gene and protein expression analyses suggest that ONC201 shifts macrophages towards a pro-inflammatory phenotype.

Data reported in Figures 1–4 indicate that ONC201 induces a metabolic and pro-inflammatory shift in macrophages. We next investigated whether this profile could be induced by ONC201 in macrophages co-cultured with tumor cells and thus support or even increase the anti-tumor activities of ONC201.

ONC201 activates the DRD2 signaling cascade in macrophages co-cultured with GB cells

We investigated whether co-cultured macrophages react to ONC201 by activating the integrated stress response and by modulating the expression of *DRD5*. Co-cultures of macrophages with each GB cell line were incubated in the absence or presence of ONC201 for 3 and 6 days. We did not test for day 1 because of the lack of visible change in the monocultures at that time. A comparative analysis of the ΔCT values obtained from qPCR analyses of mono- and co-cultured macrophages indicated that, in the presence of GB cells, macrophages decreased their basal expression of *DDIT-3* and increased *DRD5* and *TNFSF10* expression (data not shown). The addition of ONC201 to the co-cultures induced concentration- and time-dependent alterations in the expression levels of the four analyzed genes in macrophages (Figure 5). Similar tendencies were detected irrespective of the GB cell line used. As shown for macrophages in monoculture (Figure 1C), ONC201 increased *DDIT-3* and *DRD5* expression levels. Increase in *DDIT-3* expression was however detected earlier in co-cultured macrophages, possibly due to their lower basal *DDIT-3* expression. Of note, expression of the down-stream target of ATF4, *SLC7A11*, was consistently increased on days 3 and 6 (Figure 6B). *DRD2* and *TNFSF10* expression was slightly enhanced on day 3 but returned to basal levels on day 6, except for *TNFSF10* expression in macrophages co-cultured with NCH82 cells. These latter alterations were not observed in macrophages in monoculture. Altogether these data indicate that the presence of GB cells

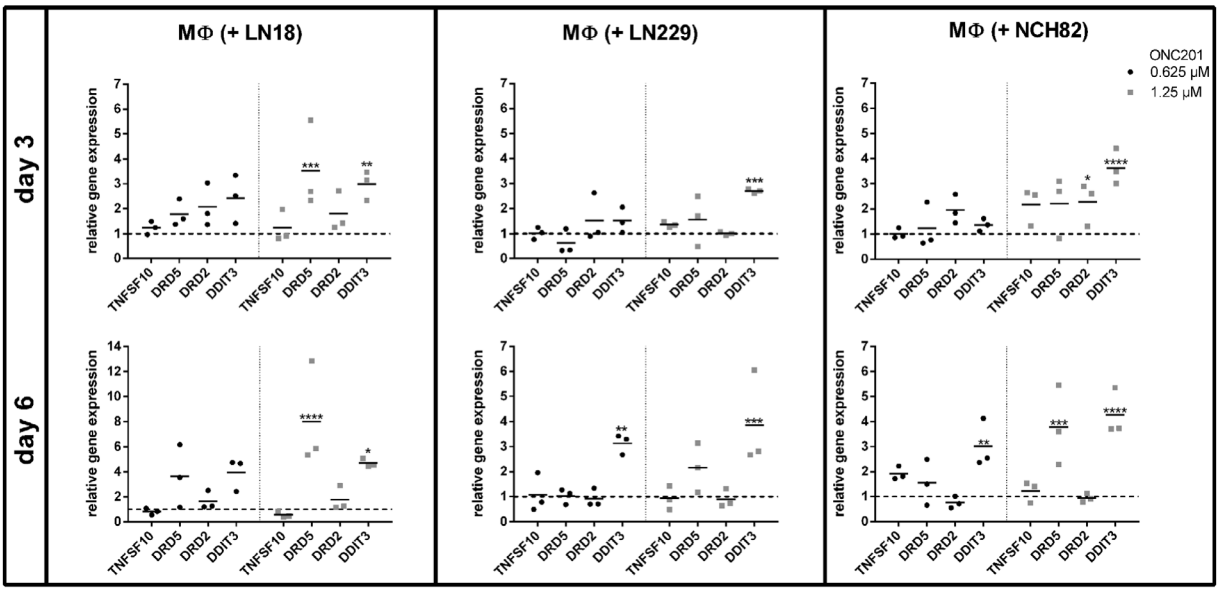

Figure 5. Expression of *TNFSF10*, *DRD5*, *DRD2*, and *DDIT-3* in primary macrophages co-cultured with the respective GB cell line and treated with ONC201. Preparations of macrophages from three different donors were used for co-cultures with GB cells in three independent experiments. Gene expression in macrophages was determined by qPCR. Values are normalized to the gene expression of the respective DMSO-treated controls (dashed line). Data are given as mean ± SEM of the three biological replicates. Each biological replicate was run in three technical replicates. $^{*}p \leq 0.05$, $^{**}p \leq 0.01$, $^{***}p \leq 0.001$, $^{****}p \leq 0.0001$ (two-way ANOVA corrected for multiple comparisons using Tukey test).

did not prevent macrophages to activate the DRD2 signaling cascade in response to ONC201.

ONC201 induces metabolic changes in macrophages/GB cells co-cultures

Technical limitations prevented us to monitor ONC201 effects on energy metabolism at the cell level in the co-culture. We therefore took advantage of the ratio of extracellular lactate and pyruvate that is described as a reliable parameter for estimating the energy state of cells [33]. ONC201 treatment increased this ratio, suggesting that a metabolic switch to glycolysis took place or was enhanced in either macrophages and/or GB cells after treatment (Figure 6A).

We next evaluated changes in glucose and glutamate transport by analyzing *SLC2A1*, *SLC1A2*, and *SLC7A11* expression in macrophages and by measuring the concentration of extracellular glutamate released by the co-cultured cells. As shown in Figure 6B, *SLC2A1* expression was slightly increased at day 3, though non significantly except for the LN229 co-cultures. Similarly, *SLC1A2* expression showed only slight changes at day 3 but not at day 6. As already observed in the monocultures, the clearest effect of ONC201 on co-cultured macrophages was on *SLC7A11* expression which increased in a concentration- and time-dependent manner irrespective of the GB cell line used (Figure 6B). The amount of extracellular glutamate measured at day 3 positively correlated with the increasing concentrations of ONC201 (Figure 6C). At day 6, we observed an ONC201 concentration-dependent decrease of extracellular glutamate in LN18 and NCH82 co-cultures, whereas glutamate levels continued to increase in LN229 co-cultures. Comparison of glutamate concentrations measured in monocultures and co-cultures suggests that most of the glutamate was contributed by GB cells. As shown in Supporting Information Table S1, untreated monocultured macrophages released up to 50 µM glutamate and monocultured GB cells between 100 and 700 µM whereas concentrations in the co-culture supernatants amounted to approximately 50 to 500 µM depending on the GB cell line. This, moreover, indicates a net decrease in the amount of extracellular glutamate that accumulates in co-cultures.

In conclusion, ONC201 induced a global glycolytic shift and altered glutamate transport also in the co-cultures.

Cytotoxicity of ONC201 and inflammatory status of macrophages/GB cells co-cultures

The results above confirmed that ONC201 activated the integrated stress response and induced transcriptional changes in macrophages as well as metabolic changes in the co-cultures. We next assessed whether these changes support an increased cytotoxicity towards GB cells. As shown in Figure 7A and Supporting Information Figure S1B, we observed a trend for GB cells sensitivity to ONC201 in the presence of macrophages which was very similar to that observed in absence of macrophages (Figure 1A, Supporting Information Figure S1A). LN18 cells were the most sensitive to ONC201 cytotoxicity, followed by NCH82 and LN229 cells that were the most resistant. These two latter were even more resistant to ONC201 in the

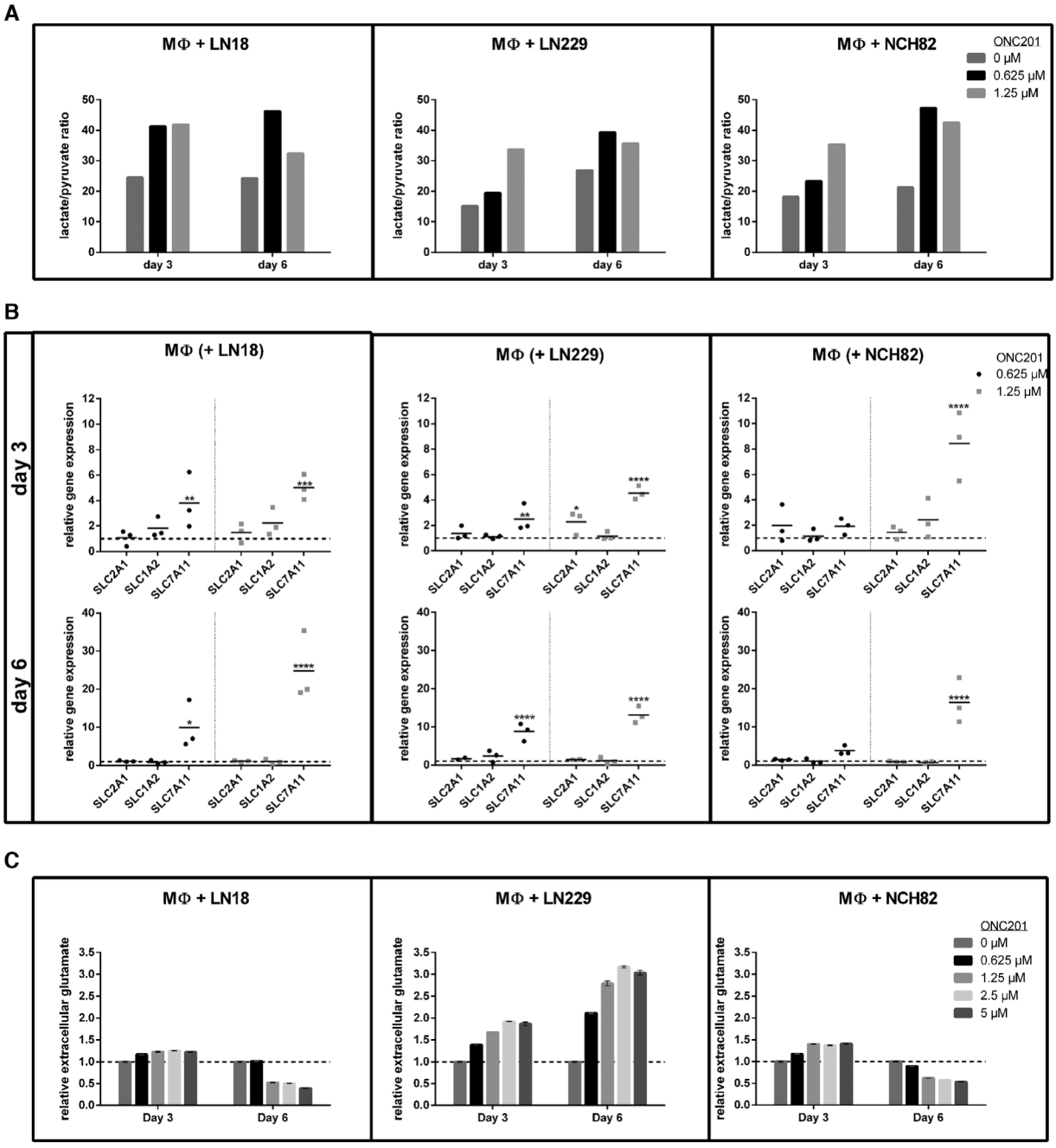

Figure 6. ONC201 induces changes in the energy and glutamate metabolism of co-cultured cells. Supernatants (A, C) and cells (B) harvested from the co-cultures (three independent experiments; same as in Figure 5) were analyzed as follows. (A) The supernatants of the three independent co-cultures were pooled, lactate and pyruvate were measured (technical replicate = 1) and the lactate/pyruvate ratio determined. (B) Relative gene expression levels of *SLC2A1*, *SLC1A2*, and *SLC7A11* were measured in macrophages by qPCR. Values are normalized to the gene expression of the respective DMSO-treated controls (dashed line). Data are given as mean ± SEM of three biological replicates. Each biological replicate was run in three technical replicates. $^{*}p \leq 0.05$, $^{**}p \leq 0.01$, $^{***}p \leq 0.001$, $^{****}p \leq 0.0001$ (two-way ANOVA corrected for multiple comparisons using Tukey test). (C) Extracellular glutamate concentration was determined in the pooled supernatants (same as in panel A) with the Glutamate-Glo™ Assay. Data are given as mean ± SEM of two technical replicates; one measurement was performed.

co-culture as indicated by a higher viability, whereas LN18 cells were still efficiently killed, except at the lowest dose (0.625 µM) of ONC201. Actually, dying LN18 cells most likely triggered the decrease in macrophages viability observed on day 6. Altogether the results reported in Figure 7A indicate that the presence of macrophages was not increasing the efficacy of ONC201 treatment.

We next assessed the inflammatory profile of the co-cultured macrophages. Gene expression analysis indicated a general trend of reduced levels of the anti-inflammatory markers *CD163* and

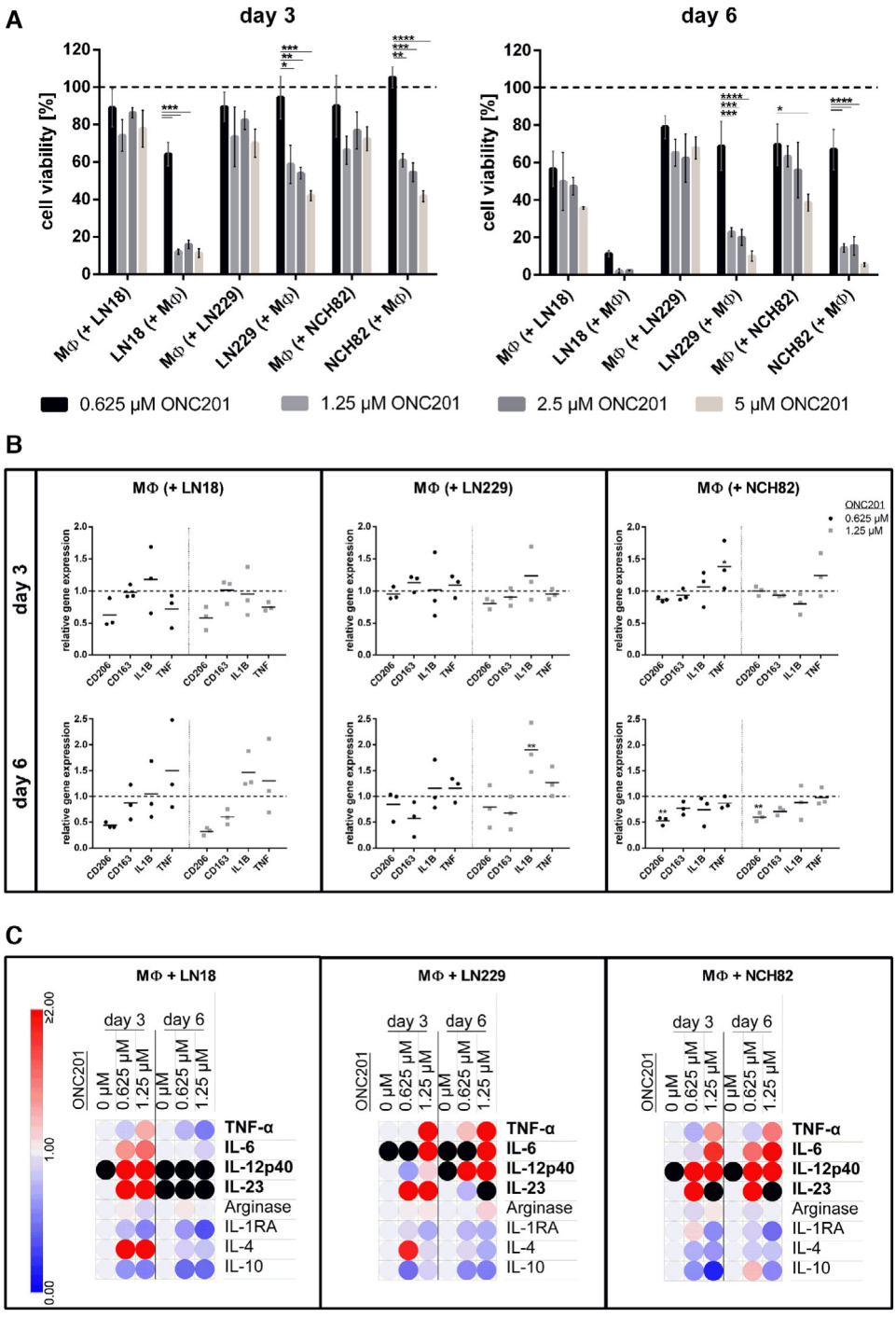

Figure 7. ONC201 induces glioblastoma cell death and a pro-inflammatory profile in the co-culture milieu. Cells and supernatants harvested from the co-cultures (three independent experiments; same as in Figure 5) were analyzed as follows. (A) Cell viability of the co-cultured cells after ONC201 treatment was analyzed with the PrestoBlue reagent. MΦ (+GB cell) = viability of macrophages co-cultured with the respective GB cell line; GB cell (+MΦ) = viability of the respective GB cell line co-cultured with primary macrophages. Values are normalized to the respective DMSO treated controls (dashed line). Data are given as mean ± SEM of the three biological replicates. Each biological replicate was run in three technical replicates. (B) Relative gene expression levels of *CD206*, *CD163*, *IL1B*, *and TNF* were determined by qPCR in macrophages co-cultured with the respective GB cell line and treated with ONC201. Values are normalized to the gene expression of the respective DMSO-treated controls (dashed line). Data are given as mean ± SEM of the three biological replicates . Each biological replicate was run in three technical replicates. $^{*}p \leq 0.05$, $^{**}p \leq 0.01$, $^{***}p \leq 0.001$, $^{****}p \leq 0.0001$ (two-way ANOVA corrected for multiple comparisons using Tukey test). (C) Inflammatory secretome of the co-cultures. The supernatants of the three co-cultures were pooled and analyzed for the indicated molecules with the LEGENDplex™ Human Macrophage/Microglia Panel and the Human ProQuantum Immunoassay Kit. One measurement was performed. Data (mean of two technical replicates ± SEM see Supplementary Table 2 for complete data) are expressed as a heat map (created with [50]). Pro-inflammatory cytokines are written in bold. Color-coding is by mean protein concentration relative to the concentration measured at 0 µM ONC201 at the respective day. In case that molecules were not detectable at 0 µM ONC201, threshold values were used to calculate relative changes. Black dot: not detectable. Measurement was performed once.

CD206 with a significant decrease for this latter in one co-culture. Changes in the expression of the pro-inflammatory markers *TNF* and *IL1B* were minor, with only one significant increase observed for each gene in one co-culture (Figure 7B). This observation suggests that ONC201 mitigates the anti-inflammatory status of macrophages in the presence of GB cells. We further analyzed the secretome of the co-cultures for a set of pro- and anti-inflammatory molecules. As shown in Figure 7C and in Supporting Information Table S2, treatment of each co-culture with ONC201 at 1.25 µM led to an increase in the extracellular concentration of the pro-inflammatory cytokines TNF-α, IL-6, and IL-12p40 and a concomitant decrease of the anti-inflammatory cytokines IL-1RA, IL-4, and IL-10. These changes were stable over the period of time analyzed except for the pro-inflammatory cytokine IL-23 in which production was concentration-dependent. ONC201 treatment did not affect the amount of extracellular arginase, an enzyme that can be produced both by immune and tumor cells and is associated with an anti-inflammatory environment (Supporting

Information Table S2) [34]. IL-1ß, which was secreted by ONC201-treated macrophages (Figure 4B), was not detected in the supernatants of the co-cultures. The consistent shift towards a pro-inflammatory milieu, irrespective of the GB cell line used, was not observed with the lower concentration of ONC201. Note that the cytokine decrease observed at day 6 in the supernatants of co-cultures with the LN18 cells likely results from the decreased number of LN18 cells (see Figure 7A).

Altogether these data suggest that treatment of macrophages/GB cells co-cultures with ONC201, despite inducing a pro-inflammatory shift of the co-culture milieu and decreasing the macrophage anti-inflammatory profile, does not result in an increased onco-toxicity.

Discussion

We hypothesized that ONC201 not only affects GB cells viability but also stimulates the anti-tumor activities of macrophages, by inducing a metabolic and inflammatory switch. We indeed observed that ONC201 reprograms macrophages, as single cells or in co-culture with GB cells. Whereas this reprogramming does not lead to an improved elimination of glioblastoma cells, it contributes to a pro-inflammatory shift of the tumor environment that might provide appropriate conditions for the recruitment and activation of additional immune cells.

Two main modes of action for ONC201-induced cytotoxicity have been described, the most studied being through the antagonism of the DRD2 dopamine receptor leading to TRAIL-dependent or independent cell death [19, 28, 30]. Irrespective of the cell type we analyzed in this study, the cell's sensitivity to ONC201 cytotoxic effects positively correlated with their ratio of *DRD2* and *DRD5* gene expression, not with changes in *TNFSF10* expression. These data are in accordance with reported observations [24, 28] and contribute further support to the use of the *DRD2/DRD5* ratio as an indicator for cell's sensitivity to ONC201 cytotoxicity.

The second mode of action consists in ONC201 binding to and activating the mitochondrial caseinolytic protease P (ClpP) [20, 21], consistent with its targeting of mitochondria [24]. ClpP activation leads to mitochondrial dysfunctions, including inhibition of oxidative phosphorylation. Various facts speak in favor of ClpP activation in ONC201-treated macrophages. A glycolytic switch and severe loss of mitochondria integrity are detected after 3 days of treatment, concomitantly to an increase in *SLC7A11* expression and before an increase in *DDIT-3* expression. These two genes are direct targets of ATF4 of which expression has been reported to increase after ClpP activation [21]. ATF4 thus likely activates *SLC7A11* and *DDIT-3* transcription in macrophages, and might do so in GB cells as well. We hypothesize that macrophages, given their low level of *DRD2* expression, predominantly respond to ONC201 with a mitochondrial stress which, at the ONC201 concentrations used in this study, does not affect -or only minimally- their survival but affects their metabolic and inflammatory status.

Concomitant to the severe loss of mitochondrial integrity, ONC201 induces a time- and concentration-dependent switch to a glycolytic ATP production. This switch is accompanied by alterations in the expression levels of glutamatergic and inflammatory genes. These alterations lead to changes in amounts of extracellular glutamate and cytokines produced by treated macrophages, resulting in a pro-inflammatory profile of macrophages. Whereas the glycolytic switch might be the direct consequence of the integrated stress response induced by ONC201 and inactivation of Akt, a hub for metabolic and inflammatory pathways [35], it might as well be a compensatory mechanism to ensure ATP production in absence of functional mitochondria. Furthermore, it likely triggers the pro-inflammatory profile [2]. Further experiments would be needed to define the cause-to-effect relationship between these events.

The inflammatory reprogramming induced by ONC201 in macrophages might not only rely on the glycolytic switch. CHOP, the product of the *DDIT3* gene is involved in triggering apoptosis and inflammation [36–38]. According to our results, CHOP is more likely to have contributed to inflammation than cell death in ONC201-treated macrophages. It is worth noting that a late increase in *DDIT3* expression was observed in murine macrophages treated with the pro-inflammatory molecule LPS: in those conditions, macrophages did not die but activated the IL-1ß pathway [36]. Dopamine receptors are important players in the regulation of inflammation in the brain levels [39]. Recently, DRD5 has been shown to inhibit NF-kB activation and modulate levels of inflammation [40]. The increased *DRD5* expression induced by ONC201 might reflect the contribution of this receptor signaling in returning macrophages to homeostasis after ONC201 treatment.

Considering that glutamate transport, energy metabolism, and oxidative stress are closely linked [41], ONC201-treated macrophages might first react to the mitochondrial stress by increasing their intracellular glutamate pool to sustain ATP production via the TCA cycle and to generate glutathione for scavenging oxidative species. Excess glutamate however must be removed in time to guarantee homeostasis of the cells and this might be accomplished by the glutamate/cystine antiporter which gene (*SLC7A11)* expression is increased 3 days after ONC201 treatment.

Changes induced by ONC201 in glutamate import/export are also observed in GB cells. They occur from the first day of treatment, indicating a fast adjustment of the cell metabolism to ONC201-induced stress. The increased expression of *SLC7A11* and the extracellular accumulation of glutamate might indicate enhancement of their anti-oxidant response. ONC201-treated LN18 cells are the only cells to react with an increased *SLC1A2* expression. The transporter encoded by this gene facilitates uptake of glutamate but also aspartate which might both be used to fuel the TCA cycle. This increased *SLC1A2* expression is intriguing given its very low or even silenced expression in glioblastoma cells [42] and might indicate an unknown aspect of ONC201 activity.

Given the metabolic shift and pro-inflammatory response of macrophages to ONC201, we expected a decreased proliferation and/or increased death of GB cells in a co-culture model. This is not what we observed at the concentrations tested. A simple explanation might rely on the amount of ONC201 available to both cell types in co-culture. On the one hand side, GB cells that express higher levels of *DRD2* than macrophages might capture more ONC201 and thus mitigate the effects of ONC201 on macrophages. On the other hand side, macrophages, as cells endowed with a high endocytic capacity, certainly take up ONC201 and hence lower the dose that would have led to the death of GB cells if they would have been in monoculture. Whatever the explanation may be, the current data suggest that in presence of ONC201, macrophages do not support tumor growth as they do in its absence [6].

A very interesting effect of ONC201 in the co-culture is the dampening of the anti-inflammatory gene expression profile of macrophages and the sustained change of the extracellular milieu in metabolites and inflammatory molecules. It is beyond our capabilities to determine which cell type contributed to the development of the pro-inflammatory milieu that emerged after ONC201 treatment. IL-23, for instance, is reported to be a direct target of CHOP [37] which gene expression was observed to be upregulated in macrophages and GB cells after ONC201 treatment. ONC201 was reported to increase the secretion of IL-12p70 and TNF-α by colorectal carcinoma cell lines [43]. Thus, not only macrophages but also GB cells might secrete TNF-α after ONC201 treatment. These data indicate that ONC201 is a potentially very interesting modulator of the tumor environment as it can turn it into a pro-inflammatory milieu by targeting both tumor cells and macrophages, thus creating conditions for recruiting and activating other immune cells such as NK- and T-cells. Moreover, ONC201 might protect macrophages from being reprogrammed toward an anti-inflammatory status by GB cells. Indeed, loss of mitochondria integrity, which ONC201 triggers in these immune cells, has been reported to prevent reprogramming of pro-inflammatory macrophages towards an anti-inflammatory status [44].

Although these observations speak for the potential of ONC201 to activate macrophage anti-tumor activities, they emphasize its limitations in a multicellular environment and point to the need of combining it with other drugs. GB cells that resisted six days of treatment expressed a high level of *DRD5*, suggesting DRD5 as a possible target for combinatorial therapy [45, 46]. The glycolytic switch and the correlated glucose uptake represent another interesting target. Pruss et al [45, 46] have demonstrated that combining ONC201 with 2-Deoxyglucose, an analogue of glucose that inhibits its uptake, increased the anti-tumor activities of ONC201. Inhibitors of glucose transporters have recently been shown to kill tumor cells expressing high level of SLC7A11 [45, 46].

In this study, we have addressed ONC201 activities in an *in vitro* cellular system characterized by a high level of heterogeneity. As expected, primary macrophages exhibit inter-individual variations but mount a similar response to ONC201. This response is differently affected by each of the three different GB cell lines, suggesting a context-dependent efficacy of ONC201. We provide first evidence for the potential of ONC201 to act on macrophage plasticity. How these changes operate in ONC201-treated macrophages and other immune cells is worth investigating to develop a more efficient therapeutic use of this drug for cancer therapy.

Material and methods

Monocyte isolation and differentiation into macrophages

Buffy coats were purchased from the Transfusion Center of the University Medical Center of the Johannes Gutenberg University (Mainz, Germany) and were obtained from anonymized healthy blood donors. All buffy coats used in this study are residual biological materials made available by the Transfusion Center to scientists on a randomized basis. Blood samples are collected and processed in accordance with the relevant German guidelines and regulations. Personal data is neither collected nor shared for this material.

Peripheral blood mononuclear cells were isolated from buffy coats using a Ficoll gradient. Monocytes were differentiated with 20 ng/ml macrophage-colony stimulating factor [M-CSF (Biolegend, San Diego, CA, USA)] for one week. Monocyte-derived macrophages were further cultured in absence of M-CSF for another week prior to experiment. A detailed description of the protocol is reported in [13]. At the end of these two weeks, cells displayed the typical morphology of macrophages. Flow cytometry indicated that more than 94% of the cells expressed the CD11b protein (data not shown). Average yield was 1×10^7 -1.5×10^7 macrophages per preparation.

Culture of human primary astrocytes and glioblastoma cell lines

Primary astrocytes purchased from ScienCell (Carlsbad, CA, USA) were cultured at 37°C and 5% CO_2 in astrocyte medium (ScienCell) containing 2% heat-inactivated FCS (Sigma-Aldrich, St. Louis, MO, USA), 1% Astrocyte Growth Supplement (ScienCell) and 50 μg/ml Gentamicin (Gibco Invitrogen, Carlsbad, California, USA). The glioblastoma cell lines LN18 and LN229 were purchased from American Type Culture Collection. The human primary glioblastoma cell line NCH82 was generated at the Department of Neurosurgery, Heidelberg University Hospital (Heidelberg, Germany) [47]. All glioblastoma cell lines were cultured in cDMEM [DMEM (Sigma-Aldrich), 10% heat-inactivated FCS, 2 mM L-Glutamine (Gibco Invitrogen), 50 μg/ml Gentamicin] at 37°C and 5% CO_2.

In vitro cell culture and ONC201 treatment

Monoculture experiments: Cells were seeded in cDMEM in tissue culture (TC) vessels (Greiner Bio-One, Frickenhausen, Germany) and incubated for 24 h (37°C, 5% CO_2). At this time point, the medium was removed and replaced by low serum-containing cDMEM (1% FCS) supplemented with ONC201 (dissolved in DMSO; MedChemExpress, Monmouth Junction, NJ, USA) or the respective volume of DMSO (Sigma-Aldrich). Plates were further incubated for one to six days (37°C, 5% CO_2) before analysis. Low serum-containing cDMEM was used to decrease potential side effects of FCS components during treatment. One preparation of macrophages was used for one independent experiment unless otherwise stated.

Co-culture experiments: Glioblastoma cells were seeded in cDMEM onto TC inserts with 0.4 μm membrane (Sarstedt, Nümbrecht, Germany). Macrophages were seeded in cDMEM on 6-well plates. Glioblastoma cells and macrophages were incubated for 24 h (37°C, 5% CO_2). Thereafter, the medium was removed and replaced by low serum-containing cDMEM (1% FCS) supplemented with ONC201 or the respective volume of DMSO. Inserts were placed into the vessels containing macrophages and plates were incubated for three to six days (37°C, 5% CO_2) before analysis. Three independent co-culture experiments each using a macrophage preparation from a different donor, were conducted; each condition was tested in duplicate. Analysis of the cells and supernatants harvested from these co-cultures is presented in Figures 5–7, Supplementary Fig 1B and Supplementary Tables 1 and 2.

Determination of cell viability

Analysis with the Presto Blue reagent: after one to six days of treatment, PrestoBlue™ Cell viability reagent (ThermoFisher Scientific, Waltham, MA, USA) was added directly to the wells in the culture medium, according to manufacturers' instructions. After 30 min of incubation at 37°C (5% CO_2) fluorescence was measured using an Infinite® 200 PRO multiplate reader (Tecan, Männedorf, Switzerland) and cell viability calculated as described in the manufacturers' protocol.

Analysis with the crystal violet staining assay: after one to six days of treatment, cell culture supernatants were removed, cells washed with PBS and stained with crystal violet solution [0.1% crystal violet (Sigma-Aldrich) in 2% Ethanol (Carl Roth, Karlsruhe, Germany)] for 10 min at room temperature. After removal of the staining solution, cells were washed three times with H_2O and plates air-dried upside down. To solubilize the stain, 1% SDS (Carl Roth) was added and plates put on a shaker until the dye was completely dissolved. For quantification, absorbance was measured at 570 nm using an Infinite® 200 PRO multiplate reader (Tecan).

Extracellular flux measurements

Measurements of oxygen consumption rate (OCR) and extracellular acidification rate (ECAR) were performed using the XF96e Extracellular Flux analyzer (Agilent Technologies, Santa Clara, CA, USA). Macrophages were plated in cDMEM into XF96 (V3) polystyrene cell culture plates (Agilent Technologies). After 24 h, cells were treated with ONC201 for one to six days and incubated under standard conditions. Prior to performing the assay, the medium was exchanged with the XF assay medium [XF RPMI with 1 mM HEPES (Agilent Technologies) supplemented with 1 mM Pyruvate (Sigma-Aldrich), 2 mM L-Glutamine (Sigma-Aldrich), 10 mM Glucose (Sigma-Aldrich)]. Three baseline measurements were taken prior to addition of any compound and three response measurements were taken after addition of each compound. For Real-Time ATP Rate Assay, sequential injections of ATP Synthase inhibitor Oligomycin (final concentration 1.5 μM), Complex 1 Inhibitor Rotenone and Complex 3 inhibitor Antimycin A (each 0.5 μM) were applied. For Mito Stress Tests, Oligomycin (1.5 μM), Carbonyl cyanide-4 (trifluoromethoxy)phenylhydrazone (FCCP; 1 μM) and Rotenone/Antimycin A (0.5 μM each) were used. ECAR (mpH/min) and OCR (pmoles/min) are reported as absolute rates normalized against cell counts. Cell counts were obtained post flux measurements using the EarlyTox integrity assay (Molecular devices, San Jose, CA, USA) according to manufacturers' instructions. Cells were imaged with a SpectraMax MiniMax 300 Imaging Cytometer (Molecular Devices) using green (541 nm emission) and red (713 nm emission) channels. Cell nuclei were automatically identified by setting size and threshold for object identification in the red channel.

Analysis and quantification of extracellular metabolites and cytokines

Supernatants from the three co-cultures were pooled according to conditions and immediately centrifuged (10 min, 400 rcf, 4°C). Aliquots from each pooled supernatant were prepared. Aliquots saved for the determination of glutamate were diluted (1:40) in ice-cold PBS and stored at -80°C. Aliquots saved for the determination of extracellular lactate and pyruvate, and extracellular cytokines (see below) were stored undiluted at -80°C.

Concentration of extracellular glutamate in cell culture supernatants was determined with the Glutamate-Glo™ Assay (Promega, Madison, WI, USA). The assay was performed according to manufacturers' instructions.

Determination of extracellular lactate and pyruvate was adapted from Uran et al [48]. Supernatants were diluted with ultra-pure water 1:10 (v/v) and mixed with ice-cold methanol 1:4.5 (v/v). 50 μl of these extracts were mixed with 25 μl 140 mM 3-Nitrophenylhydrazine hydrochloride (Sigma-Aldrich), 25 μl methanol, and 100 μl 50 mM Ethyl-3-(3-dimethylaminopropyl) carbodiimide hydrochloride (Sigma–Aldrich) and incubated for 20 min at 60°C. Separation was carried out using an Acquity

H-class UPLC system coupled to a QDa mass detector (Waters, Milford, MA, USA) using an Acquity HSS T3 column (100 mm × 2.1 mm, 1.8 μm, Waters) heated to 40°C. Separation of derivates was achieved by increasing the concentration of 0.1 % formic acid in acetonitrile (B) in 0.1% formic acid in water (A) at 0.55 ml/min as follows: 2 min 15% B, 2.01 min 31% B, 5 min 54% B, 5.01 min 90% B, hold for 2 min, and return to 15% B in 2 min. Mass signals for the following compounds were detected in single ion record mode using negative detector polarity and 0.8 kV capillary voltage: Lactate (224.3 *m/z*; 25 V CV) and pyruvate (357.3 *m/z*; 15 V).

The concentration of extracellular cytokines was determined as follows. Supernatants and cells were harvested from monocultures of macrophages after ONC201 treatment. Supernatants were centrifuged (10 min, 400 rcf, 4°C), aliquoted and stored at -80°C. Cells were lysed in Triton-X 100 buffer (150 mM NaCl [Carl Roth], 1.0% [v/v] Triton X-100 [Carl Roth], 50 mM Tris-HCl [Carl Roth], pH 7.4) supplemented with freshly added protease inhibitor [cOmplete, Roche Diagnostics GmbH, Mannheim, Germany] and their protein content measured with the bicinchoninic acid assay (ThermoFisher Scientific). After adjusting the protein concentrations to equal levels, the samples of the three preparations were pooled. IL-1ß and TNF-α were measured in supernatants and cell lysates using Human ProQuantum Immunoassay Kits (ThermoFisher Scientific) according to manufacturers' instructions.

Co-culture supernatants were analyzed using the LEGENDplex™ Human Macrophage/Microglia Panel (BioLegend) and an Attune NxT Flow cytometer (ThermoFisher Scientific). The panel of analyzed cytokines is composed of IL-12p70, TNF-α, IL-6, IL-4, IL-10, IL-1β, Arginase, TARC, IL-1RA, IL-12p40, IL-23, IFN- γ, and IP-10. Since the concentrations of IL-4 and IL-10 were below the detection limit, we used the Human ProQuantum Immunoassay Kit (ThermoFisher Scientific) for quantification of these cytokines. The assays were performed according to manufacturers' instructions.

Total RNA isolation, cDNA transcription, and gene expression profiling

After PrestoBlue incubation, cells were washed with PBS and total RNA isolation was performed using RNeasy Mini Kit (Qiagen, Hilden, Germany) according to manufacturers' instructions. RNA concentration and quality were determined using a Nanodrop 2200 (ThermoFisher Scientific). Only samples showing a 260/280 nm ratio between 1.8 and 2.1 were selected for cDNA transcription performed with the FastGene Scriptase II - Ready Mix (NIPPON Genetics Europe, Düren, Germany). Quantitative PCR (qPCR) analysis was done using TaqMan® primers and a StepOnePlus System (Applied Biosystems, Foster City, CA, USA). Briefly, for each well of the 96-well qPCR plate (Sarstedt), 10 μl of qPCRBIO Probe Mix (NIPPON Genetics Europe) were mixed with 5 ng cDNA, 1 μl of the appropriate primer (Table 1), and 4 μl H_2O. Relative quantification (RQ) of gene expression was determined using the $2^{-\Delta\Delta Ct}$ method [49]. Reference genes: *SDHA* and *HPRT1* were used in PCR conducted with samples of monocyte-derived macrophages; *SDHA* was used for analyses of astrocytes and tumor cells.

Table 1. List of TaqMan® primers used for qPCR

Target gene (associated protein)	Assay ID
CD163 (Scavenger receptor cysteine-rich type 1 protein M130)	Hs00174705_m1
CD206 (Macrophage mannose receptor 1)	Hs00267207_m1
DDIT-3 (DNA damage-inducible transcript 3 protein)	Hs00358796_g1
DRD2 (D(2) dopamine receptor)	Hs00241436_m1
DRD5 (D(1B) dopamine receptor)	Hs00361234_s1
HPRT1 (Hypoxanthine-guanine phosphoribosyltransferase)	Hs02800695_m1
IL1B (Interleukin-1 beta)	Hs01555410_m1
SDHA (Succinate dehydrogenase (ubiquinone) flavoprotein subunit, mitochondrial)	Hs00188166_m1
SLC1A2 (Glutamine synthetase)	Hs01102423_m1
SLC2A1 (Solute carrier family 2, facilitated glucose transporter member 1)	Hs00892681_m1
SLC7A11 (Cystine/glutamate transporter)	Hs00921938_m1
TNF (Tumor necrosis factor)	Hs00174128_m1
TNFSF10 (Tumor necrosis factor ligand superfamily member 10)	Hs00921974_m1

Statistics

Statistical analysis was performed using GraphPad Prism software. The difference between means of unpaired samples was performed using two-way ANOVA with a significance defined by an α of 0.05. The resulting p-values were corrected for multiple comparisons using the Tukey test. $*p \leq 0.05$, $**p \leq 0.01$, $***p \leq 0.001$, $****p \leq 0.0001$.

Acknowledgments: We thank the Metabolomics Core Technology Platform of the Excellence cluster "CellNetworks" (University of Heidelberg) for support with UPLC-based metabolite quantification. C.G. was supported by the FAZIT-STIFTUNG, G.P. by the Deutsche Forschungsgemeinschaft (grant ZUK 40/2010-3009262) and W.R. by the Alexander von Humboldt Foundation and the Boehringer Ingelheim Foundation. The graphical abstract was created with BioRender.com.
Open access funding enabled and organized by Projekt DEAL.

Author contributions: C.G., C.W., and A.R.-V. were associated with conception and design of the work. C.G., C.W., and G.P. performed experimental work and acquisition of data. C.G., C.W., and

G.P. performed the analysis of data. C.G., C.W., G.P., and A.R.-V. were associated with the interpretation of data. C.G. and A.R.-V. drafted the manuscript. C.G., C.W., G.P., W.R., and A.R.-V. were associated with critical revision for important intellectual content. All authors read and approved the final manuscript.

Conflict of interest: The authors declare no commercial or financial conflict of interest.

Peer review: The peer review history for this article is available at https://publons.com/publon/10.1002/eji.202048957

Data availability statement: The datasets generated and analyzed during the current study are available from the corresponding author upon reasonable request.

References

1 **Locati, M.**, **Curtale, G.**, and **Mantovani, A.**, Diversity, Mechanisms, and Significance of Macrophage Plasticity. *Annu. Rev. Pathol. Mech. Dis.* 2020. **15**: 123–147.

2 **Viola, A.**, **Munari, F.**, **Sánchez-Rodríguez, R.**, **Scolaro, T.**, and **Castegna, A.**, The metabolic signature of macrophage responses. *Front. Immunol.* 2019. **10**. https://doi.org/10.3389/fimmu.2019.01462.

3 **Lewis, C. E.**, and **Pollard, J. W.**, Distinct role of macrophages in different tumor microenvironments. *Cancer Res*. 2006. **66**: 605–612.

4 **Kim, J.**, and **Bae, J. S.**, Metabolic regulation of macrophages in tumor microenvironment. *Curr. Opin. Hematol.* 2018. **25**: 52–59.

5 **Ohgaki, H.**, and **Kleihues, P.**, The definition of primary and secondary glioblastoma. *Clin. Cancer Res.* 2013. **19**: 764–772.

6 **Wei, J.**, **Chen, P.**, **Gupta, P.**, **Ott, M.**, **Zamler, D.**, **Kassab, C.**, and **Bhat, K. P.** et al., Immune biology of glioma-associated macrophages and microglia: functional and therapeutic implications. *Neuro. Oncol.* 2020. **22**: 180–194.

7 **Poon, C. C.**, **Sarkar, S.**, **Yong, V. W.**, and **Kelly, J. J. P.**, Glioblastoma-associated microglia and macrophages: Targets for therapies to improve prognosis. *Brain*. 2017. **140**: 1548–1560.

8 **Kees, T.**, **Lohr, J.**, **Noack, J.**, **Mora, R.**, **Gdynia, G.**, **Tödt, G.**, and **Ernst, A.** et al., Microglia isolated from patients with glioma gain antitumor activities on poly (I:C) stimulation. *Neuro. Oncol*. 2012. **14**: 64–78.

9 **Soga, T.**, Cancer metabolism: Key players in metabolic reprogramming. *Cancer Sci*. 2013. **104**: 275–281.

10 **Ye, Z. C.**, and **Sontheimer, H.**, Glioma cells release excitotoxic concentrations of glutamate. *Cancer Res*. 1999. **59**: 4383–4391.

11 **Corsi, L.**, **Mescola, A.**, and **Alessandrini, A.**, Glutamate Receptors and Glioblastoma Multiforme: An Old "Route" for New Perspectives. *Int. J. Mol. Sci.* 2019. **20**: 1796.

12 **Choi, J.**, **Stradmann-Bellinghausen, B.**, **Yakubov, E.**, and **Savaskan, N. E.**, Regnier-Vigouroux A. Glioblastoma cells induce differential glutamatergic gene expressions in human tumor-associated microglia/macrophages and monocyte-derived macrophages. *Cancer Biol. Ther.* 2015. https://doi.org/10.1080/15384047.2015.1056406.

13 **Geiß, C.**, **Alanis-Lobato, G.**, **Andrade-Navarro, M.**, and **Régnier-Vigouroux, A.**, Assessing the reliability of gene expression measurements in very-low-numbers of human monocyte-derived macrophages. *Sci. Rep.* 2019. **9**: 17908.

14 **Abuawad, A.**, **Mbadugha, C.**, **Ghaemmaghami, A. M.**, and **Kim, D. H.**, Metabolic characterisation of THP-1 macrophage polarisation using LC–MS-based metabolite profiling. *Metabolomics*. 2020. **16**: 1–14.

15 **Ralff, M. D.**, **Lulla, A. R.**, **Wagner, J.**, and **El-Deiry, W. S.**, ONC201: a new treatment option being tested clinically for recurrent glioblastoma. *Transl. Cancer Res.* 2017. **6**: S1239–S1243.

16 **Karpel-Massler, G.**, and **Siegelin, M. D.**, TIC10/ONC201-a potential therapeutic in glioblastoma. *Transl. Cancer Res.* 2017. **6**: S1439–S1440.

17 **Arrillaga-Romany, I.**, **Chi, A. S.**, **Allen, J. E.**, **Oster, W.**, **Wen, P. Y.**, and **Batchelor, T. T.**, A phase 2 study of the first imipridone ONC 201, a selective DRD 2 antagonist for oncology, administered every three weeks in recurrent glioblastoma. *Oncotarget*. 2017. **8**: 79298–79304.

18 **Stein, M. N.**, **Bertino, J. R.**, **Kaufman, H. L.**, **Mayer, T.**, **Moss, R.**, **Silk, A.**, and **Chan, N.** et al., First-in-Human Clinical Trial of Oral ONC201 in Patients with Refractory Solid Tumors. *Clin. Cancer Res.* 2017. **23**: 4163–4169.

19 **Madhukar, N. S.**, **Khade, P. K.**, **Huang, L.**, **Gayvert, K.**, **Galletti, G.**, **Stogniew, M.**, and **Allen, J. E.** et al., A Bayesian machine learning approach for drug target identification using diverse data types. *Nat. Commun.* 2019. **10**: 5221.

20 **Graves, P. R.**, **Aponte-Collazo, L. J.**, **Fennell, E. M. J.**, **Graves, A. C.**, **Hale, A. E.**, **Dicheva, N.**, and **Herring, L. E.** et al., Mitochondrial Protease ClpP is a Target for the Anticancer Compounds ONC201 and Related Analogues. *ACS Chem. Biol.* 2019. **14**: 1020–1029.

21 **Ishizawa, J.**, **Zarabi, S. F.**, **Davis, R. E.**, **Halgas, O.**, **Nii, T.**, **Jitkova, Y.**, and **Zhao, R.** et al., Mitochondrial ClpP-Mediated Proteolysis Induces Selective Cancer Cell Lethality. *Cancer Cell.* 2019. **35**: 721–737.e9.

22 **Allen, J. E.**, **Krigsfeld, G.**, **Patel, L.**, **Mayes, P. A.**, **Dicker, D. T.**, **Wu, G. S.**, and **El-Deiry, W. S.**, Identification of TRAIL-inducing compounds highlights small molecule ONC201/TIC10 as a unique anti-cancer agent that activates the TRAIL pathway. *Mol. Cancer.* 2015. **14**. https://doi.org/10.1186/s12943-015-0346-9.

23 **Kline, C. L. B.**, **Van Den Heuvel, A. P. J.**, **Allen, J. E.**, **Prabhu, V V.**, and **Dicker, D. T.**, El-Deiry WS. ONC201 kills solid tumor cells by triggering an integrated stress response dependent on ATF4 activation by specific eIF2a kinases. *Sci. Signal.* 2016. **9**: ra18.

24 **Greer, Y. E.**, **Porat-Shliom, N.**, **Nagashima, K.**, **Stuelten, C.**, **Crooks, D.**, **Koparde, V. N.**, and **Gilbert, S. F.** et al., ONC201 kills breast cancer cells in vitro by targeting mitochondria. *Oncotarget*. 2018. **9**: 18454–18479.

25 **Ishida, C. T.**, **Zhang, Y.**, **Bianchetti, E.**, **Shu, C.**, **Nguyen, T. T. T.**, **Kleiner, G.**, and **Sanchez-Quintero, M. J.** et al., Metabolic reprogramming by dual AKT/ERK inhibition through imipridones elicits unique vulnerabilities in glioblastoma. *Clin. Cancer Res.* 2018. **24**: 5392–5406.

26 **Pruss, M.**, **Dwucet, A.**, **Tanriover, M.**, **Hlavac, M.**, **Kast, R. E.**, **Debatin, K. M.**, and **Wirtz, C. R.** et al., Dual metabolic reprogramming by ONC201/TIC10 and 2-Deoxyglucose induces energy depletion and synergistic anti-cancer activity in glioblastoma. *Br. J. Cancer.* 2020. https://doi.org/10.1038/s41416-020-0759-0.

27 **Zhao, R.**, **Li, Y.**, **Gorantla, S.**, **Poluektova, L. Y.**, **Lin, H.**, **Gao, F.**, and **Wang, H.** et al., Small molecule ONC201 inhibits HIV-1 replication in macrophages via FOXO3a and TRAIL. *Antiviral Res*. 2019. **168**: 134–145.

28 **Prabhu, V. V.**, **Madhukar, N. S.**, **Gilvary, C.**, **Kline, C. L. B.**, **Oster, S.**, **El-Deiry, W. S.**, and **Elemento, O.** et al., Dopamine Receptor D5 is a Modulator of Tumor Response to Dopamine Receptor D2 Antagonism. *Clin. Cancer Res.* 2019. **25**: 2305–2313.

29 **Allen, J. E.**, **Krigsfeld, G.**, **Mayes, P. A.**, **Patel, L.**, **Dicker, D. T.**, **Patel, A. S.**, and **Dolloff, N. G.** et al., Dual inactivation of Akt and ERK by TIC10 signals Foxo3a nuclear translocation, TRAIL gene induction, and potent antitumor effects. *Sci. Transl. Med.* 2013. **5**: 171ra17.

30 **Kline, C. L. B.**, **Ralff, M. D.**, **Lulla, A. R.**, **Wagner, J. M.**, **Abbosh, P. H.**, **Dicker, D. T.**, and **Allen, J. E.** et al., Role of Dopamine Receptors in the Anticancer Activity of ONC201. *Neoplasia (United States)*. 2018. **20**: 80–91.

31 **Beaulieu, J. M.**, **Espinoza, S.**, and **Gainetdinov, R. R.**, Dopamine receptors - IUPHAR review 13. *Br. J. Pharmacol.* 2015. **172**: 1–23.

32 **Lewerenz, J.**, **Sato, H.**, **Albrecht, P.**, **Henke, N.**, **Noack, R.**, **Methner, A.**, and **Maher, P.**, Mutation of ATF4 mediates resistance of neuronal cell lines against oxidative stress by inducing xCT expression. *Cell Death Differ*. 2012. **19**: 847–858.

33 **Zoremba, N.**, **Homola, A.**, **Rossaint, R.**, and **Syková, E.**, Interstitial lactate, lactate/pyruvate and glucose in rat muscle before, during and in the recovery from global hypoxia. *Acta Vet. Scand.* 2014. **56**: 72.

34 **Grzywa, T. M.**, **Sosnowska, A.**, **Matryba, P.**, **Rydzynska, Z.**, **Jasinski, M.**, **Nowis, D.**, and **Golab, J.**, Myeloid Cell-Derived Arginase in Cancer Immune Response. *Front. Immunol.* 2020. **11**: 938.

35 **Covarrubias, A. J.**, **Aksoylar, H. I.**, and **Horng, T.**, Control of macrophage metabolism and activation by mTOR and Akt signaling. *Semin. Immunol.* 2015. **27**: 286–296.

36 **Nakayama, Y.**, **Endo, M.**, **Tsukano, H.**, **Mori, M.**, **Oike, Y.**, and **Gotoh, T.**, Molecular mechanisms of the LPS-induced non-apoptotic ER stress-CHOP pathway. *J. Biochem.* 2010. **147**: 471–483.

37 **Goodall, J. C.**, **Wu, C.**, **Zhang, Y.**, **McNeill, L.**, **Ellis, L.**, **Saudek, V.**, and **Gaston, J. S. H.**, Endoplasmic reticulum stress-induced transcription factor, CHOP, is crucial for dendritic cell IL-23 expression. *Proc. Natl. Acad. Sci. U. S. A.* 2010. **107**: 17698–17703.

38 **Li, Y.**, **Guo, Y.**, **Tang, J.**, **Jiang, J.**, and **Chen, Z.**, New insights into the roles of CHOP-induced apoptosis in ER stress. *Acta Biochim. Biophys. Sin. (Shanghai)*. 2014. **46**: 629–640.

39 **Xia, Q. P.**, **Cheng, Z. Y.**, and **He, L.**, The modulatory role of dopamine receptors in brain neuroinflammation. *Int. Immunopharmacol.* 2019. **76**: 105908.

40 **Wu, Y.**, **Hu, Y.**, **Wang, B.**, **Li, S.**, **Ma, C.**, **Liu, X.**, and **Moynagh, P. N.** et al., Dopamine Uses the DRD5-ARRB2-PP2A Signaling Axis to Block the TRAF6-Mediated NF-κB Pathway and Suppress Systemic Inflammation. *Mol. Cell.* 2020. **78**: 42–56.e6.

41 **Gras, G.**, **Porcheray, F.**, **Samah, B.**, and **Leone, C.**, The glutamate-glutamine cycle as an inducible, protective face of macrophage activation. *J. Leukoc. Biol.* 2006. **80**: 1067–1075.

42 **de Groot, J.**, and **Sontheimer, H.**, Glutamate and the biology of gliomas. *Glia*. 2011. **59**: 1181–1189.

43 **Wagner, J.**, **LeahKline, C.**, **Zhou, L.**, **Campbell, K. S.**, **MacFarlane, A. W.**, **Olszanski, A. J.**, and **Cai, K. Q.** et al., Dose intensification of TRAIL-inducing ONC201 inhibits metastasis and promotes intratumoral NK cell recruitment. In: *Journal of Clinical Investigation*.Vol **128**. American Society for Clinical Investigation. 2018: 2325–2338. https://doi.org/10.1172/JCI96711.

44 **Van den Bossche, J.**, **Baardman, J.**, **Otto, N. A.**, **van der Velden, S.**, **Neele, A. E.**, **van den Berg, S. M.**, and **Luque-Martin, R.** et al., Mitochondrial Dysfunction Prevents Repolarization of Inflammatory Macrophages. *Cell Rep*. 2016. **17**: 684–696.

45 **Leng, Z. G.**, **Lin, S. J.**, **Wu, Z. R.**, **Guo, Y. H.**, **Cai, L.**, **Shang, H. B.**, and **Tang, H.** et al., Activation of DRD5 (dopamine receptor D5) inhibits tumor growth by autophagic cell death. *Autophagy*. 2017. **13**: 1404–1419.

46 **Liu, X.**, **Olszewski, K.**, **Zhang, Y.**, **Lim, E. W.**, **Shi, J.**, **Zhang, X.**, and **Zhang, J.** et al., Cystine transporter regulation of pentose phosphate pathway dependency and disulfide stress exposes a targetable metabolic vulnerability in cancer. *Nat. Cell Biol.* 2020. **22**: 476–486.

47 **Karcher, S.**, **Steiner, H. H.**, **Ahmadi, R.**, **Zoubaa, S.**, **Vasvari, G.**, **Bauer, H.**, and **Unterberg, A.** et al., Different angiogenic phenotypes in primary and secondary glioblastomas. *Int. J. Cancer.* 2006. **118**: 2182–2189.

48 **Uran, S.**, **Landmark, K. E.**, **Hjellum, G.**, and **Skotland, T.**, Quantification of 13C pyruvate and 13C lactate in dog blood by reversed-phase liquid chromatography-electrospray ionization mass spectrometry after derivatization with 3-nitrophenylhydrazine. *J. Pharm. Biomed. Anal.* 2007. **44**: 947–954.

49 **Livak, K. J.**, and **Schmittgen, T. D.**, Analysis of Relative Gene Expression Data Using Real-Time Quantitative PCR and the $2-\Delta\Delta CT$ Method. *Methods*. 2001. **25**: 402–408.

50 **broadinstitute.org**. **Morpheus**. Available at: https://software.broadinstitute.org/morpheus [Accessed November 2, 2020].

Abbreviations: **DRD2**: dopamine receptor D2 · **GB**: glioblastoma · **OXPHOS**: oxidative phosphorylation · **TAM**: tumor-associated macrophage

Full correspondence: Dr. Anne Régnier-Vigouroux, Institute of Developmental Biology & Neurobiology, Johannes Gutenberg Universität-Mainz, Germany
e-mail: vigouroux@uni-mainz.de

Received: 7/9/2020
Revised: 23/11/2020
Accepted: 12/1/2021
Accepted article online: 13/1/2021

Supporting information

Metabolic and inflammatory reprogramming of macrophages by ONC201 translates in a pro-inflammatory environment even in presence of glioblastoma cells

Carsten Geiß, Claudius Witzler, Gernot Poschet, Wolfram Ruf, Anne Régnier-Vigouroux

Supplementary Figure 1

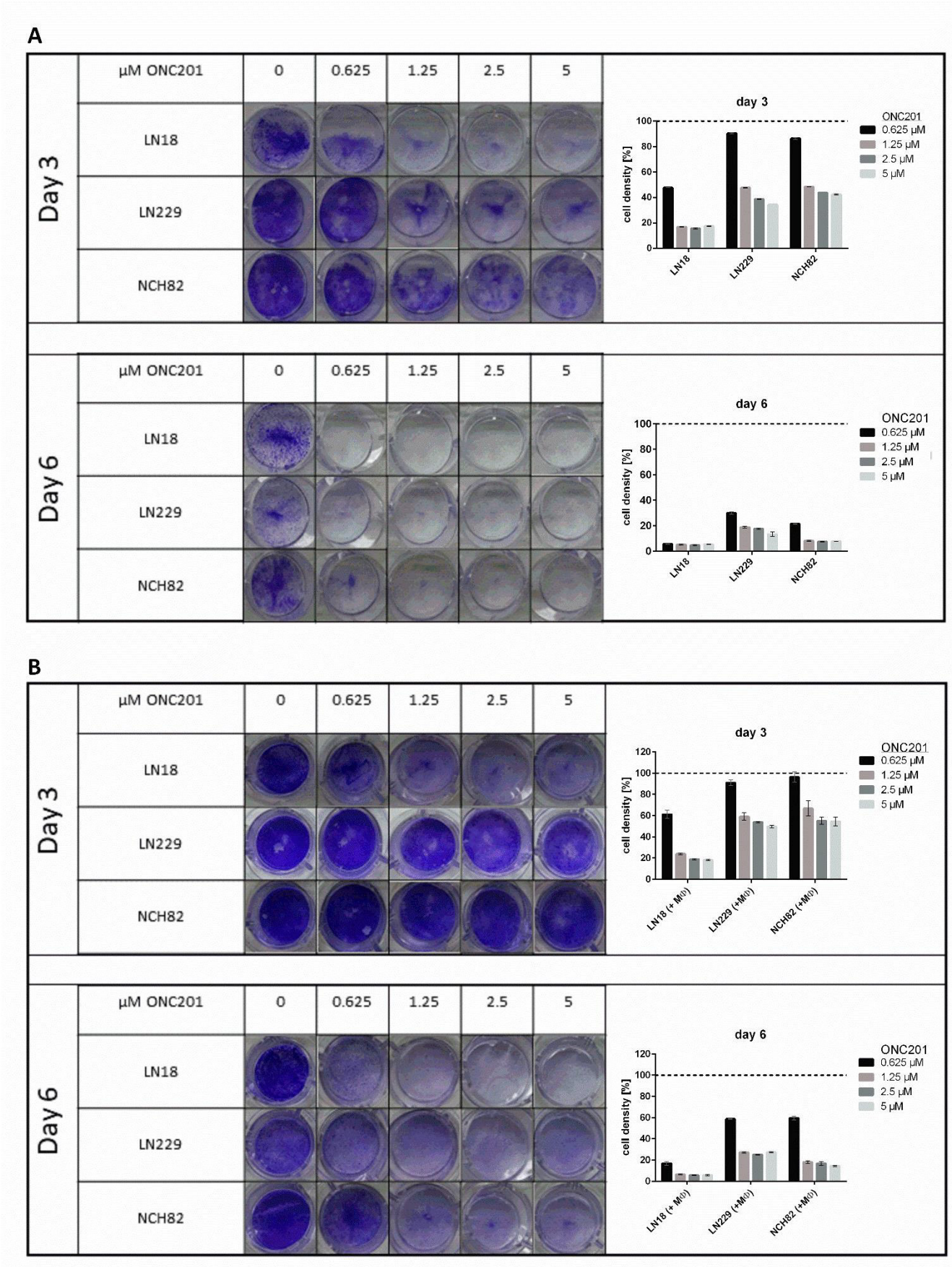

Supplementary Figure 1. Glioblastoma cells viability after ONC201 treatment. Crystal violet staining (left) and quantitative analysis (right) of LN18, LN229 and NCH82 cells treated for the indicated periods of time and ONC201 concentrations. Cristal violet images are shown for one representative experiment. Quantification: Values are normalized to the respective DMSO treated controls (dashed line). (A) monocultures; data are given as mean ± SEM of three technical replicates and are from one experiment. (B) co-cultures with macrophages; data are given as mean ± SEM of three biological replicates; each biological replicate was run in three technical replicates. Data are from three independent experiments.

Supplementary Figure 2

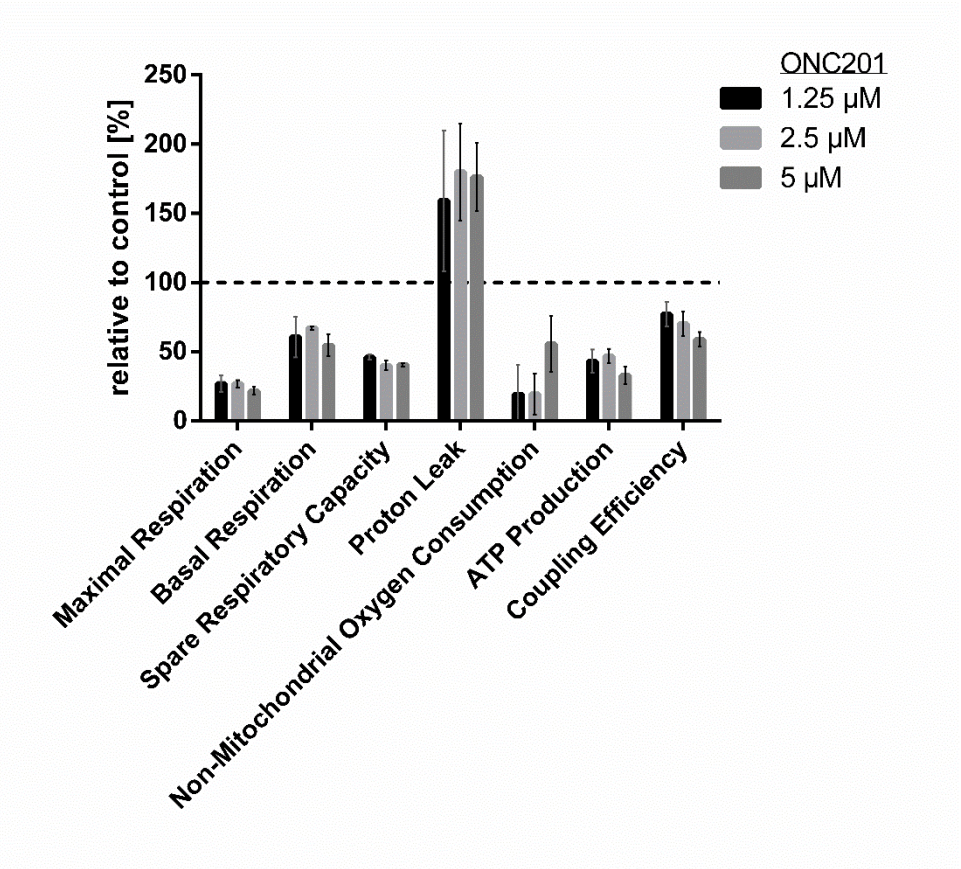

Supplementary Figure 2. ONC201 reduces mitochondrial integrity of primary macrophages. Mito Stress Tests of macrophages treated with indicated doses of ONC201 for three days. Values for each calculated parameter are normalized to the respective DMSO treated controls (dashed line). Data are given as mean ± SEM of four technical replicates and are from one experiment representative of two independent experiments.

Supplementary Figure 3

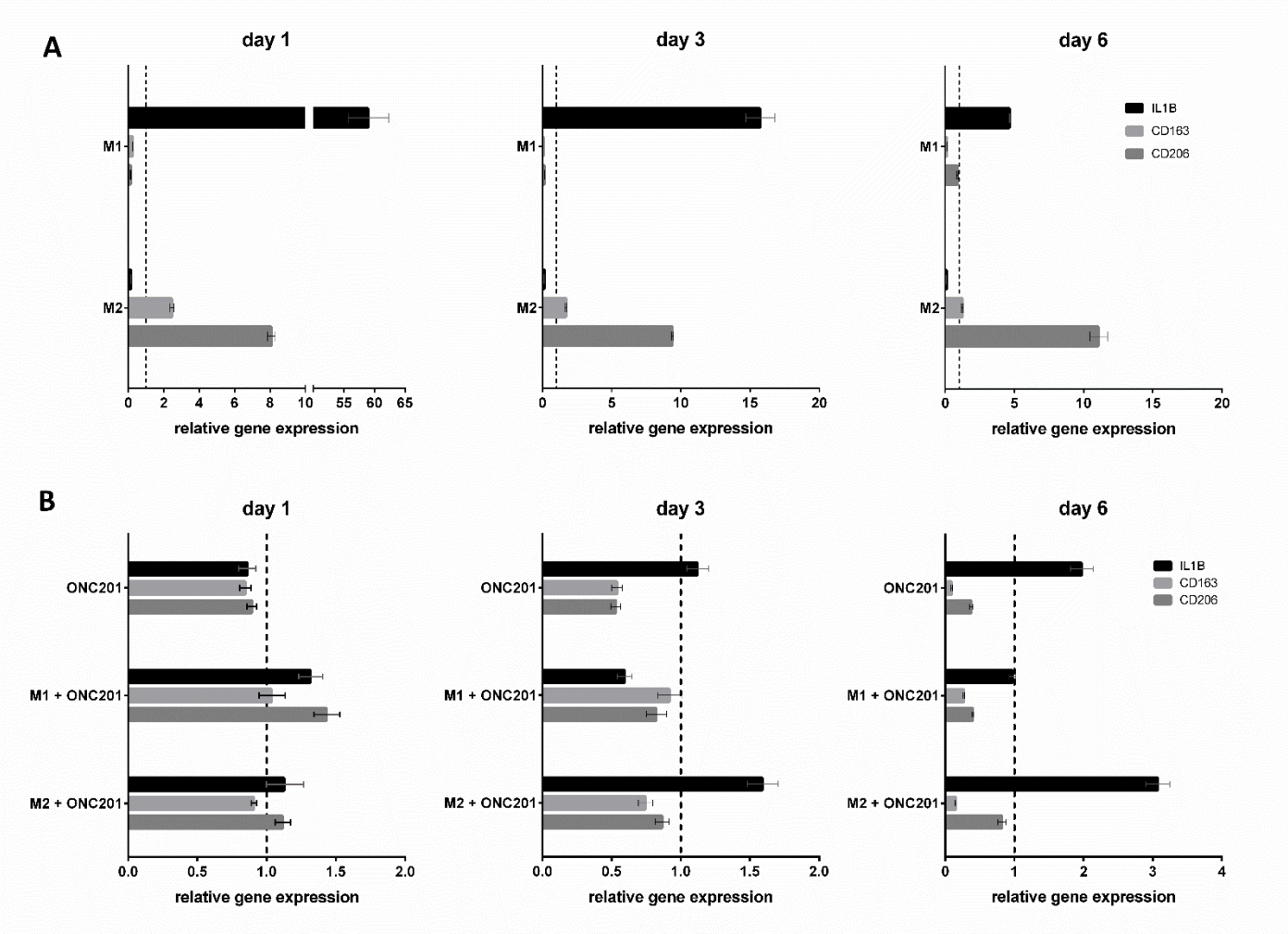

Supplementary Figure 3. Expression of *IL1B*, *CD163* and *CD206* in primary macrophages after ONC201 treatment. Macrophages were stimulated for the indicated periods of time with pro-inflammatory M1 [10 µg/ml polyinosinic-polycytidylic acid (InvivoGen) + 10 ng/ml lipopolysaccharide (Sigma Aldrich)] or anti-inflammatory M2 [10 ng/ml Interleukin-4 (BioLegend) + 10 ng/ml Interleukin-10 (BioLegend)] stimuli in the absence (A) or in the presence (B) of 5 µM ONC201. Relative gene expression was determined by qPCR as described in *Materials and methods*. Values are normalized to the gene expression of the respective DMSO-treated controls (dashed line). Data are given as mean ± SEM of three technical replicates and are from one experiment.

Supplementary Table 1

Extracellular Glutamate in µM		Day 1	Day 3	Day 6
Mono-culture	**MΦ**	49.50 (± 3.54)	48.16 (± 6.87)	39.54 (± 12.72)
	LN18	231.98 (± 0.50)	677.20 (± 0.22)	496.56 (± 11.10)
	LN229	119.68 (± 0.55)	300.01 (± 3.89)	263.01 (± 1.34)
	NCH82	210.07 (± 0.21)	611.99 (± 0.84)	492.03 (± 7.30)
Co-culture	**MΦ + LN18**	Not tested	381.20 (± 3.52)	426.63 (± 6.72)
	MΦ + LN229	Not tested	146.72 (± 1.72)	45.22 (± 0.60)
	MΦ + NCH82	Not tested	500.06 (± 7.07)	487.68 (± 3.43)

Glutamate concentrations measured in supernatants of control conditions. Extracellular glutamate concentration was determined in culture supernatants with the Glutamate-Glo™ Assay. Data from cells in monoculture (related to Figure 3): data are given as mean ± SEM of two technical replicates. Macrophages, six independent experiments; GB cells, one experiment. Data from cells in co-culture were obtained from pooled supernatants of three independent experiments (related to Figure 6): data are given as mean ± SEM of two technical replicates; one measurement.

Supplementary Table 2

Pro-inflammatory molecules

	time point	ONC201	TNF-α (pg/ml)	IL-6 (pg/ml)	IL-12p40 (pg/ml)	IL-23 (pg/ml)
MΦ + LN18	day 3	0 µM	18.23 (± 4.29)	35.55 (± 0.93)	<1.22	0.68 (*)
		0.625 µM	15.62 (± 4.71)	48.76 (± 5.65)	229.77 (± 125.86)	14.04 (*)
		1.25 µM	23.43 (± 0.35)	55.43 (± 1.31)	289.96 (*)	3.87 (*)
	day 6	0 µM	18.32 (± 2.46)	28.73 (± 0.24)	<1.22	<0.24
		0.625 µM	14.09 (± 8.69)	28.58 (± 3.21)	<1.22	<0.24
		1.25 µM	10.05 (± 3.33)	24.86 (± 0.26)	<1.22	<0.24
MΦ + LN229	day 3	0 µM	7.63 (± 0.07)	<15.09	326.22 (*)	0.79 (*)
		0.625 µM	7.56 (± 1.05)	<15.09	215.75 (± 27.20)	11.08 (± 1.31)
		1.25 µM	18.19 (± 2.87)	70.61 (± 3.97)	353.11 (*)	2.77 (*)
	day 6	0 µM	5.06 (± 2.08)	<15.09	<1.22	23.96 (*)
		0.625 µM	6.11 (± 3.47)	<15.09	499.03 (*)	18.36 (*)
		1.25 µM	23.10 (± 3.30)	70.27 (± 3.68)	519.42 (*)	<0.24
MΦ + NCH82	day 3	0 µM	50.99 (± 10.55)	1935.36(± 36.27)	<1.22	5.03 (± 0.94)
		0.625 µM	38.63 (± 1.78)	1764.53 (± 10.94)	229.85 (*)	10.68 (*)
		1.25 µM	69.80 (± 11.85)	3525.87 (± 651.53)	162.92 (*)	<0.24
	day 6	0 µM	38.10 (± 5.93)	502.29 (± 6.49)	<1.22	2.53 (*)
		0.625 µM	32.84 (± 1.49)	766.20 (± 38.54)	336.43 (± 204.13)	9.10 (± 3.13)
		1.25 µM	56.95 (± 14.36)	4097.65 (± 157.04)	419.54 (± 66.43)	<0.24

Anti-inflammatory molecules

	time point	ONC201	Arginase (pg/ml)	IL-1RA (pg/ml)	IL-4 (fg/ml)	IL-10 (pg/ml)
MΦ + LN18	day 3	0 µM	31903.65 (± 2485.45)	1872.05 (± 109.25)	99.70 (± 2.79)	6.72 (± 0.54)
		0.625 µM	32219.65 (± 1792.45)	1473.15 (± 33.85)	225.84 (± 8.64)	4.19 (± 0.54)
		1.25 µM	28307.00 (± 1556.80)	1053.70 (± 33.30)	209.58 (± 5.16)	3.75 (± 1.94)
	day 6	0 µM	30303.85 (± 1201.65)	3573.00 (± 1085.50)	178.63 (± 12.09)	25.92 (± 0.44)
		0.625 µM	31441.00 (± 2248.75)	2258.65 (± 136.35)	157.16 (± 6.62)	11.18 (± 2.00)
		1.25 µM	29864.65 (± 1470.65)	1234.90 (± 10.50)	143.67 (± 9.46)	11.26 (± 0.06)
MΦ + LN229	day 3	0 µM	30458.00 (± 531.50)	1375.60 (± 9.40)	138.33 (± 0.34)	5.42 (± 1.76)
		0.625 µM	30538.00 (± 70.25)	1237.65 (± 34.15)	255.85 (± 46.71)	2.59 (± 0.24)
		1.25 µM	31559.46 (± 1401.35)	1003.70 (± 109.60)	126.74 (± 0.13)	4.81 (± 0.68)
	day 6	0 µM	26779.15 (± 894.25)	1636.65 (± 36.45)	200.89 (± 5.03)	11.84 (± 1.44)
		0.625 µM	26681.00 (± 1724.45)	1258.00 (± 13.70)	182.43 (± 2.70)	6.80 (± 2.39)
		1.25 µM	29882.10 (± 573.80)	1230.85 (± 146.55)	144.40 (± 7.70)	6.58 (± 0.06)
MΦ + NCH82	day 3	0 µM	31482.55 (± 1708.75)	3009.25 (± 21.55)	236.29 (± 4.62)	16.06 (± 0.16)
		0.625 µM	28301.00 (± 975.95)	3243.80 (± 6.60)	178.51 (± 3.17)	9.67 (± 2.71)
		1.25 µM	32894.55 (± 325.75)	1782.40 (± 203.20)	149.63 (± 5.20)	2.74 (± 1.48)
	day 6	0 µM	31937.40 (± 554.20)	4456.40 (± 167.90)	141.86 (± 2.28)	10.39 (± 0.76)
		0.625 µM	30125.70 (± 2016.60)	3869.30 (± 236.70)	122.33 (± 0.18)	12.79 (± 2.68)
		1.25 µM	31191.85 (± 1929.85)	2081.35 (± 227.85)	113.82 (± 3.46)	6.06 (± 3.39)

Concentrations of extracellular inflammatory molecules in the co-culture supernatants. The values reported in this table are those presented in the heat map of Figure 7C. Briefly, three independent experiments were performed, the supernatants were harvested, pooled and extracellular cytokine concentrations was measured in each pool of the three biological samples using the LEGENDplex™ Human Macrophage/Microglia Panel and the Human ProQuantum Immunoassay Kit. Please note that the concentrations of IL-4 are indicated in fg/ml. Data are given as the mean of two technical replicates ± SEM, except for data marked with an asterisk (*) for which the mean could not be calculated because only one technical replicate was above the detection threshold. Analytes detected in less than 50% of the samples (IL-12p70, IL-1ß, IFN- γ, IP-10) are not shown. Data from TARC measurements had to be excluded because of too high intra -sample variability.